

Design and Analysis of Three Phase Double Sided Rotor Line Start Axial Flux Permanent Magnet Synchronous Motor

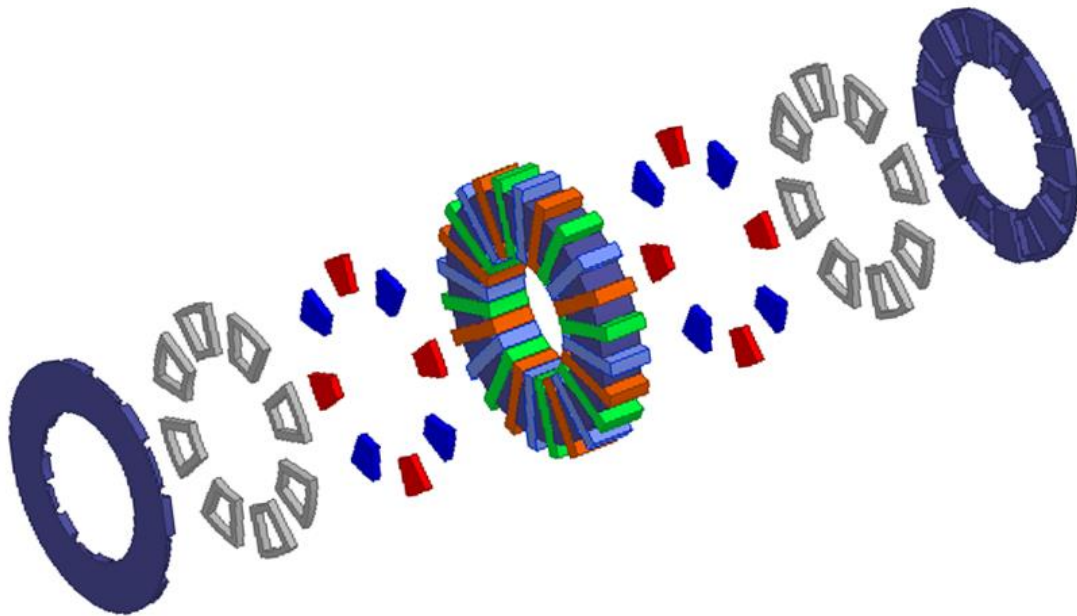
Parth Patel

Master of Engineering (Electronics)

Flinders University

Supervisor: Dr. Amin Mahmoudi

October 2017



Submitted to the School of Computer Science, Engineering and Mathematics in the Faculty of Science and Engineering in partial fulfilment of the requirements for the degree of Master Engineering (Electronics).

Abstract

This thesis presents design, analysis and simulation of Line-start axial flux permanent magnet synchronous motor (LSAFPMSM) with double sided rotor single stator slotted configuration. Design of this type of motor used in many constant speed applications. This thesis presents comparison between three phase double sided rotor line-start axial flux permanent magnet synchronous motor (LSAFPMSM) with three phase Induction motor. Three axial flux motor designs with different type of rotor with magnet and inductor bar configuration is designed. These three designs are analysed with aluminium and copper material of inductor bar. The design and analysis of the motor is performed in ANSYS Maxwell 3D software. The Finite Element Analysis is used to analyse the motor performance and comparison of both motors. Moreover, the steady state and dynamic performance of both motors are performed under no load and under load condition. The characteristic of motor such as speed, torque, output power, losses, induced voltage and magnetic flux density are studied. From the comparison of LSAFPMSM and induction motor, the results confirm that speed of LSAFPMSM is stable at synchronous speed while operation under loading conditions. The efficiency and power factor of the LSAFPMSM is higher than induction motor. It is suitable to replace induction motor to LSAFPMSM due to advantages of higher efficiency. The main disadvantage of the LSAFPMSM is the higher cost of motor due to adding permanent magnets.

Declaration of Academic Integrity

'I certify that this thesis does not incorporate without acknowledgment any material previously submitted for a degree or diploma in any university; and that to the best of my knowledge and belief it does not contain any material previously published or written by another person except where due reference is made in the text.'

Parth Patel

Acknowledgements

I would like to acknowledge my family for supporting me throughout this project. I would also like to specially acknowledge my supervisor, Dr. Amin Mahmoudi for providing me the knowledge and help during this project.

Table of Contents

Abstract.....	2
Declaration of Academic Integrity	3
Acknowledgements.....	3
List of Figures	7
List of Tables	11
Chapter 1: Introduction	12
1.1 Background.....	13
1.2 Problem statement.....	15
1.3 Objectives	16
1.4 Methodology.....	16
1.5 Limitations	16
1.6 Scope.....	17
1.7 Outline	17
Chapter 2: Literature Review.....	19
2.1 Introduction.....	20
2.2 Induction Motor	20
2.3 Axial Flux and Radial Flux Machine.....	21
2.4 Line-start Axial Flux permanent magnet synchronous motor	22
2.6 Gap Statement.....	23
2.7 Contribution.....	24
Chapter 3: Design Aspects and Justification.....	25
3.1 Induction motor as a benchmark model.....	26
3.1.1 Specification of induction motor	28
3.1.2 Stator	28
3.1.3 Rotor	29

3.2 Design of Axial-flux machine.....	30
3.3 Machine arrangement of Axial-flux machine.....	31
3.4 Stator configuration for LSAFPMSM	31
3.4.1 Windings of Stator	32
3.5 Rotor configuration for LSAFPMSM.....	33
3.5.1 Design of Inductor bar	34
3.5.2 Shape of magnets	37
3.6 Electrical Steel	38
Chapter 4: Method of Simulation.....	40
4.1 Simulation using Maxwell 3D FEA.....	41
4.2 Magnetostatic Analysis.....	42
4.3 Magnetostatic Flux Linkage	48
4.4 Summary of Magnetostatic Analysis	53
4.5 No load test analysis	54
4.5.1 Induced voltage measurement.....	54
4.6 Transient analysis	57
Chapter 5: Results and Discussion	58
5.1 Start-up of the Motor	59
5.2 Winding current of Motors	70
5.3 Losses of the machine.....	73
5.4 Torque produced by Machine	79
5.5 Power Rating of machine.....	84
5.6 Efficiency of motor	90
5.7 Power Factor	91
Chapter 6: Conclusion and Future work.....	94
6.1 Conclusion	95

6.2 Key Findings.....	95
6.3 Future work.....	96
References.....	97
Appendices.....	99
Appendix A: Mesh plots	99

List of Figures

Fig 3.1 Exploded view of Induction motor	26
Fig 3.2 Different views of induction motor in 3-D	27
Fig 3.3 Design of slotted stator	29
Fig 3.4 Rotor with Inductor bars	29
Fig 3.5 Exploded view of Axial-flux synchronous motor	30
Fig 3.6 Different views of AFPMSM	30
Fig 3.7 Single stator, single rotor (SSSR)	31
Fig 3.8 Single stator, double rotor (SSDR)	31
Fig 3.9 Stator of LSAFPMSM with windings	32
Fig 3.10 Stator Dimension	32
Fig 3.11 3-phase winding diagram of stator	33
Fig 3.12 Rotor of LSAFPMSM with magnets	34
Fig 3.13 Rotor dimension	34
Fig 3.14 Inductor type 1	35
Fig 3.15 Inductor type 2	35
Fig 3.16 Inductor type 3	35
Fig 3.17 Inductor type 1 with rotor	35
Fig 3.18 Inductor type 2 with rotor	35
Fig 3.19 Inductor type 3 with rotor	36
Fig 3.20 Magnet shape	37
Fig 3.21: B-H curve for M19_29G electrical steel	38
Fig 4.1: Maxwell 3D model of motor	41
Fig 4.2: Magnetic flux density of motor at no load	43
Fig 4.3: Magnetic flux density of motor at 2Nm load	44
Fig 4.4: Magnetic flux vector of motor at no load	46
Fig 4.5: Magnetic flux vector of motor at 2Nm load	47
Fig 4.6: Magnetic flux linkage at no load	50
Fig 4.7: Magnetic flux linkage at 2Nm load	53
Fig 4.8: Induced voltage waveform of LSAFPMSM	56

Fig 5.1: Speed of induction motor at no load	59
Fig 5.2: Speed of LSAFPMSM type 1 Aluminium inductor at no load	59
Fig 5.3: Speed of LSAFPMSM type 1 Copper inductor at no load	60
Fig 5.4: Speed of LSAFPMSM type 2 Aluminium inductor at no load	60
Fig 5.5: Speed of LSAFPMSM type 2 Copper inductor at no load	61
Fig 5.6: Speed of LSAFPMSM type 3 Aluminium inductor at no load	61
Fig 5.7: Speed of LSAFPMSM type 3 Copper inductor at no load	61
Fig 5.8: Speed of induction motor at 2Nm load	62
Fig 5.9: Speed of LSAFPMSM type 1 Aluminium inductor at 2Nm load	63
Fig 5.10: Speed of LSAFPMSM type 1 Copper inductor at 2Nm load	63
Fig 5.11: Speed of LSAFPMSM type 2 Aluminium inductor 2Nm no load	63
Fig 5.12: Speed of LSAFPMSM type 2 Copper inductor at 2Nm load	64
Fig 5.13: Speed of LSAFPMSM type 3 Aluminium inductor at 2Nm load	64
Fig 5.14: Speed of LSAFPMSM type 3 Copper inductor at 2Nm load	65
Fig 5.15: Speed of induction motor at 14Nm load	65
Fig 5.16: Speed of LSAFPMSM type 1 Aluminium inductor at 14Nm load	66
Fig 5.17: Speed of LSAFPMSM type 1 Copper inductor at 14Nm load	66
Fig 5.18: Speed of LSAFPMSM type 2 Aluminium inductor at 14Nm load	66
Fig 5.19: Speed of LSAFPMSM type 2 Copper inductor at 14Nm load	67
Fig 5.20: Speed of LSAFPMSM type 3 Aluminium inductor at 14Nm load	67
Fig 5.21: Speed of LSAFPMSM type 3 Copper inductor at 14Nm load	67
Fig 5.22: Winding current of all model at no load	72
Fig 5.23: Losses of Induction motor at no load	73
Fig 5.24: Losses of LSAFPMSM type 1 Aluminium inductor at no load	74
Fig 5.25: Losses of LSAFPMSM type 1 Copper inductor at no load	74
Fig 5.26: Losses of LSAFPMSM type 2 Aluminium inductor at no load	74
Fig 5.27: Losses of LSAFPMSM type 2 Copper inductor at no load	75
Fig 5.28: Losses of LSAFPMSM type 3 Aluminium inductor at no load	75
Fig 5.29: Losses of LSAFPMSM type 3 Copper inductor at no load	75
Fig 5.30: Losses of Induction motor at 2Nm load	76
Fig 5.31: Losses of LSAFPMSM type 1 Aluminium inductor at 2Nm load	76
Fig 5.32: Losses of LSAFPMSM type 1 Copper inductor at 2Nm load	77
Fig 5.33: Losses of LSAFPMSM type 2 Aluminium inductor at 2Nm load	77

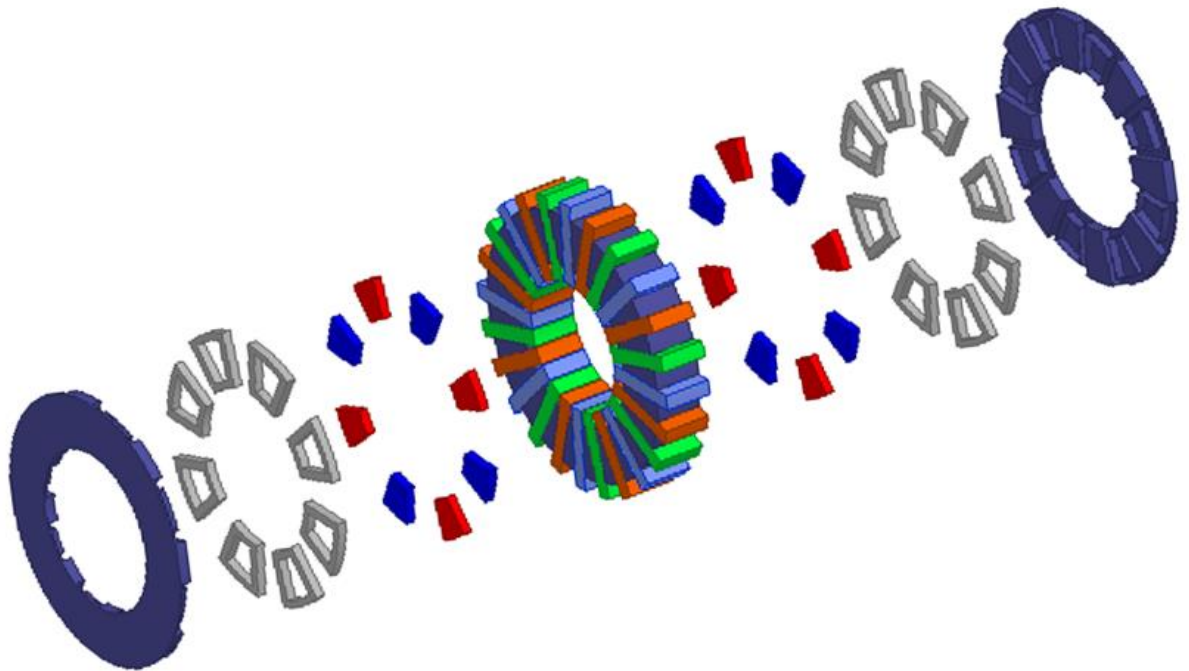
Fig 5.34: Losses of LSAFPMSM type 2 Copper inductor at 2Nm load	77
Fig 5.35: Losses of LSAFPMSM type 3 Aluminium inductor at 2Nm load	78
Fig 5.36: Losses of LSAFPMSM type 3 Copper inductor at 2Nm load	78
Fig.5.37: Torque of Induction motor at no load	79
Fig 5.38: Torque of LSAFPMSM type 1 Aluminium inductor at no load	79
Fig 5.39: Torque of LSAFPMSM type 1 Copper inductor at no load	80
Fig 5.40: Torque of LSAFPMSM type 2 Aluminium inductor at no load	80
Fig 5.41: Torque of LSAFPMSM type 2 Copper inductor at no load	80
Fig 5.42: Torque of LSAFPMSM type 3 Aluminium inductor at no load	81
Fig 5.43: Torque of LSAFPMSM type 3 Copper inductor at no load	81
Fig.5.44: Torque of Induction motor at 2Nm load	82
Fig 5.45: Torque of LSAFPMSM type 1 Aluminium inductor at 2Nm load	82
Fig 5.46: Torque of LSAFPMSM type 1 Copper inductor at 2Nm load	82
Fig 5.47: Torque of LSAFPMSM type 2 Aluminium inductor at 2Nm load	83
Fig 5.48: Torque of LSAFPMSM type 2 Copper inductor at 2Nm load	83
Fig 5.49: Torque of LSAFPMSM type 3 Aluminium inductor at 2Nm load	83
Fig 5.50: Torque of LSAFPMSM type 3 Copper inductor at 2Nm load	84
Fig 5.51: Input and output power of Induction motor at no load	85
Fig 5.52: Input and output power of LSAFPMSM type 1 aluminium inductor at no load	85
Fig 5.53: Input and output power of LSAFPMSM type 1 copper inductor at no load	85
Fig 5.54: Input and output power of LSAFPMSM type 2 aluminium inductor at no load	86
Fig 5.55: Input and output power of LSAFPMSM type 2 copper inductor at no load	86
Fig 5.56: Input and output power of LSAFPMSM type 3 aluminium inductor at no load	86
Fig 5.57: Input and output power of LSAFPMSM type 3 copper inductor at no load	87
Fig.5.58: Input and output power of Induction motor at 2Nm load	87
Fig 5.59: Input and output power of LSAFPMSM type 1 aluminium inductor at 2Nm load	88
Fig 5.60: Input and output power of LSAFPMSM type 1 copper inductor at 2Nm load	88
Fig 5.61: Input and output power of LSAFPMSM type 2 aluminium inductor at 2Nm load	88

Fig 5.62: Input and output power of LSAFPMSM type 2 copper inductor at 2Nm load	89
Fig 5.63: Input and output power of LSAFPMSM type 3 aluminium inductor at 2Nm load	89
Fig 5.64: Input and output power of LSAFPMSM type 3 copper inductor at 2Nm load	89
Fig 5.65: Efficiency of all motor at 2Nm load	90
Fig 5.66: Power factor of motor at no load and 2Nm load	91

List of Tables

Table 1.1: Overall Electricity consumption by motor	13
Table 1.2: Minimum 3-phase motor efficiency standards in Australia	14
Table 3.1: Specification of Induction motor	28
Table 3.2: Properties of copper material for rotor	33
Table 3.3: Properties of aluminium material for inductor	36
Table 3.4: Properties of copper material for inductor	36
Table 3.5: Properties of N36Z_20 material for magnet	37
Table 3.6: Properties of M19_29G Electrical steel	38
Table 3.7: Summary of dimensions of LSAFPMSM	39
Table 4.1: Summary of peak Induced voltage of open circuit test	56
Table 5.1: Speed response of motor under different load condition	68
Table 5.2: Overall performance of motors	92

Chapter 1: Introduction



1.1 Background

Today, Induction machines are considered as a backbone of the industries. Because, these kinds of motors are having very simple and robust construction. Even they are easy to install for different variable speed applications. Majority of the industrial apparatus are working with the motors. So, because of this much use the induction motor is the major consumer of the electrical energy in the industries. The aim of the electrical motors is to convert the electrical energy to the mechanical energy. So, these conversion of energy is not possible for 100%. Some of the electrical energy is wasted and this waste of energy can be considered as a loss of the motor.

There are majority of the power consumers in Australia in 2011. Such as, industrial, commercial, residential, transport and agriculture. So, for these different consumers the amount of consumption is illustrated below in the table below,

Table 1.1: Overall Electricity consumption by Motor [1].

Sector	Electricity consumption	% of all EMDS electricity	% of sector electricity
Industrial	4488 TWh/year	64%	69%
Commercial	1412 TWh/year	20%	38%
Residential	948 TWh/year	13%	22%
Transport and agriculture	260 TWh/year	3%	39%

Here, from the table it can be clearly seen that industries are one of the major consumer of electricity with 69% [1]. In industries, the motors are mostly having high consumption for different operations such as packaging of the mass-produced products in refrigerator compressors, extractor fans, computer hard drives etc. Among all this motor, the rating of 0.75kW and 375kW motors are mostly used in industrial sector [1].

From the previous studies, it can be noticed that these traditionally use induction motors are having major losses quantity than the losses from other electric motors. So, these losses take place because of more current carrying material in the construction of motor. These losses can be result in the heating of the machine and the heating of machine cause the CO2 emission, which also affects the environment.

To overcome this kind of losses in the motors, today there are so many researches going on. Because it is the biggest threat on the world. International Electrotechnical commission has introduced the international standards in the production of the electric motor. They stated some of the efficiency levels for different rating of the motors. Also, the Australian government has started initiative named MEPS from the year 2011. Table 1.2, shows the minimum efficiency standards for Australia.

Table 1.2 Minimum three phase motor efficiency standards in Australia [2].

Rated Output kW	Minimum Efficiency %			
	2 pole	4 pole	6 pole	8 pole
0.73	78.8	80.5	76.0	71.8
0.75	78.8	80.5	76.0	71.8
1.1	80.6	82.2	78.3	74.7
1.5	82.6	83.5	79.9	76.8
2.2	84.1	84.9	81.9	79.4
3	85.3	86.0	83.5	81.3
4	86.3	87.0	84.7	82.8
5.5	87.2	87.9	86.1	84.5
7.5	88.3	88.9	87.3	86.0
11	89.5	89.9	88.7	87.7
15	90.8	90.8	89.6	88.9

Also, the European union has placed new standards of efficiency to produce the electric motor. In those standards, they divided in four various parts such as IE1, IE2, IE3 and IE4. Where, IE1 is the standard efficiency, IE4 stands for super premium efficiency. Also, the researchers are continuously trying to achieve the ultra-premium efficiency IE5 [2]. So, here the aim is to design the axial flux double sided rotor line-start PM motor.

1.2 Problem statement

Traditionally, the induction motors are majorly used in the industries and also for the house hold applications. Due to lower efficiency of induction motor, motor takes more input power. The more generation of power leads to the CO₂ emission. It is the serious environmental problem.

Basically, the reason for the losses in the machines are the copper winding and the friction during the rotation as well as the core of the motor. So, the copper quantity can be reduced by designing the new motor with the inductor bars.

Also, the radial flux machines are bulkier and occupy more space during its application. So, the idea arises in mind to design the motor working with axial flux phenomenon. And there are plenty of advantages of developing the axial flux motor.

There are many developers in the market named ABB, SIEMENS, GE, SEW in the production of electrical machine. But, for this new configuration of the design another idea was attached of self-starting of the motor. So, to overcome these problems the whole modern design of the axial flux line start motor with the PM is developed.

The Axial flux motor is having large cogging torque compared to traditionally used motors. So, these types of motors can be used in the different applications such as ship propulsion, elevators. Also, because of high efficiency and high torque, it can be also used in the application of the transport and military. These types of the motors reduce the losses and the overall efficiency of these machines is high. Which is ultimately helps to reduce the emission of CO₂.

For the optimization of the best design, there are basically 3 design of line-start axial flux permanent magnet synchronous motor were finalized with different design of inductor bars with aluminium and copper material of inductor bar.

1.3 Objectives

- To study the performance of 8 pole 50Hz 1.1kW, average 335V induction motor as a benchmark model.
- To design a double-sided rotor line-start axial flux permanent magnet synchronous motor of 1.5kW 8 pole 50Hz.
- To simulate LSAFPMSM with three different type of inductor bar with aluminium and copper material.
- To compare the performance of LSAFPMSM and induction motor under different load condition.

1.4 Methodology

The Finite Element Analysis (FEA) is used for simulation of motor. The ANSYS Maxwell 3D 2015 version software is used for simulation of motor. Mostly, this software is industry standard simulation program to performed Magnetostatic, open circuit test and transient analysis for better accurate result of motor. First, the induction motor is designed in ANSYS Maxwell 3D software and the simulation is done with the help of finite element analysis method. Three-phase 8 pole 50Hz, 1.3kW induction motor is designed. This motor is taken as a benchmark model. And the motor is simulated for magnetostatic and transient analysis. The line-start axial flux permanent magnet synchronous motor is designed in same software. The stator design is same as induction motor but the rotor design is different for both model. The three types of inductor bar are designed for LSAFPMSM. The simulation of these three types of LSAFPMSM is carried out using this software. The magnetostatic and transient analysis of LSAFPMSM is obtained. Finally, the FEA application is used with ANSYS Maxwell 3D in this research.

1.5 Limitations

All the motors are designed in Maxwell 3D using FEA. The 3D design takes too much time for simulation. The 3D design is also very expensive with respect to processor of computer. So, 2D design model is often used in replace of 3D design because 2D model take less computational time. But, the axial flux machine cannot be converted to 2D design. So, the results of 2D model is not accurate as 3D model simulation.

1.6 Scope

The scope of the research is to design and analysis of 1.5kW line-start axial flux permanent magnet synchronous motor with double sided rotor slotted stator and to design 1.3kW induction motor with slotted stator configuration. the simulation for both motor will be performed under different loading condition. The three-type inductor bar is designed for LSAFPMSM. The magnetostatic and transient analysis of all motor is performed using Maxwell 3D FEA method. The Maxwell 3D is used to design all motor for better results of motors.

1.7 Outline

Chapter 1: Introduction

Chapter 1 gives an overview and background of project. The problem statement describes the problem with other motor. The methodology, limitation and scope of the project are also included in this chapter.

Chapter 2: Literature Review

Chapter 2 consists the previous research information which guide the direction of research in different area of this thesis. The literature review also gives the detail of previous research paper which is contributing and related to this project. Mostly, the research paper is presented on the LSAFPMSM for design and analysis process.

Chapter 3: Design Aspects and Justification

This chapter provides the design aspects and justification which are used for designing of machine. The whole machine geometry and design properties of stator, rotor, inductor bar and magnet of motor is specified in this chapter. The final 3D design of all model is illustrated in this chapter.

Chapter 4: Method of Simulation

The chapter 4 gives the detail information about the simulation method and about the software which is used for simulation in 3D. The magnetic analysis and open circuit test is included in this chapter. This chapter ends with the simulation results.

Chapter 5: Results and Discussion

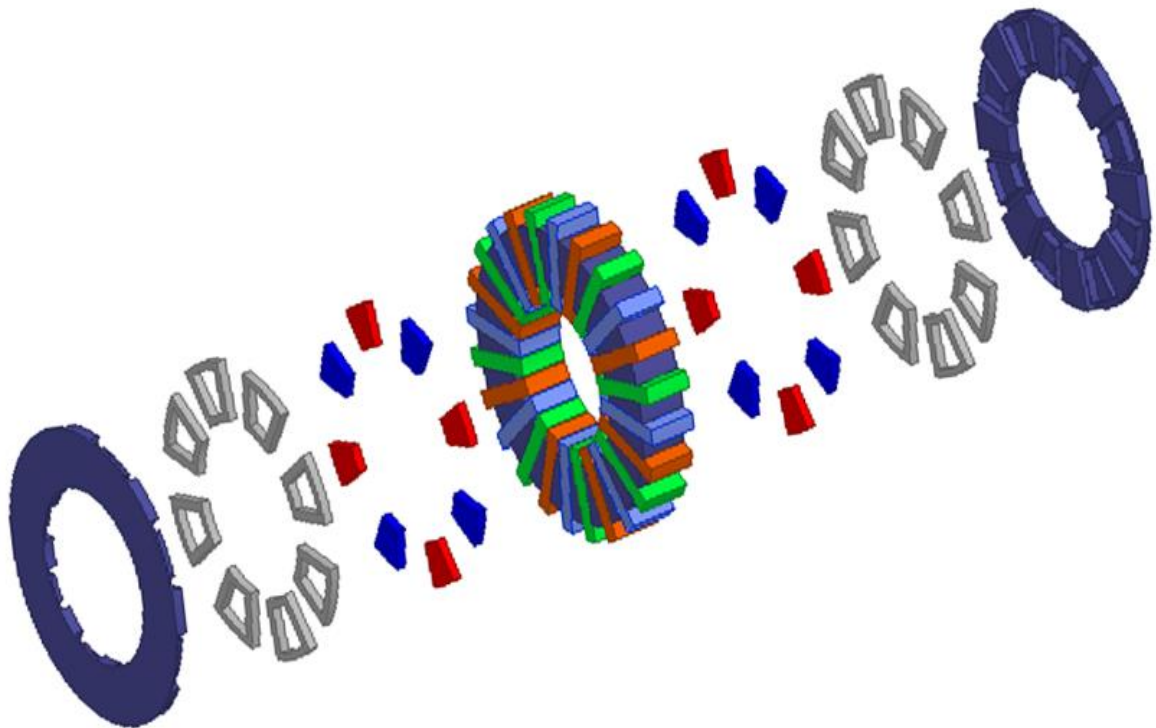
Chapter 5 represents the results of transient analysis. The motor is tested to evaluate for its performance parameter at different loading condition. The results are obtained for

LSAFPMSM and Induction motor. The results of both motor are compared to obtained the better performance of motor.

Chapter 6: Conclusion and Future work

Chapter 6 provides the brief conclusion from the results of all motors. This chapter ends with discussion of key finding and future direction of this project from the obtained result of motor.

Chapter 2: Literature Review



2.1 Introduction

In last 10 years, there are many research executed in the field of electrical engineering. The different type of motors is developed in these researches. There are many types of motors are designed for different types of applications. All the new designs have its advantages and disadvantages. There is not specific method for design and analysis purpose, all the researches are carried out with different methods using different software. This literature review starts with previous paper discussing general design and analysis of line start axial flux permanent magnet synchronous motor and induction motor. In the second part of review research gap is discussed.

2.2 Induction Motor

The different methods of electrical motor design and analysis is illustrated in many research paper. But, there are few paper which discussed about design of the motor. Livadaru L, Simion A, Munteanu A, Sandru M [3] have published a paper for designing and simulation of induction motor. In this study, a high-power induction motor rating of 630kW is designed. The deep bar double squirrel cage rotor is used to increase torque and to decrease starting current. While the stator has double layer winding. The finite element method is used for steady-state operation and transient analysis of the motor. It concludes, due to special construction of rotor, it required a high starting torque and low starting current.

Contreras S, Cortes C and Guzman M [4] present their study with modelling of squirrel cage induction motors of rating 3.7kW two pole. This motor is modelled in two ways such as finite element method and analytic equivalent circuit. The Bio-inspired multi-objective optimization algorithm is used to improve the design of motor and motor is validate through FEM. It is concluded that an equivalent circuit of motor can be used with given algorithm technic and discussed different parameters of motor.

Ruthes J, Nau S and Nied A [5] conducted a study on analysis of induction motor under non-sinusoidal supply voltage. The three methods Analytical Models (AM), Finite element method (FEM) and Magnetic Equivalent Circuit (MEC) are used for modelling and design of induction motor. But AM has disadvantages of accuracy so this method is used in analyzing in small changes while FEM method has provided stator rotor slot, distribution of stator winding but this method takes more computation time. The MEC method is very precious and less complexity of model. This paper concluded that the FEM and MCA methods are better with results as compared to AM and MEC takes less simulation time and more suitable.

Srinivasan J, Selvaraj K, Chitrarasu J and Resmi R [6] compared the full pitch and short pitch winding configuration of three phase squirrel cage induction motor rated 1.1kW, 500 rpm and 12 poles. Using the finite element method, the harmonic of winding current of motor is compared for both configuration. The stator has double layer winding with two coils placed in a single slot and simple rotor construction is used. In the results, the graph of air gap flux density of full and short pitch and magnetic flux density of motor are obtained. From the results, it concluded that full pitch winding has more harmonics as compared to short pitch winding.

Pyrhonen J, Jokinen T and Hrabovcova V [7] published a book name “Design of Rotating Electrical Machines”. They provide a theoretical background for designing of electrical machine with equations which are used for designing. In the detail, they discussed on method of design, winding of machines, design of magnetic circuit, calculation of airgap, flux line and obtained the graph of speed and efficiency at different load conditions.

2.3 Axial Flux and Radial Flux Machine

Cavagnino A, Lazzari M and Profumo F [8] have compared axial flux structure and conventional radial flux structure machines. The two motor designs are selected and compared both in terms of electromagnetic torque with different dimensions and pole numbers. During the test the overall volume of motor, losses and flux density are taken as constant. It concluded that the axial flux machine is more suitable when number pole is high and axial length is short.

Patterson D, Colton J, Mularcik B and Kennedy B [9] have studied on comparison of radial and axial structures in electrical machine. The single sided geometry is used for axial flux and for radial flux inside rotor geometry is used. This paper concludes that axial flux has large torque arm with same radius and it required less material as compared to radial flux machines. So, the cost of radial flux machine is high.

Upadhyay P.R. and Rajagopal K.R. [10] have compared axial and radial field permanent magnet brushless DC motor rating of 350 rpm and 70W. Two methods, Computer aided design (CAD) and finite element method are used for comparison. The different parameters of motor are calculated in CAD and EFM is used for validation in 2-D and 3-D. From the obtain results it concludes that axial field motor is preferable than radial field. The axial field motor has high efficiency.

Sitapati K and Krishnan R [11] discussed on comparison of radial and axial field permanent magnet brushless machines. The four-novel design of machine such as single gap and dual gap

slotted axial field machine and single gap and dual gap slot less axial field machine are compared with one radial filed machine. The five-different power rating and two rated speed is used for designing. The comparison consists in terms of losses, power, torque, magnet size and inertia of machine. It concludes that, the axial filed machine is superior in terms of smaller volume of material and high-power density.

Pravaniem A, Niemela M and Pyrhonen J [12] has compared low speed axial and radial flux surface mounted machines. The comparison is based on the efficiency and volume of the machine. This research concludes that efficiency of axial flux machine is low with same electrical loading and air fap flux density but the efficiency can be improved by increasing volume. The efficiency also improved by using more poles.

2.4 Line-start Axial Flux permanent magnet synchronous motor

Mahmoudi A, Kahourzade S, Uddin M, Rahim N and Hew W.P. [13] present a novel design of line-start axial flux permanent magnet synchronous motor using finite element analysis method. The 4-pole slot less double-sided rotor configuration is used for high torque density and stable rotation of motor so the motor can operate at synchronous speed and the prototyping of the motor is presented. The steady state and transient performance is analyzed with FEM. From the results, the speed of the motor synchronizes at rated speed and sufficient starting torque. This type of motor is suitable for high-speed application.

Ugale R.T., Bhanuji A and Chaudhari B. N. [14] conducted a study on novel design of rotor. The permanent magnet which is place in rotor so the design of the rotor is very complex. So, this paper presents a new two-part rotor design which gives synchronous speed and performance of motor. The two-part rotor design gives a wide choice of machine parameters and axial length does not depend on it. The result shows that torque of two-part rotor is 1.3 times higher than spoke rotor. So, motor run with high starting torque in starting and torque is constant at steady state performance.

Tsuboi K, Takegami T, Hirotsuka I and Nakamura M [15] have discussed about the performance and calculation of three phase LSPMM using general analytical method. Using this method, the current and torque is calculated. Moreover, the vibratory torque can be calculated in less time. In the conclusion, the characteristics of three phase LSPMM can be calculated in very less time by using this method. This method also can be used for reducing vibration and noise of the motor. The combination of this method and FEM method gives better design and magnetic flux of the motor.

Feng X, Bao Y, Liu L, Huang L and Zhang Y have [16] compared line start-up permanent magnet synchronous motor (LSPMSM) to the premium efficient induction motor (PEIM) in terms of design and starting performance of these motor using finite element analysis (FEA). Two types of rotor design, semi-closes slot and fully closed slot rotor are designed by combination of squirrel cage and permanent magnet poles. FEA is used to analyses starting torque, cogging torque, mechanical stress, no load voltage etc. this study concludes that LSPMSM has higher efficiency, power factor and less material used as compared to PEIM.

Fei W, Luk P.C.K, Ma J, Shen J and Yang G [17] have present an amended high performance LSPMSM from small three phase induction motor. For the modification, the stator and winding pattern are same but the size of copper wire and coil turn are changed to get unity power factor. The four-pole rotor with permanent magnet is used for high energy at high temperature. 36 pyriform slots with flat bottom rotor is used for high efficiency LSPMSM. The analyses of this motor are done with FEA using ANSOFT MAXWELL 2-D. It concludes that new developed LSPMSM has increase efficiency and power factor with minimum changes at minimum extra cost.

Kul S, Bilgin O and Mutluer M [18] have discussed about the application of finite element method (FEM) to determine the performance of LSPMSM. This study focus on 1.1kW, 4-pole LSPMSM. This motor is designed in ANSYS MAXWELL Rmxprt software and then the motor can be converted into 2-D/3-D finite element modelling. The rotor consists permanent magnet and damper winding while stator has armature winding. The transient analysis is performed to get graph of efficiency, breaking torque and speed. Form the results it can be say that, efficiency, breaking torque and power factor can be depend on the magnet dimension and breaking torque is proportional to magnet dimension.

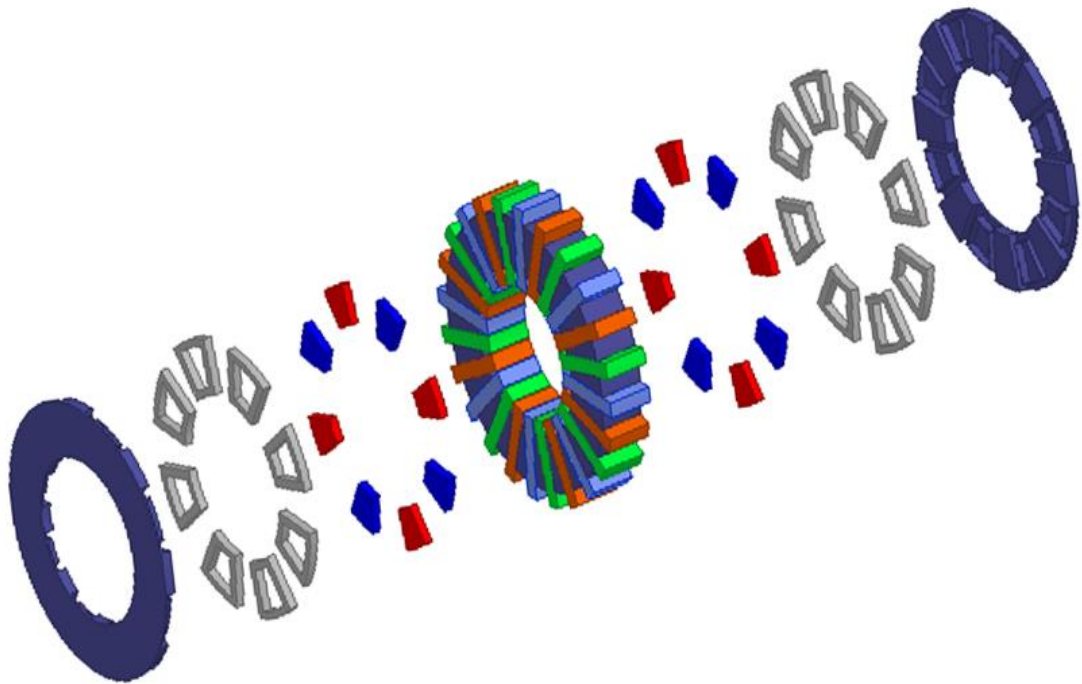
2.6 Gap Statement

Among all the mentioned literature review for the specified permanent magnet motor has been carried out. Most of the paper focus on the three-phase permanent magnet synchronous motor with different analyses method. But there is less research was done in three-phase line start permanent magnet synchronous motor for constant speed application with higher efficiency and better power factor. The novel design of the rotor can be done on the LSPMSM. The performance of this motor can be achieved by transient and steady state analysis using finite element method in ANSYS MAXWELL 3-D.

2.7 Contribution

The aim of this project is to design and analyses of three-phase double sided rotor axial-flux permanent magnet synchronous motor to get better efficiency and power factor than Induction motor. This analysis is performed for the direct drive double sided rotor with permanent magnet design motor for constant speed. The analysis is performed to get results in different loading condition of the motor.

Chapter 3: Design Aspects and Justification



3.1 Induction motor as a benchmark model

In this project, the induction motor of rating 1.1kW, 8-pole, 50Hz is taken as a benchmark model. The exploded view of the induction motor is shown in figure 3.1. Mostly, the induction motor consists rotor, stator and inductor bars. Double sided rotor configuration used for this motor. The inductor bars built in the rotor which is made from cast aluminium material. The slotted stator has 24 slots and windings are applied to three phase voltage supply. The motor is run on the principal of electromagnetic induction which obtained by rotor from the stator windings. Now a day, three-phase induction motor is widely used for industrial application and single-phase induction motor used for small household application. The induction motor always run less than synchronous speed due to lagging flux current in rotor.

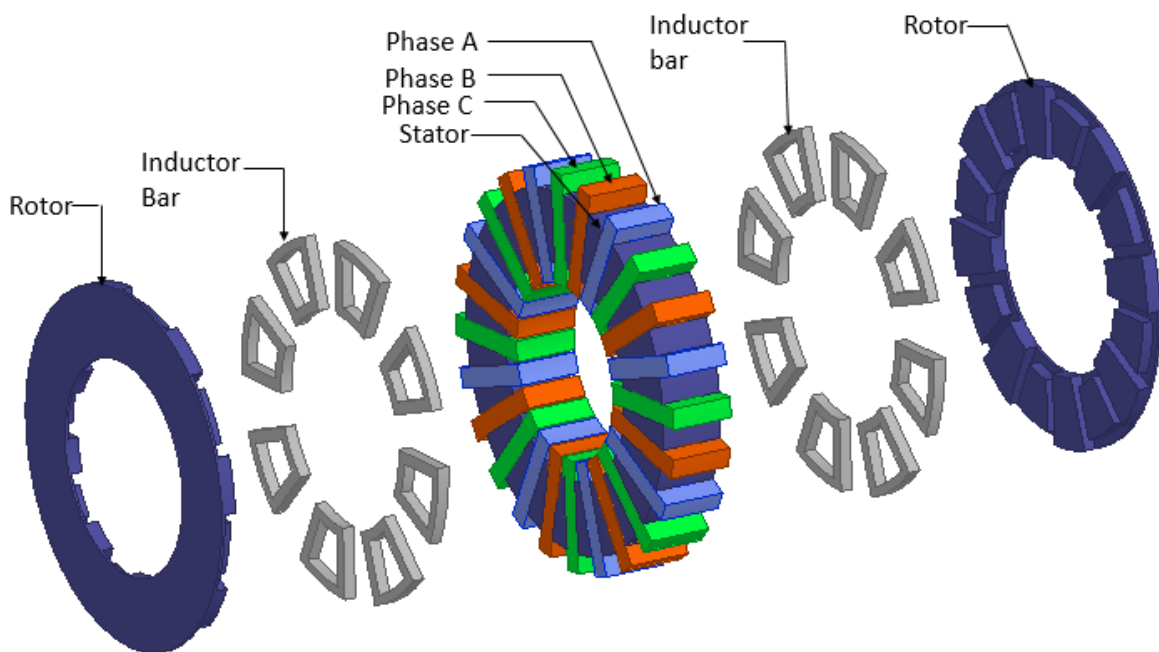


Figure.3.1: Exploded view of Induction motor

The different views of the induction motor are shown in figure 3.2. The synchronous speed is the speed of rotating magnetic field which is defined as given formula.

$$N_s = 120 \times \frac{f}{P} \text{ (RPM)}$$

Where, P is total number of poles and f is supply frequency.

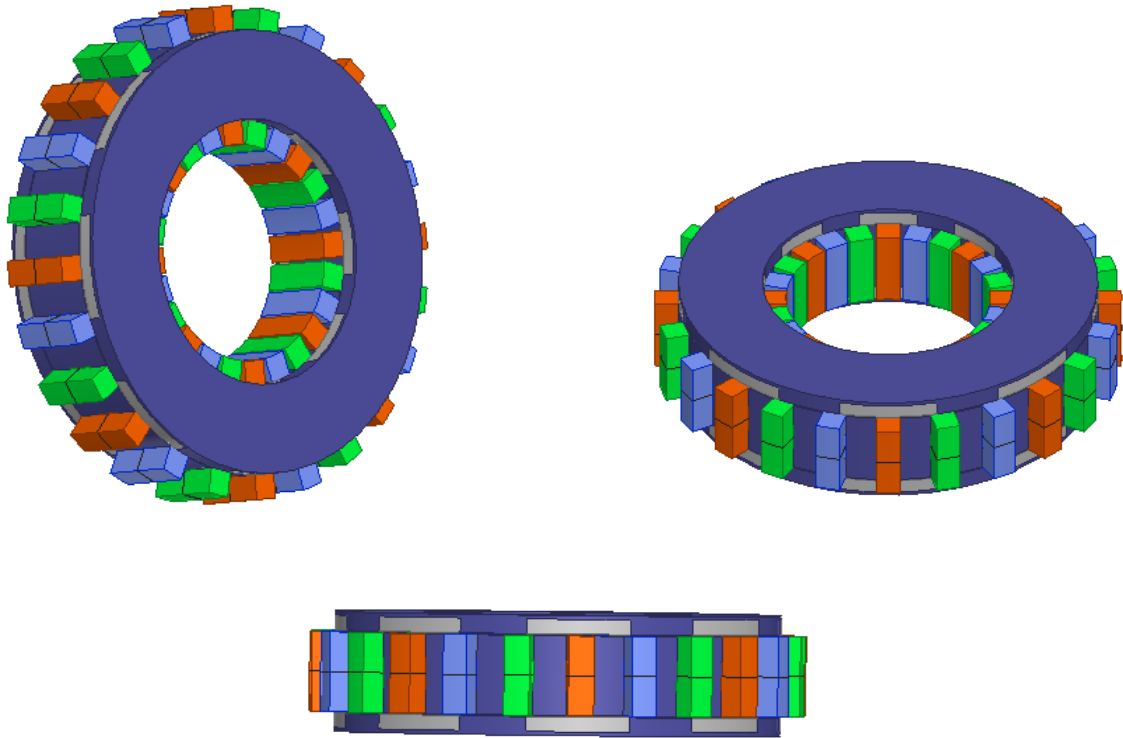


Figure 3.2: Different views of induction motor in 3-D

The difference between synchronous speed and actual speed is called percentage ration of slip s . Slip of the motor can be calculated by formula:

$$\% \text{ slip } s = \frac{N_s - N}{N_s} \times 100$$

Where, N_s is synchronous speed and N is actual speed of motor.

The torque of the induction motor is proportional to the flux per pole, rotor current and power factor which can be formulated as,

$$T \propto \phi I_2 \cos\theta_2$$

Where, T is torque. I_2 is rotor current, $\cos\theta_2$ is power factor of rotor and ϕ is flux which produced by induced emf.

The formula for maximum torque of three phase induction motor derived as,

$$T = \frac{sE_2^2 R_2}{R_2^2 + (sX_2)^2} \times \frac{3}{2\pi n_s}$$

Where, s is slip of motor. E_2 is rotor emf, R_2 is rotor resistance and X_2 is rotor reactance. N_s is synchronous speed of the motor.

3.1.1 Specification of induction motor

The dimension and general data of the induction motor is given in table. The rating of motor is 1.1kW, 8-pole at rated speed of 727 rpm.

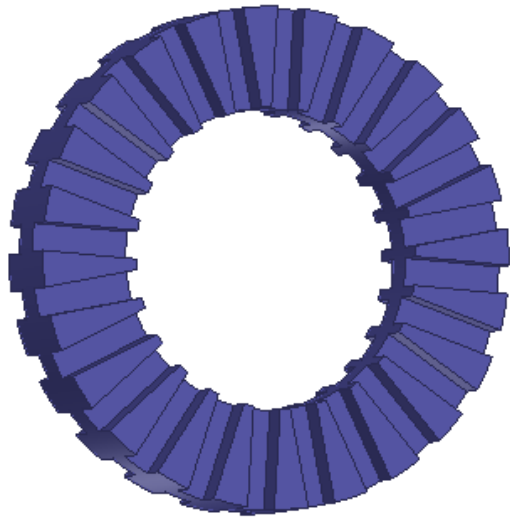
The slotted stator with 24 slots is used for motor design. The material M19_29G steel is used for stator. The inner and outer radius of stator is 90mm and 150mm respectively. The same steel material is used for rotor. The double-sided rotor geometry is used in this motor design. The inductor bar is made of aluminium material which are fit with rotor.

Table 3.1: Specification of Induction motor

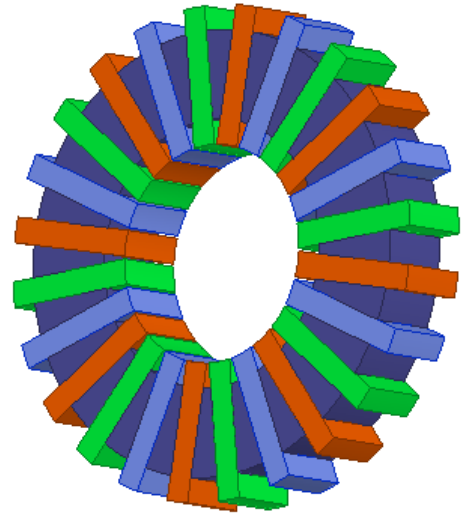
General data of machine	
Given output power (kW)	1.1
Number of poles	8
Given speed (rpm)	727
Frequency (Hz)	50
Average Voltage Rating (V)	335
Stator data	
Inner radius (mm)	90
Outer radius (mm)	150
Thickness (mm)	20
Rotor data	
Inner radius (mm)	90
Outer radius (mm)	150
Thickness (mm)	2.5

3.1.2 Stator

The slotted stator which is made from laminated iron is used in this design. The 24 stator slots are filled with same number of windings as shown in figure 3.4. The winding colour Blue, Red and Green indicates Phase A, Phase B and Phase C respectively.



(a) Slotted stator



(b) Slotted stator with windings

Fig.3.3: Design of slotted stator

3.1.3 Rotor

The main part of the project is having a double-sided rotor with inductor bars as shown in figure1. The same material M19_24G steel as stator is used in rotor. The inductor bar is fitted in the rotor which is made of aluminium material as shown in figure 3.5.

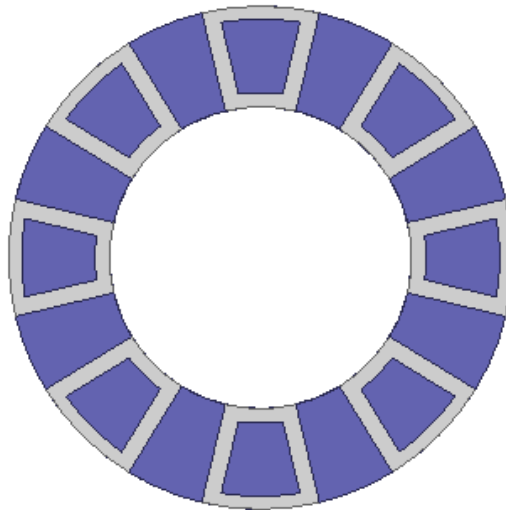


Fig.3.4: Rotor with Inductor bars

3.2 Design of Axial-flux machine

The research conducted on the axial-flux permanent magnet synchronous motor (AFPMSM) with double sided rotor slotted stator configuration using toroidal windings. This type of machine is also called as torus configuration. The exploded view of the machine is shown in figure 3.6. The double-sided rotor which covered stator and other parts of the motor. The magnets are fitted inside the rotor. The different 3-D views of AFPMSM displayed in figure 3.7.

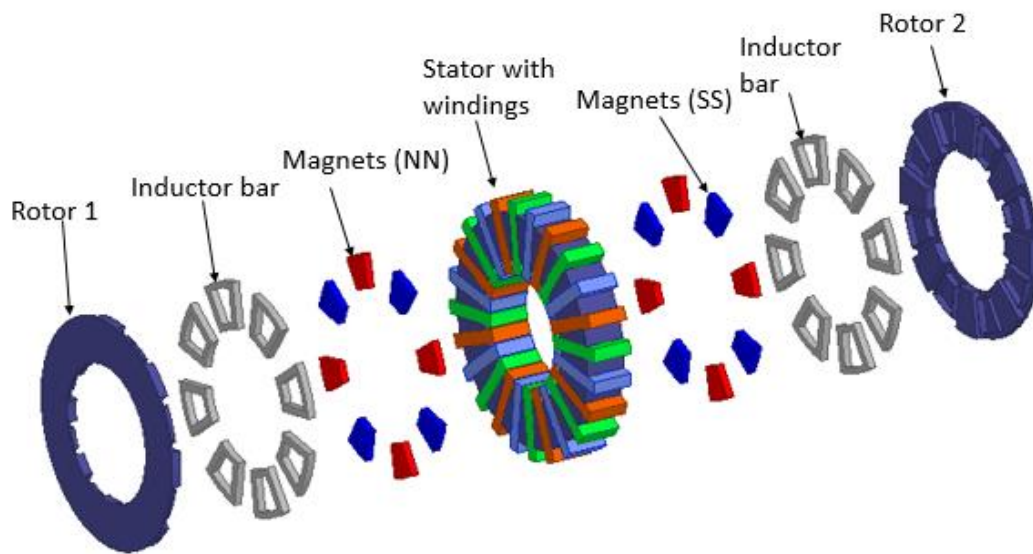


Fig.3.5: Exploded view of Axial-flux synchronous motor

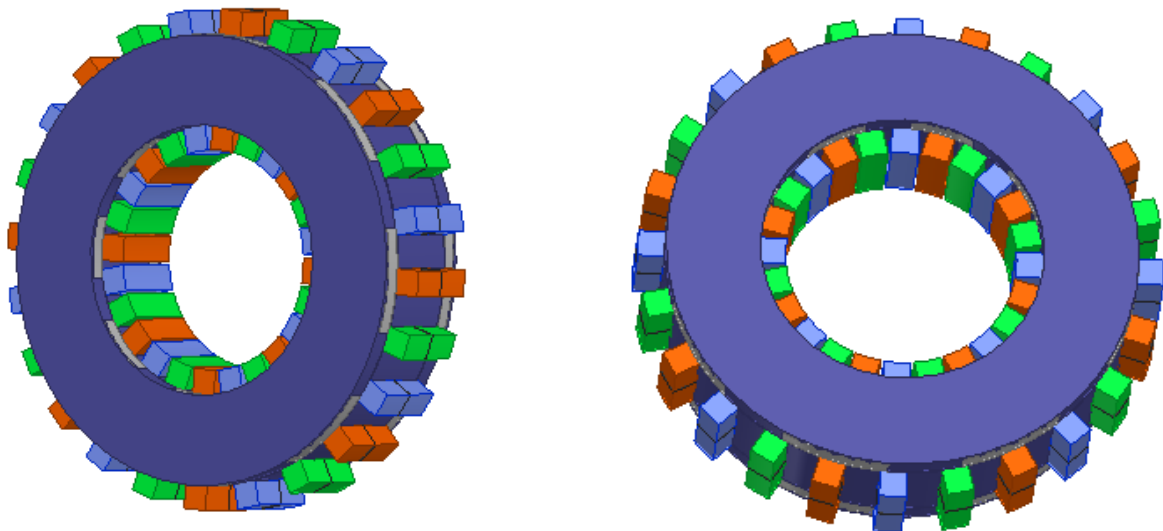


Fig.3.6: Diffrent 3-D views of AFPMSM

Here, the magnets are design as arc shape with colour red for north pole and blue for south pole. The same colour is used for phase as induction motor which is wound around the stator.

3.3 Machine arrangement of Axial-flux machine

There are mainly four different types of arrangement has done as per different application, size of motor, cost and many other specified parameters of motor.

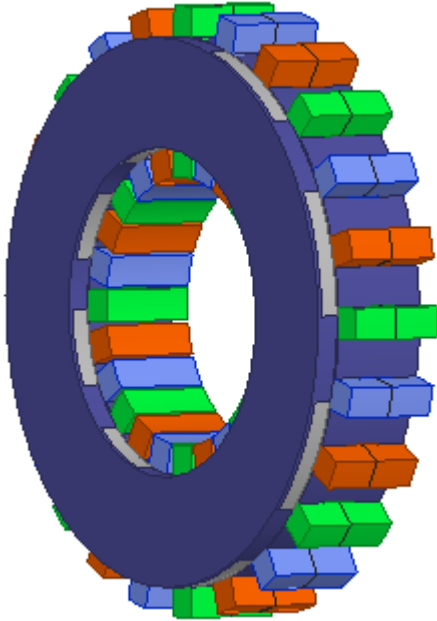


Fig.3.7: Single stator, single rotor

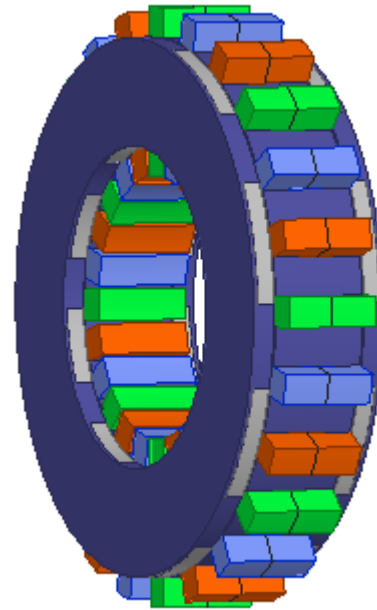


Fig.3.8: Single stator, double rotor (SSDR)

Fig 3.8 and 3.9 illustrate two machine arrangements of the AFPMSM one is single stator, single rotor (SSSR) and other is single stator, double rotor (SSDR). The other two types are double stator, single rotor (DSSR) and multistage of stator and rotor. This project mainly focuses on the single stator, double rotor which is also called as TORUS type. This configuration is used for both induction motor and AFPMSM.

3.4 Stator configuration for LSAFPMSM

The stator configuration of induction motor and LSAFPMSM is same with dimension. It has slotted stator with 24 slots. The stator diameter can be change according to the application of motor. In this project, the stator diameter is same as rotor diameter as shown in figure 3.10.

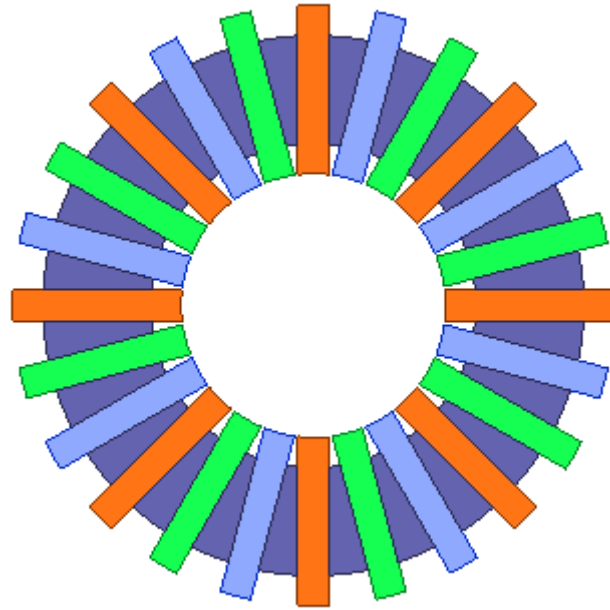


Fig.3.9: Stator of LSAFPMSM with windings

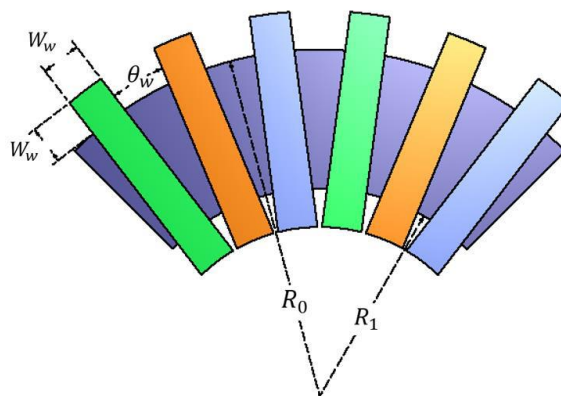


Fig.3.10: Stator dimension

3.4.1 Windings of Stator

The copper material is used for winding of stator. The I^2R losses is consider for the windings. The blue, red and green colour are set for three phases. This design has 24 copper winding around the stator. The material properties of copper are described in table 3.2. Three-phase winding diagram of stator is shown in figure 3.11.

Table 3.2: Properties of copper material for rotor

<i>Name</i>	<i>Type</i>	<i>Value</i>	<i>Units</i>
<i>Relative Permeability</i>	Simple	0.999991	B/H
<i>Bulk Conductivity</i>	Simple	580000000	Ω^{-1}/m
<i>Magnetic Coercivity</i>	Vector		-
<i>Magnitude</i>	Vector Mag	0	A/m
<i>Core Loss Model</i>		None	W/m^3
<i>Mass Density</i>	Simple	8933	kg/m^3
<i>Composition</i>		Solid	-

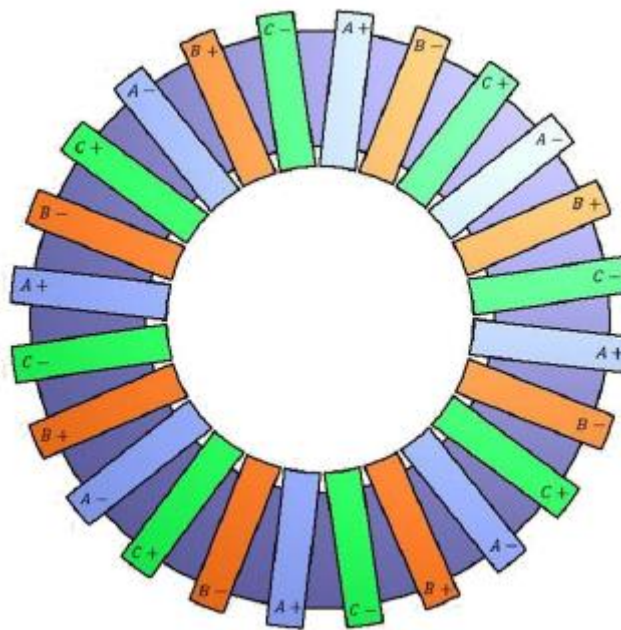


Fig.3.11: 3-phase winding diagram of stator

3.5 Rotor configuration for LSAFPMSM

The rotor configuration of the LSAFPMSM is shown in figure 3.13. The rotor design of LSAFPMSM have different than induction motor. The rotor of LSAFPMSM consists permanent magnet. The inductor bar are fitted in rotor. The arc shape of magnets are also fitted in rotor as colour blue for north pole and red for south pole. The double sided rotor is used for this design and analyses is done in the results chapter. The outer radius 150mm and inner radius 90mm is chosen. The thickness of rotor is 2.5mm. Mainly the three different type of inductor design is analysed for LSAFPMSM.

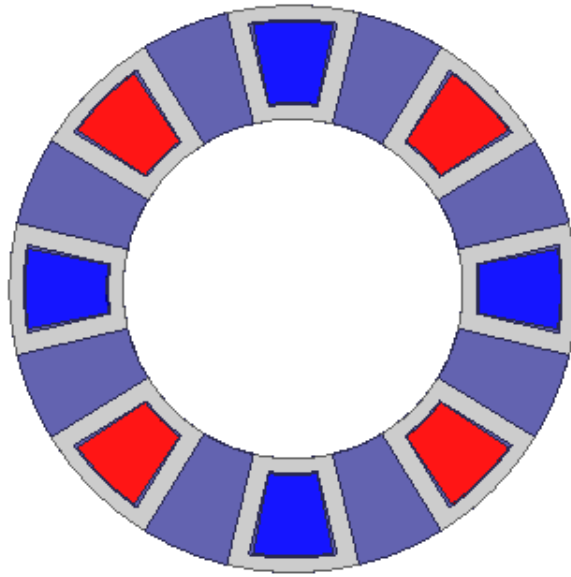


Fig.3.12: Rotor of LSAFPMSM with magnets

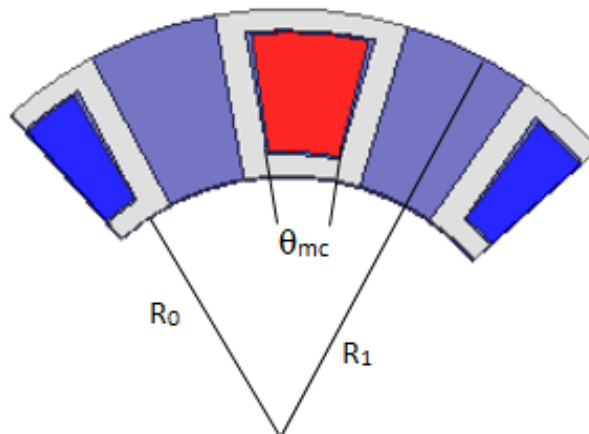


Fig.3.13: Rotor dimension

3.5.1 Design of Inductor bar

The inductor bars are fitted in the rotor as shown in figure 3.13. In this project three types of inductor bar design are analysed. The motor is tested with these three-inductor design with aluminium and copper material. The dimension of three inductor is different. The line-start axial flux permanent magnet synchronous motor is tested with three different types of inductor bar. The design and dimension of these three-inductor bar is different.

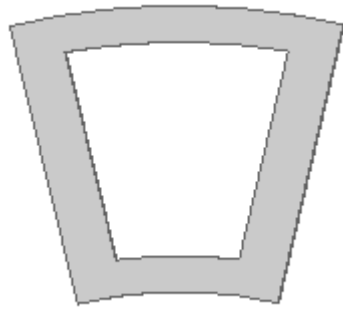


Fig.3.14: Inductor type 1

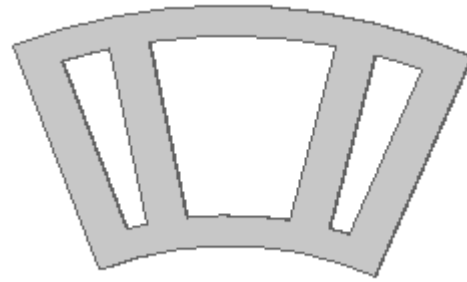


Fig.3.15: Inductor type 2

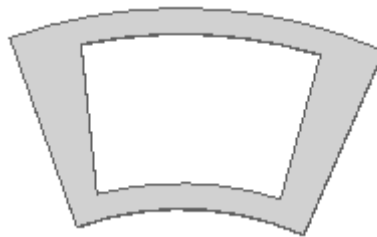


Fig.3.16 Inductor type 3

Fig 3.15-3.17 illustrate three different design of the inductor bars. Type 1 inductor bar is same size from the sides. Type 2 has double inductor bar and type 3 enclosed whole outer part of the rotor. The three inductors with rotor is shown in following figures.

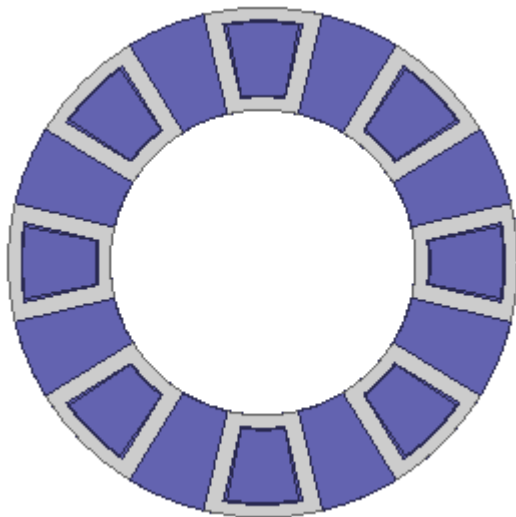


Fig.3.17: Inductor type 1 with rotor

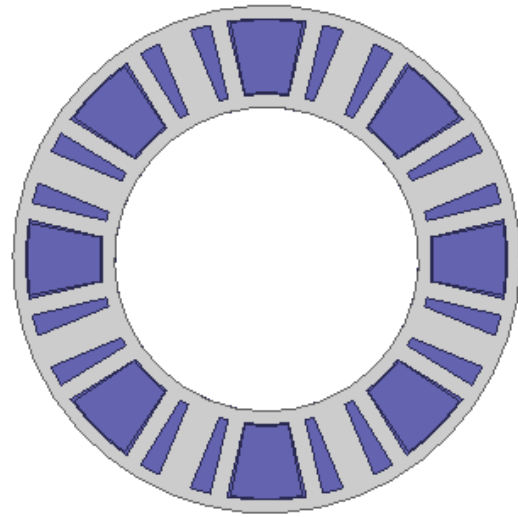


Fig.3.18: Inductor type 2 with rotor

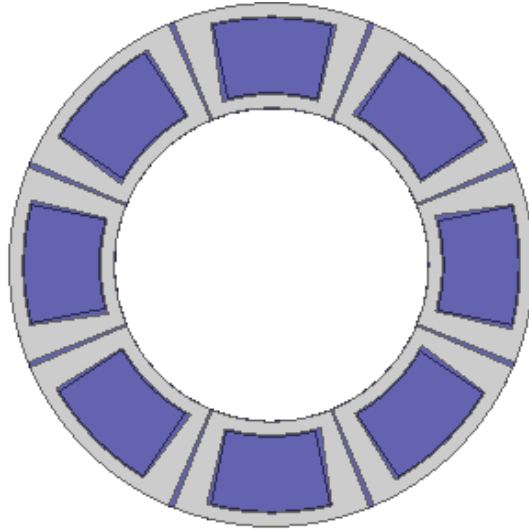


Fig.3.19: Inductor type 3 with rotor

Normally, the inductor bars are made from aluminium material. So, the eddy current losses are major concern for the motor which is the reason of low efficiency and larger losses of motor. In this project, copper material is also used for inductor bar. The properties of both material are shown in following tables.

Table 3.3: Properties of aluminium material for inductor

<i>Name</i>	Type	Value	Units
<i>Relative Permeability</i>	Simple	1.000021	<i>B/H</i>
<i>Bulk Conductivity</i>	Simple	38000000	Ω^{-1}/m
<i>Magnetic Coercivity</i>	Vector		-
<i>Magnitude</i>	Vector Mag	0	<i>A/m</i>
<i>Core Loss Model</i>		None	<i>W/m³</i>
<i>Mass Density</i>	Simple	2689	<i>kg/m³</i>
<i>Composition</i>		Solid	-

Table 3.4: Properties of copper material for inductor

<i>Name</i>	Type	Value	Units
<i>Relative Permeability</i>	Simple	0.999991	<i>B/H</i>
<i>Bulk Conductivity</i>	Simple	58000000	Ω^{-1}/m
<i>Magnetic Coercivity</i>	Vector		-
<i>Magnitude</i>	Vector Mag	0	<i>A/m</i>
<i>Core Loss Model</i>		None	<i>W/m³</i>
<i>Mass Density</i>	Simple	8933	<i>kg/m³</i>
<i>Composition</i>		Solid	-

3.5.2 Shape of magnets

The shape of the magnet is arc type used for AFPMSM. The N36Z_20 material is used for magnets with relative permeability of 1.03. This type of magnet is easily available. Thickness of magnet is 10mm with axial length of 43.06mm. The dimension of the magnet is changed for all three types of inductor.

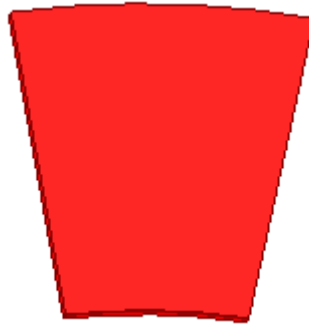


Fig.3.20: Magnet shape

Table 3.5: Properties of N36Z_20 material for magnets

<i>Name</i>	Type	Value	Units
<i>Relative Permeability</i>	Simple	1.03	B/H
<i>Bulk Conductivity</i>	Simple	620000	Ω^{-1}/m
<i>Magnetic Coercivity</i>	Vector		-
<i>Magnitude</i>	Vector Mag	-920000	A/m
<i>X – Component</i>	Unit Vector	1	-
<i>Y – Component</i>	Unit Vector	0	-
<i>Z – Component</i>	Unit Vector	0	-
<i>Core Loss Model</i>		None	W/m^3
<i>Mass Density</i>	Simple	0	kg/m^3
<i>Composition</i>		Solid	-

3.6 Electrical Steel

The electrical steel material M19_29G is assigned to the stator and rotor cores. It has 7650 kg/m³ mass density with stacking factor of 0.92. Here, letter M indicates magnetic material. The magnetic properties of steel are same in all direction. The 19 number indicate grade of core loss of non-oriented steel. The 29G indicates thickness of laminated steel. The properties of electrical steel M19_29G are listed in table 3.6 and the B-H curve is shown in figure 3.21.

Table 3.6: Properties of M19_29G material (Electrical steel)

<i>Name</i>	Typ e	Valu e	Units
<i>Relative Permeability</i>	Nonlinear		<i>B/H</i>
<i>Bulk Conductivity</i>	Simple	1960000	Ω^{-1}/m
<i>Magnetic Coercivity</i>	Vector		-
<i>Magnitude</i>	Vector Mag	0	<i>A/m</i>
<i>X – Component</i>	Unit Vector	1	-
<i>Y – Component</i>	Unit Vector	0	-
<i>Z – Component</i>	Unit Vector	0	-
<i>Core Loss Model</i>		Electrical Steel	<i>W/m³</i>
<i>K_{lh}</i>	Simple	164.2	-
<i>K_{lc}</i>	Simple	0.409	-
<i>K_{le}</i>	Simple	0	-
<i>K_{dc}</i>	Simple	0	-
<i>Mass Density</i>	Simple	7650	<i>kg/m³</i>
<i>Composition</i>		Solid	-

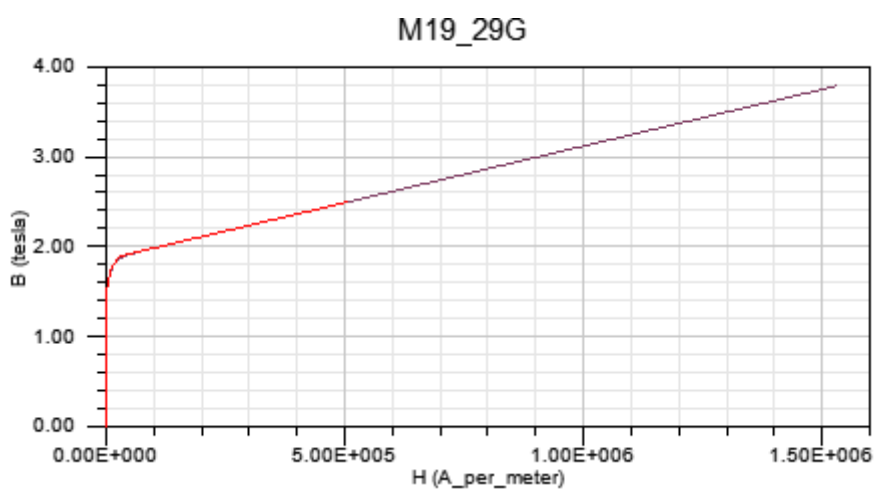


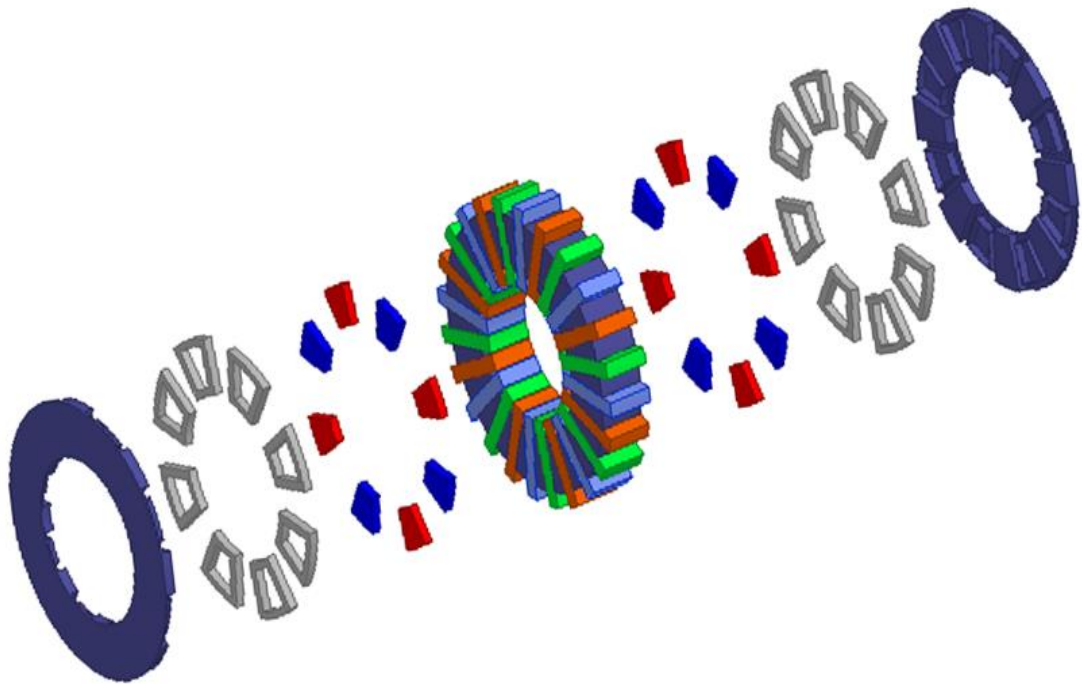
Fig.3.21: B-H curve for M19_29G electrical steel

Table.3.7: Summary of dimensions of LSAFPMSM

All dimension (mm)	Type 1 Inductor model	Type 2 inductor model	Type 3 inductor model
Rotor outer radius	150	150	150
Rotor inner radius	90	90	90
Rotor thickness	2.5	2.5	2.5
Stator outer radius	150	150	150
Stator inner radius	90	90	90
Stator thickness	20	20	20
Inductor axial width	60	60	60
Inductor length	70.6	117.8	114.5
Inductor thickness	10	10	10
Magnet axial width	43.06	43.06	43.06
Magnet length	42.5	42.5	68.5
Magnet thickness	10	10	10

Finally, all the above design of Line-start axial flux permanent magnet synchronous motor is finalised for the simulation and testing. The simulation of three models of LSAFPMSM are described in next chapter with different analysing process.

Chapter 4: Method of Simulation



4.1 Simulation using Maxwell 3D FEA

In this project, ANSYS Maxwell 3D finite element analysis software is used for simulation of different electrical operation such as magnetostatic analysis and transient analysis of the machine. The main advantage of Maxwell 3D is the better and accurate results as compared to Maxwell 2D. In Maxwell 3D, the Z-axis is also considered which is not present in Maxwell 2D. The Maxwell 2D takes less time to simulate the machine. While, the Maxwell 3D has 3D geometry which is complex than 2D design. The simulation time of the machine is increased in Maxwell 3D due to many elements of machine.

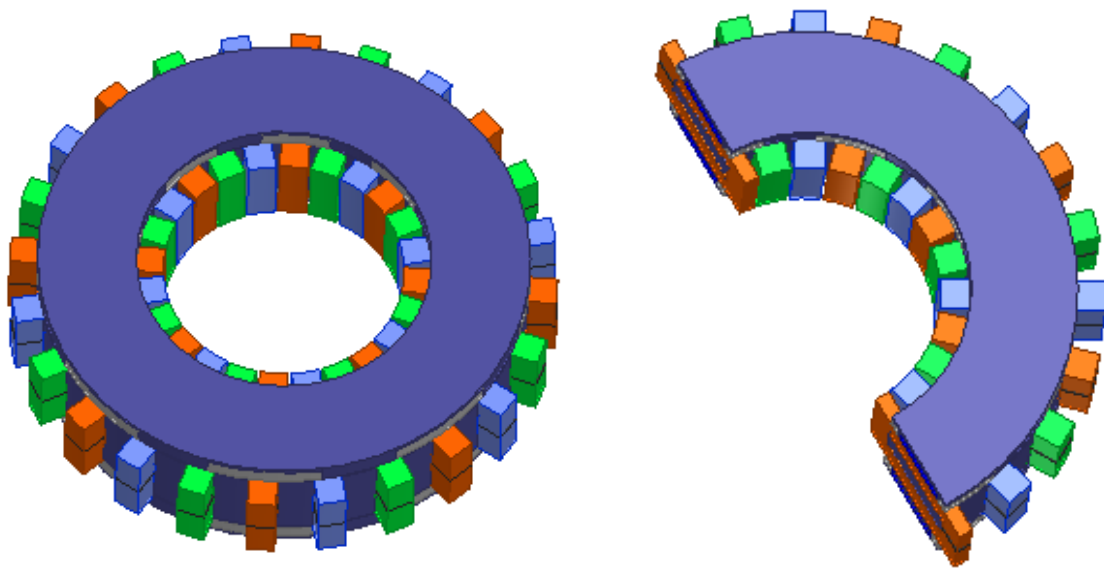


Fig.4.1: Maxwell 3D model of motor

The area of machine is divided in small element in Finite element analysis. First, the 3D element is divided for the mashing process of machine. Mashing is very important for the accuracy of the obtained results. The Maxwell software provide the wide range of mashing operation to improve the accuracy of the machine. After the mashing process, the results of all simulation element are combined to simulate the overall system response.

First, the induction motor is designed and analysed for no load test. The simulation time is 1.25s with time step of 0.002s is set in the software. After that, the motion is applied to the motor. The mesh is applied in different parts of motor. The same procedure is applied for different design of line start axil flux permanent magnet synchronous motor. The simulation time and step time is same for this motor as induction motor. The magnetostatic analysis is performed for all motor which shows the magnetic flux density of the motor. The transient analysis is computed which is described in the result chapter.

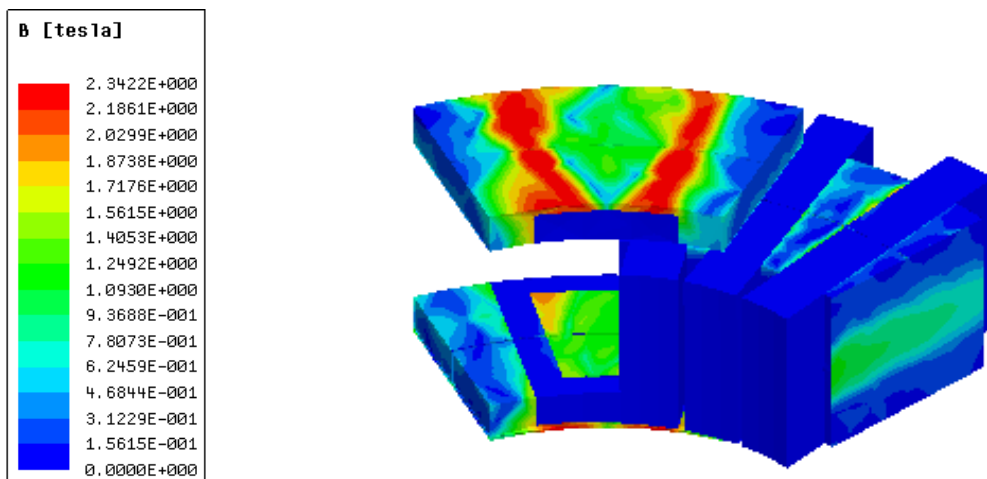
4.2 Magnetostatic Analysis

This is the first stage of analysis of machine in ANSYS Maxwell. To obtain the magnetic circuit of machine, the magnetostatic analysis is used. After performing this analysis, it shows the magnetise area of core saturation which is used to improve the magnetic path of the machine design. This process is applied for all the designed models to see the magnetic performance of the different models.

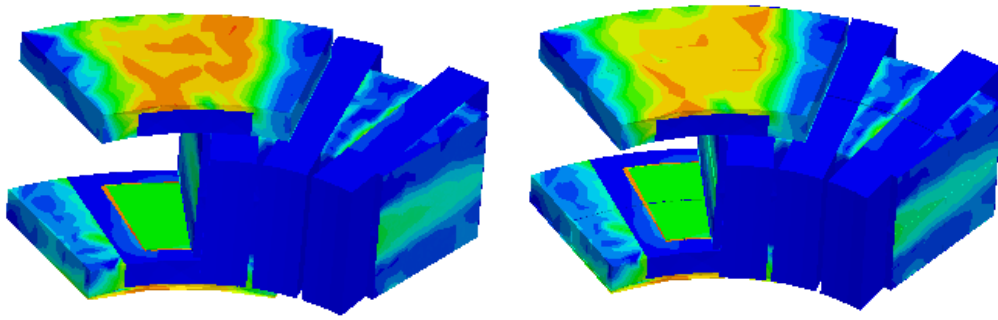
The magnetostatic analysis is performed under no load condition and under load 2Nm condition. There is no magnetic flux created by winding at no load condition. In under load condition, the 2Nm mechanical load is applied to the machine and the magnetic analysis is obtained for under load condition.

The magnetic field shows the behaviour of magnetic circuit which is flowing to entire machine at the given time. The flux density is obtained at the different parts of the machine at given degree and time. It also displays the change of flux density of rotating machine. The flux line is also presented in the different parts of machine.

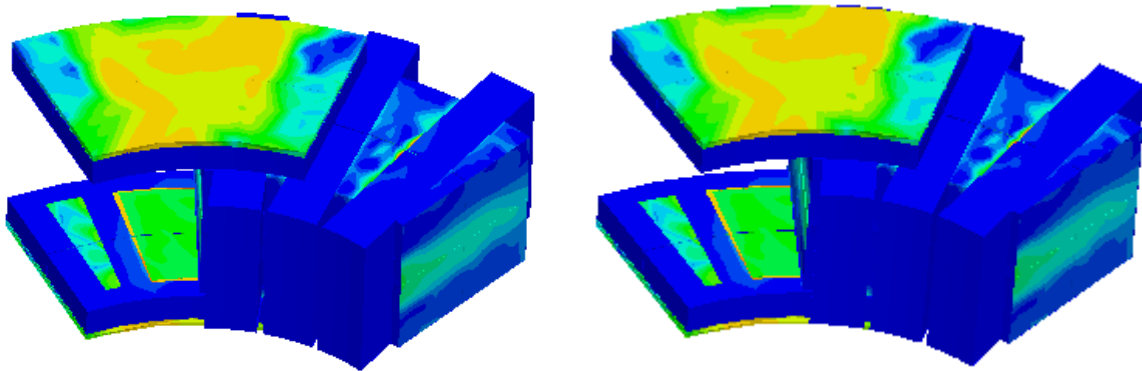
The following figure shows the flux density for no load and 2Nm load condition of all designed models.



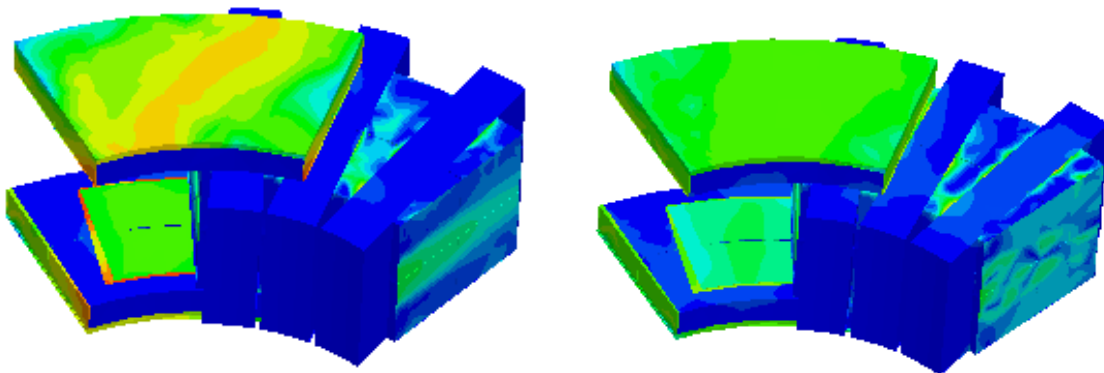
(a) Induction motor



(b) LSAFPMSM tyep 1 inductor (left) Aluminium (right) copper material

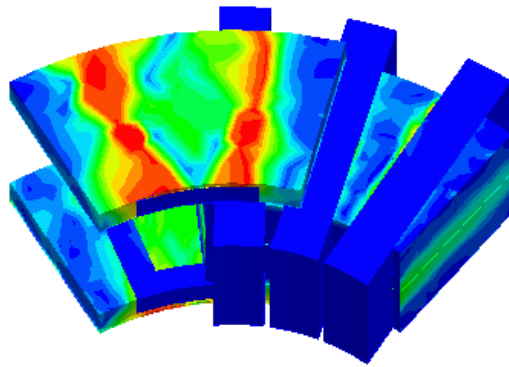
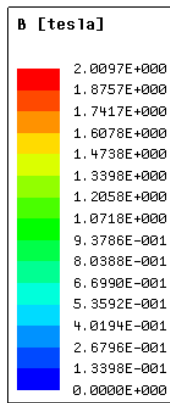


(c) LSAFPMSM tyep 2 inductor (left) Aluminium (right) copper material

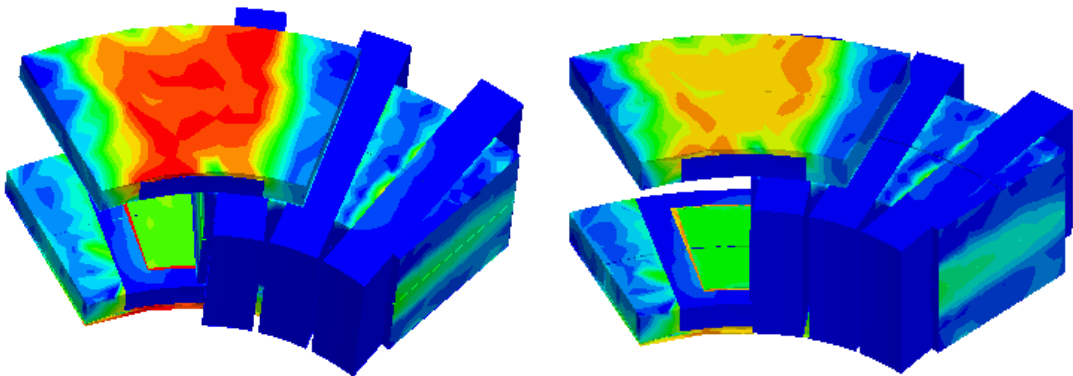


(d) LSAFPMSM tyep 3 inductor (left) Aluminium (right) copper material

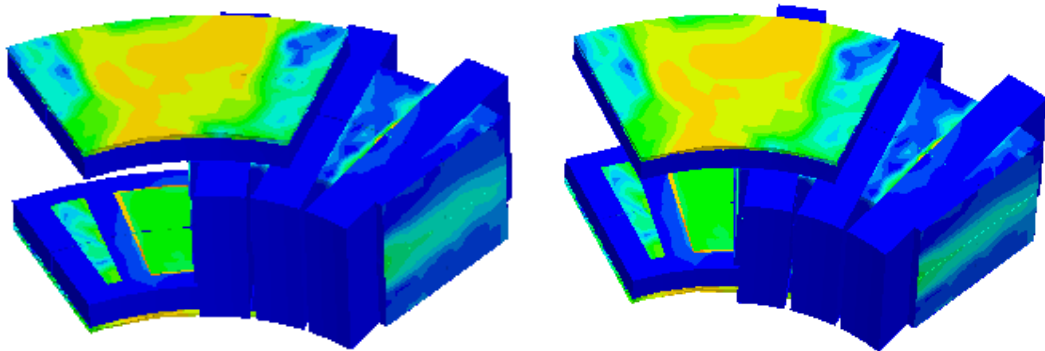
Fig. 4.2: Magnetic flux density of motors at no load



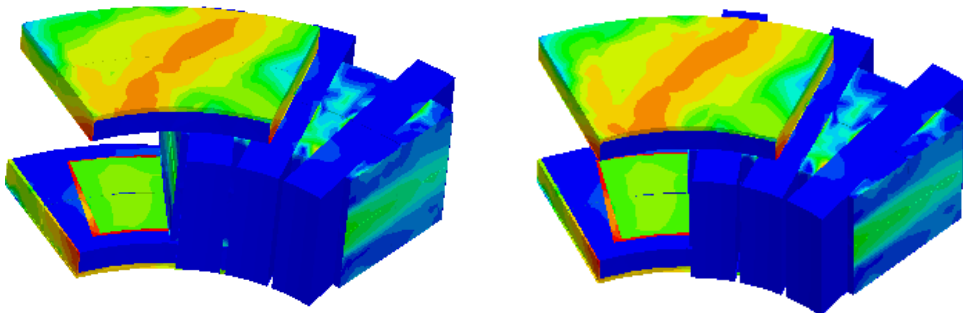
(a) Induction motor



(b) LSAFPMSM type 1 inductor (left) Aluminium (right) copper material



(c) LSAFPMSM type 2 inductor (left) Aluminium (right) copper material

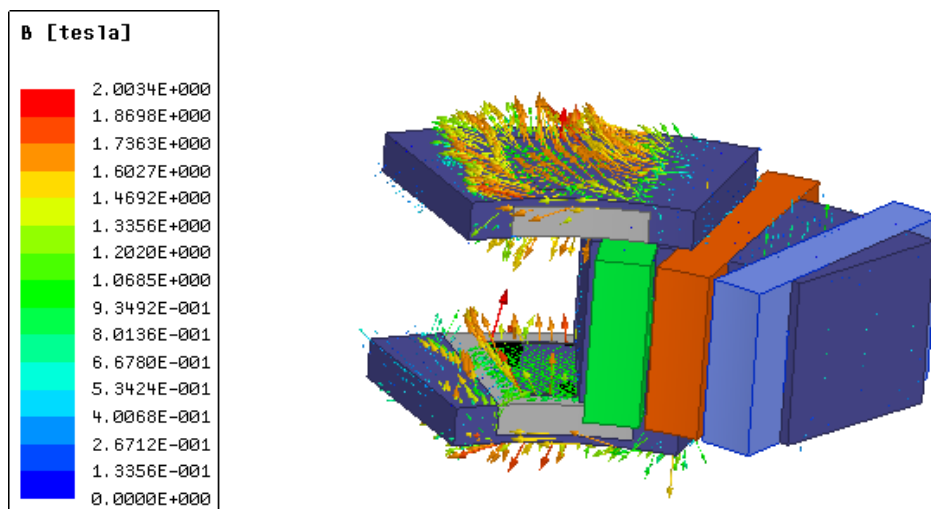


(d) LSAFPMSM type 3 inductor (left) Aluminium (right) copper material

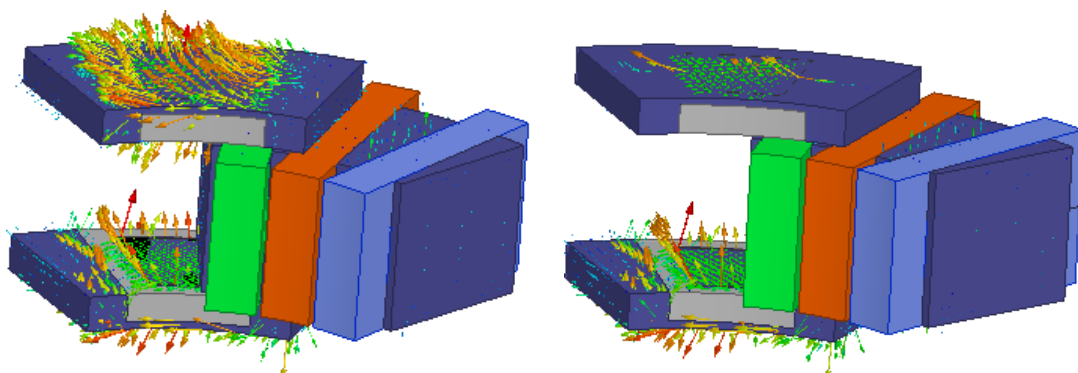
Fig.4.3: Flux density of motors at 2Nm load

The magnetic flux density of all models at no load condition is shown in figure 4.2. The magnetic flux density is high in the core part of stator and rotor of the motor. The flux density is measured in tesla with the range between 0 tesla to 2.34 tesla. Here, the orange and green area indicates the high flux density of rotor and stator while the blue area indicated low flux density of stator and rotor. It can be noticed that, the LSAFPMSM models have more magnetic flux density than the induction motor. Figure 4.3 illustrates the magnetic flux density at 2Nm under load condition. LSAFPMSM have better flux density at given load condition. The range of flux density for 2Nm load is 0 to 2 tesla. The rotor has high saturation for LSAFPMSM models at 2Nm load.

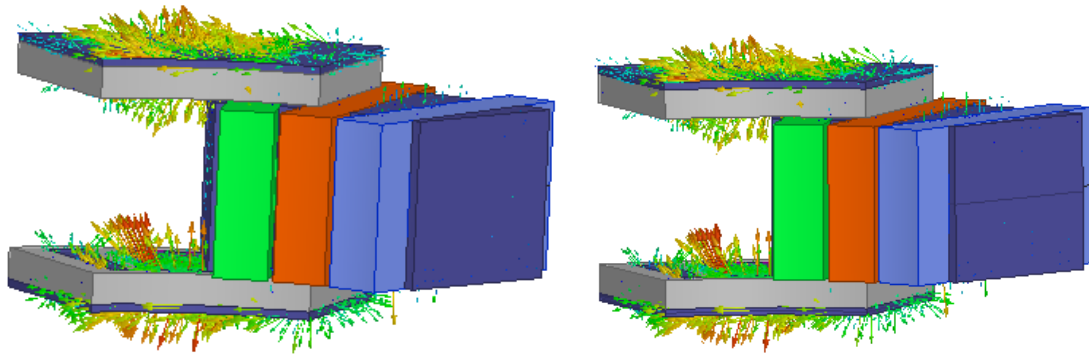
Now, the next step is to plot the magnetic flux vector for all model. Using the flux vector, the intensity of flux can be identified in the all parts of the motor. The flux vector is obtained for no load and for 2Nm load. The following figure 4.4 represents the magnetic flux vector at no load and 2Nm load condition.



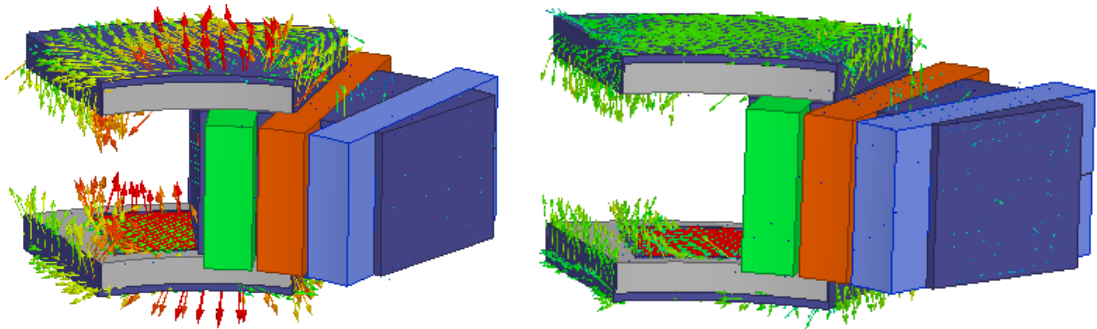
(a) Induction motor



(b) LSAFPMSM type 1 inductor (left) Aluminium (right) copper material



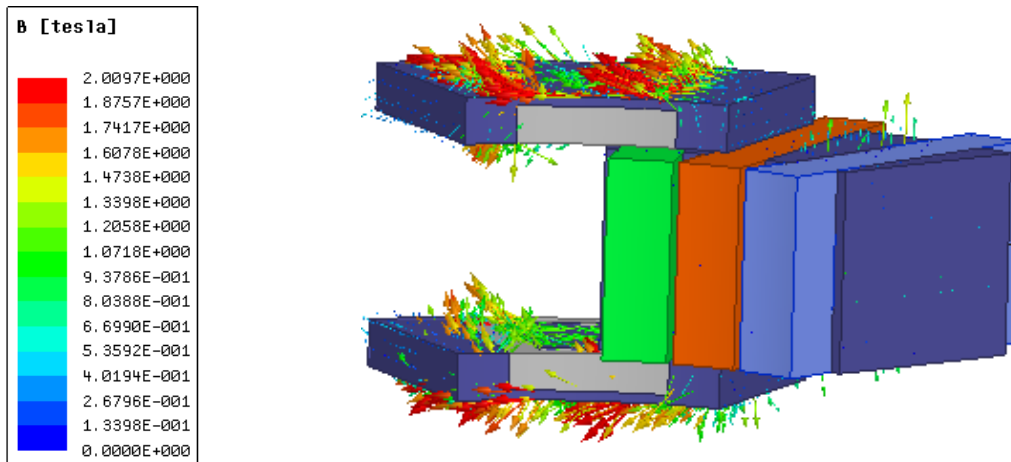
(c) LSAFPMSM tyep 2 inductor (left) Aluminium (right) copper material



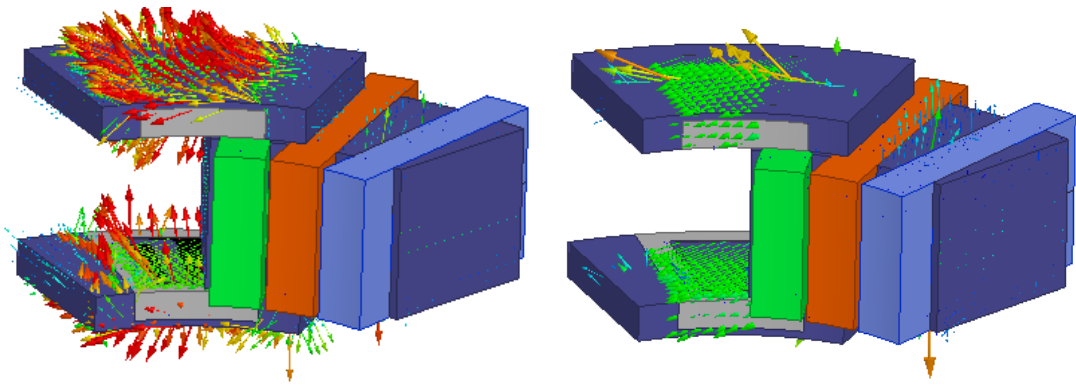
(d) LSAFPMSM tyep 3 inductor (left) Aluminium (right) copper material

Fig.4.4: Magnetic flux vector of motors at no load

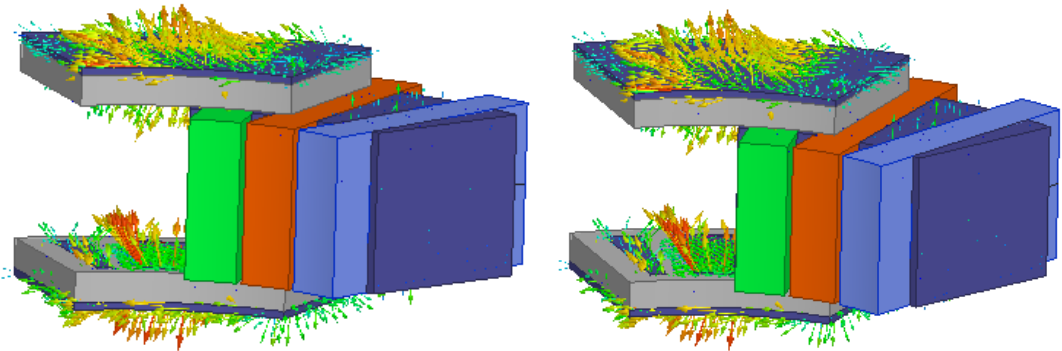
The magnetic flux vector for 2Nm load is represented in following figure 4.5.



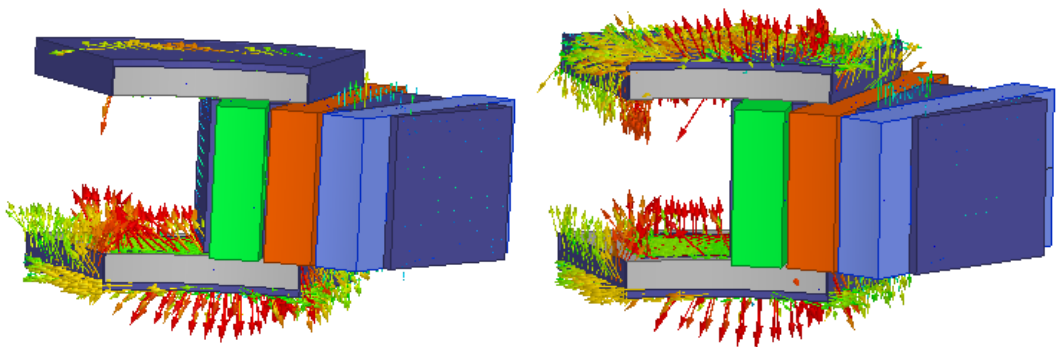
(a) Induction motor



(b) LSAFPMSM type 1 inductor (left) Aluminium (right) copper material



(c) LSAFPMSM type 2 inductor (left) Aluminium (right) copper material



(d) LSAFPMSM type 3 inductor (left) Aluminium (right) copper material

Fig.4.5: Magnetic flux vector of motors at 2Nm load

The figure 4.5 shows the magnetic flux vector at 2Nm load. The magnetic flux vector represent the direction and a magnitude of machine. The magnetic flux vector is used to predict the effect of a magnet on magnetic filed. The orange and green colour shows the high magnetic lux vector on the different parts of motor. The LSAFPMSM have better magnitude and direction of vector as compared to induction motor.

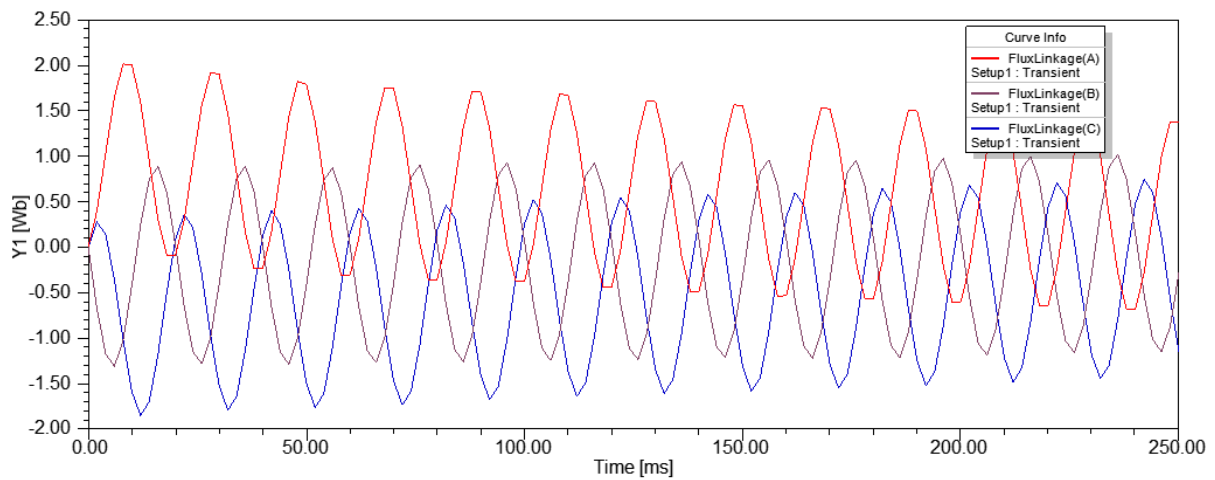
4.3 Magnetostatic Flux Linkage

The magnetic flux linkage used to indicate how much flux is passing through the coils. The induced EMF is proportional to the derivative of flux linkage which is given by the following formula:

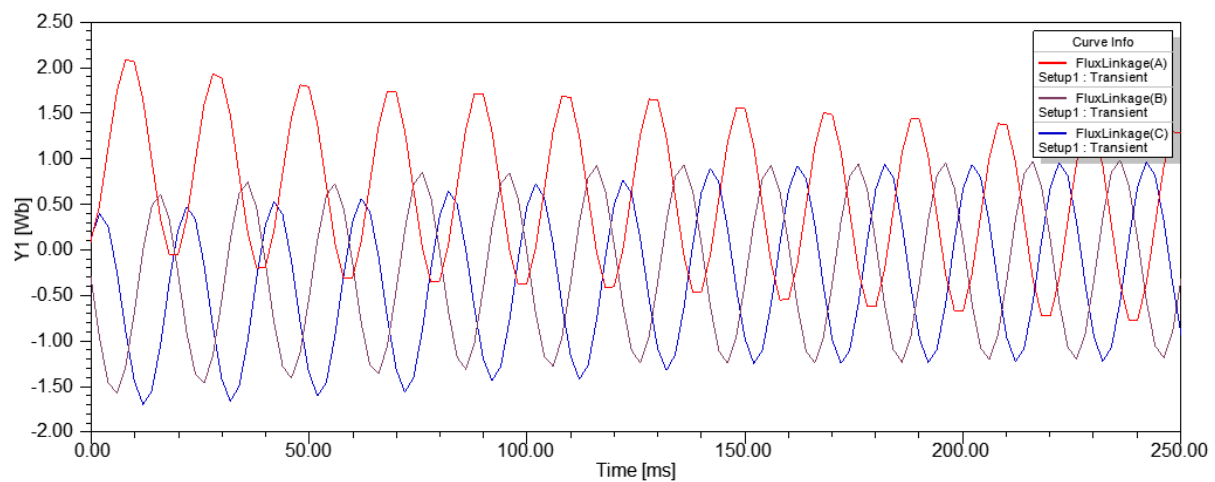
$$e = N \left(\frac{d\phi}{dt} \right)$$

Where, e is the induced EMF. N is the number of turns in coil and ϕ is the flux linkage.

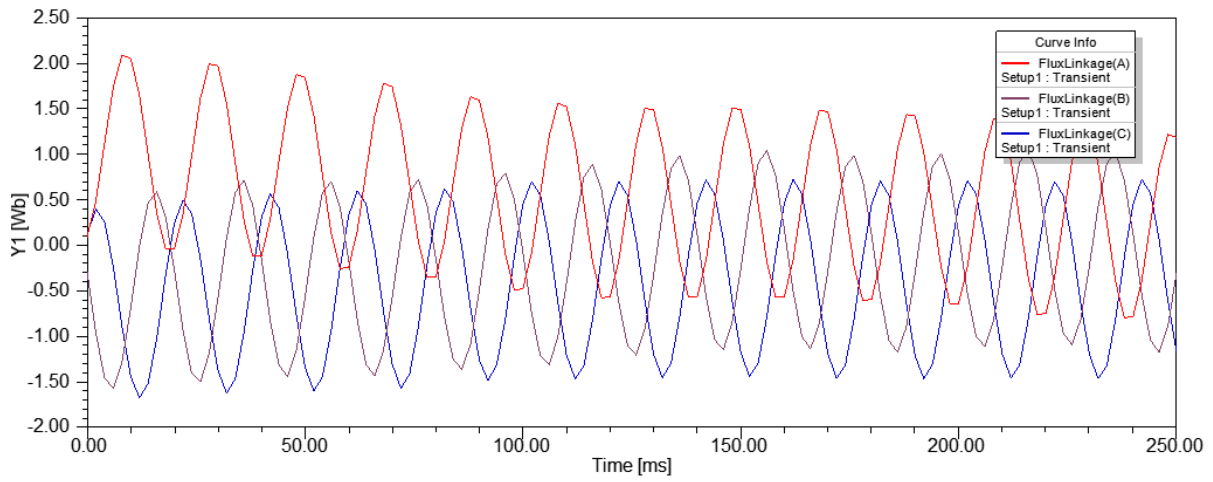
The magnetic flux linkage is obtained for all models at no load and 2Nm load.



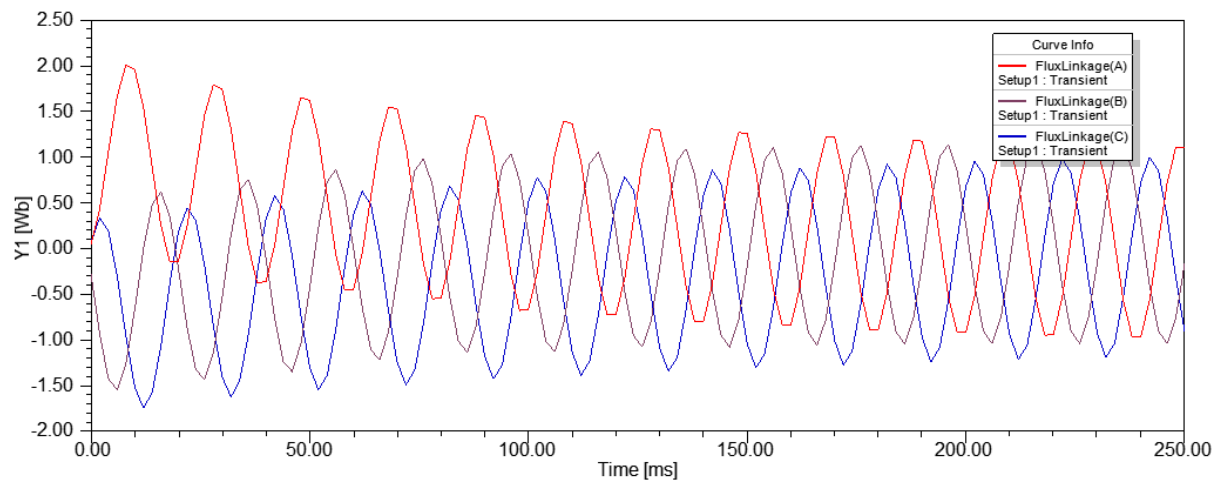
(a) Induction motor at no load



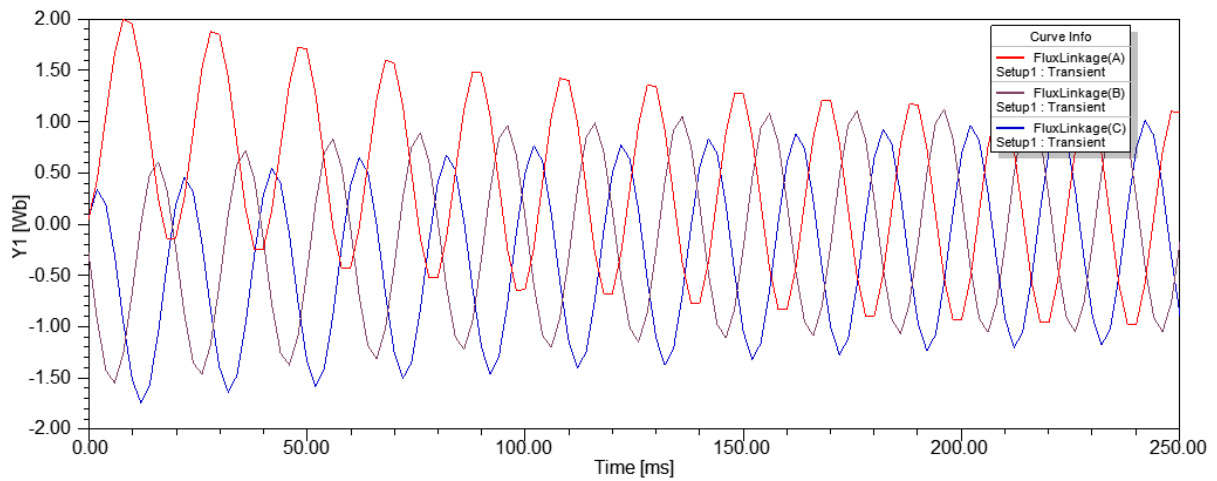
(b) LSAFPMSM type 1 aluminium inductor at no load



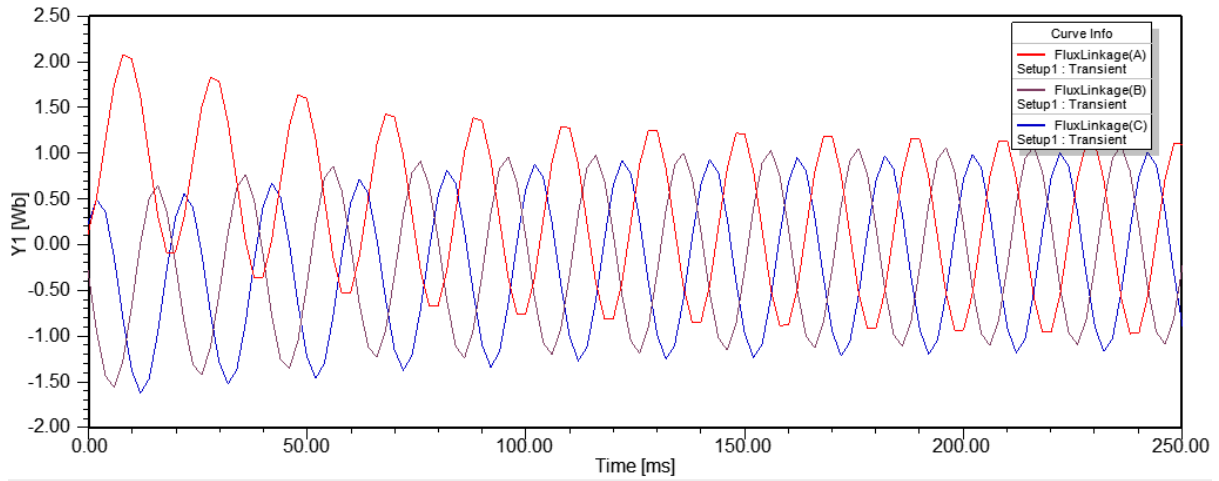
(c) LSAFPMSM type 1 copper inductor at no load



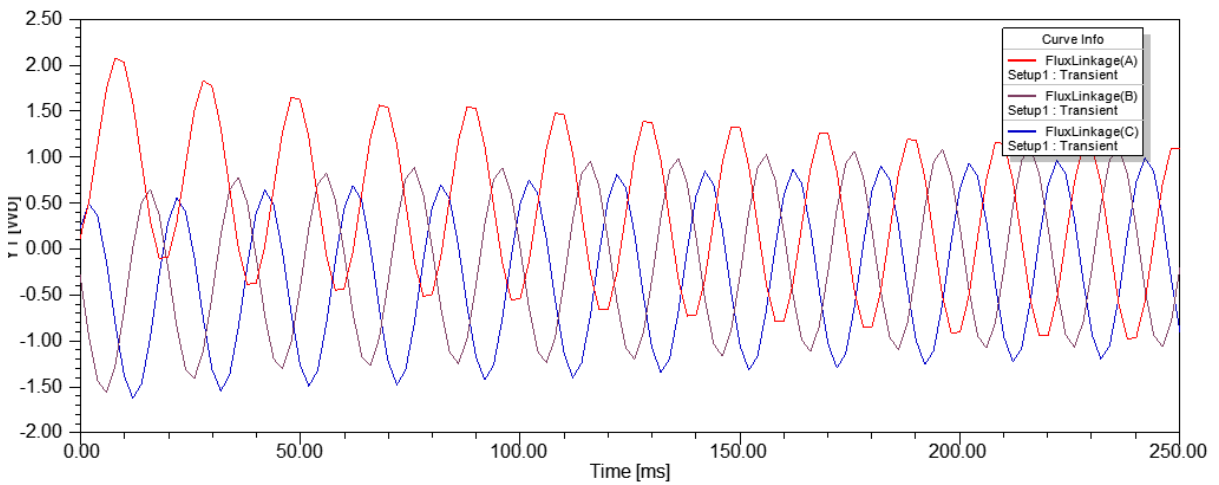
(d) LSAFPMSM type 2 aluminium inductor at no load



(e) LSAFPMSM type 2 copper inductor at no load



(f) LSAFPMSM type 3 aluminium inductor at no load

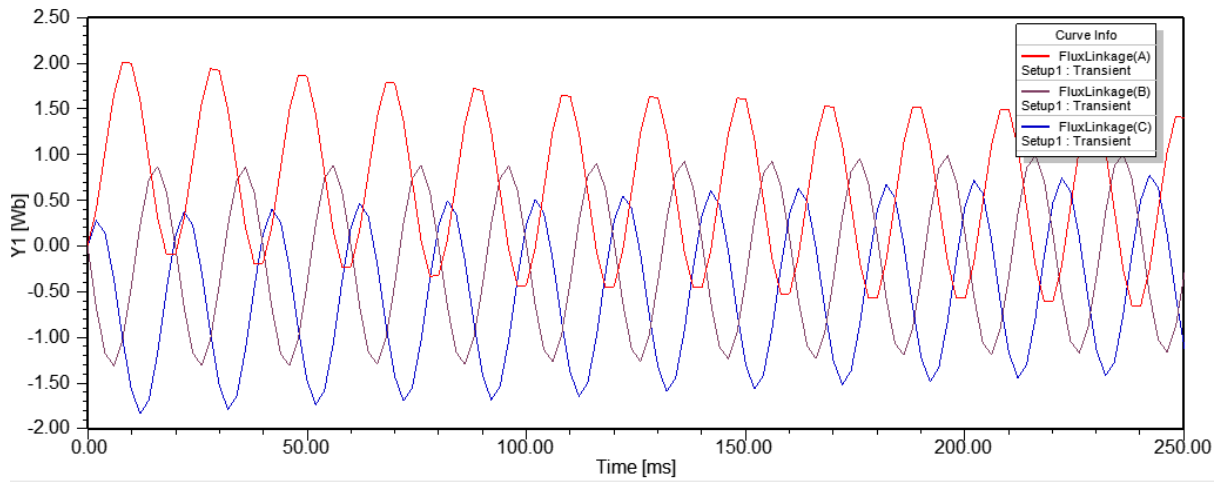


(g) LSAFPMSM type 3 copper inductor at no load

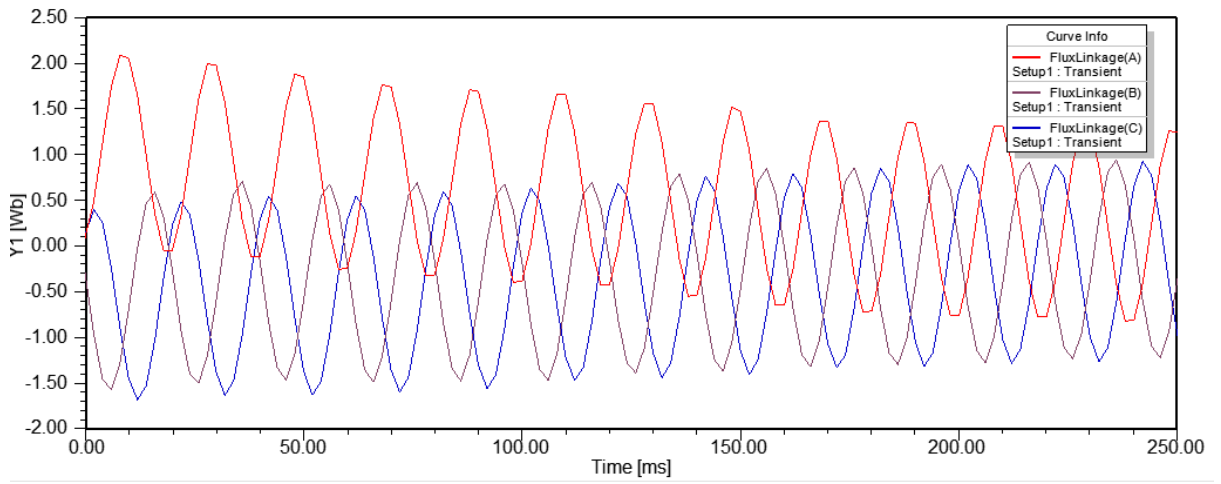
Fig.4.6: Magnetic flux linkage at No load

The above figure 4.6 shows the magnetic flux linkage at no load condition. Three-phase flux linkage is represent using the different colour. The magnetic flux linkage of all motor is sinusoidal. Due to the saturation in the core, the waveform of linkage is fluctuating in the starting condition of machine but after that the waveform get sinusoidal as shown in the results.

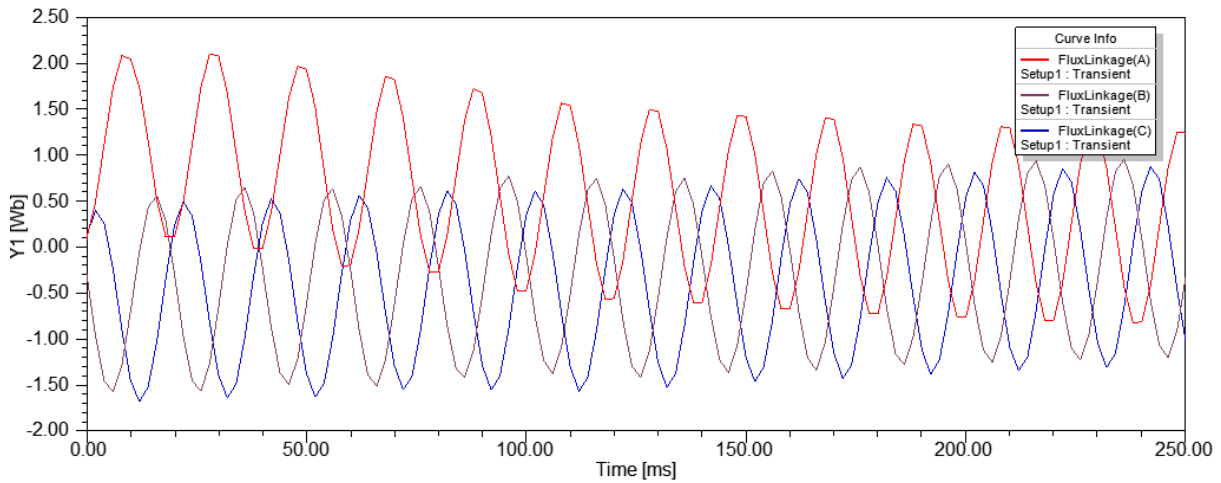
Now, the magnetic flux linkage is tested for the 2Nm load for all machines which is illustrated in the flowing figure.



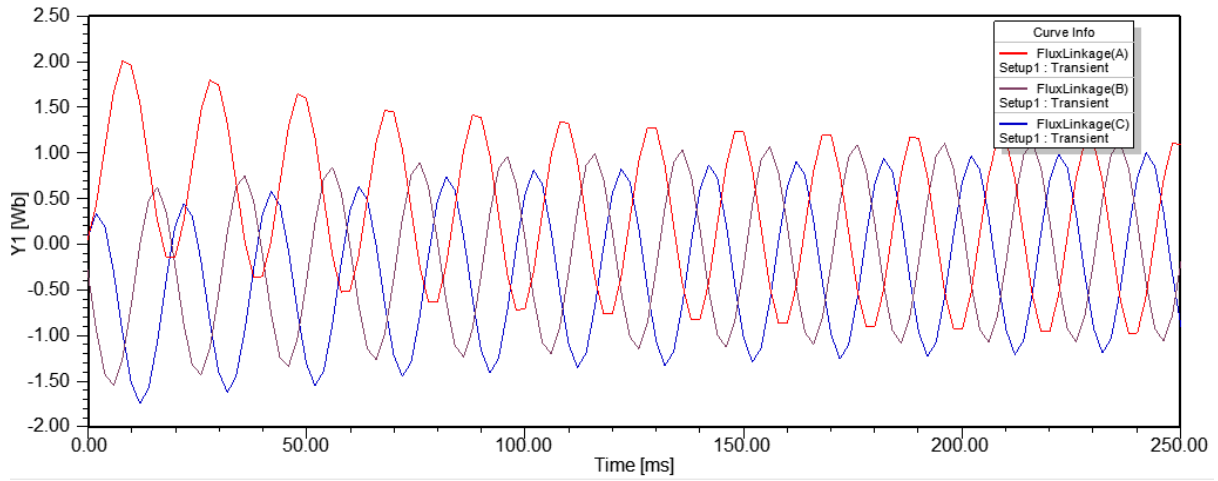
(a) Induction motor at 2Nm load



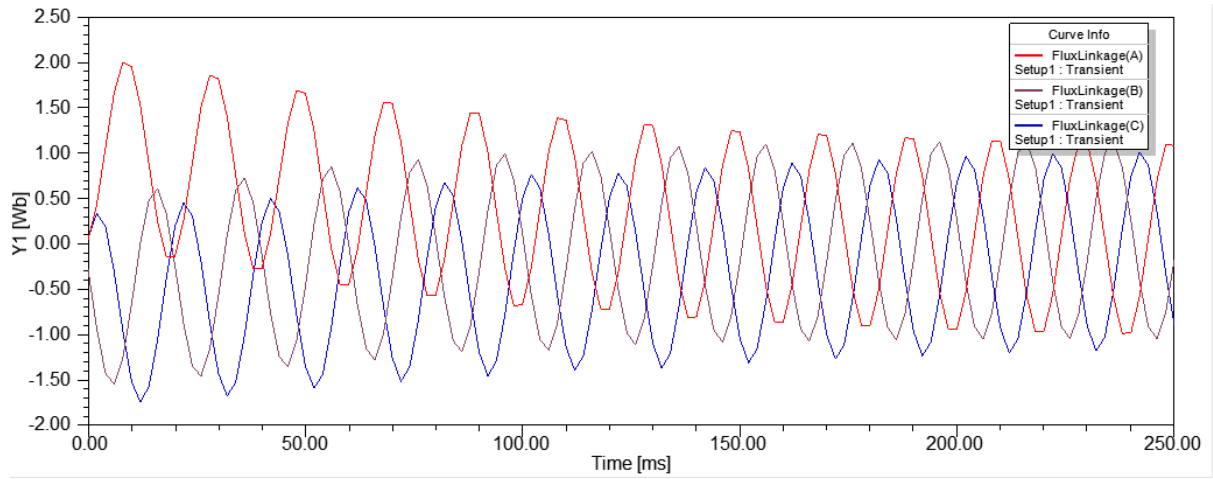
(b) LSAFPMSM type 1 aluminium inductor at 2Nm load



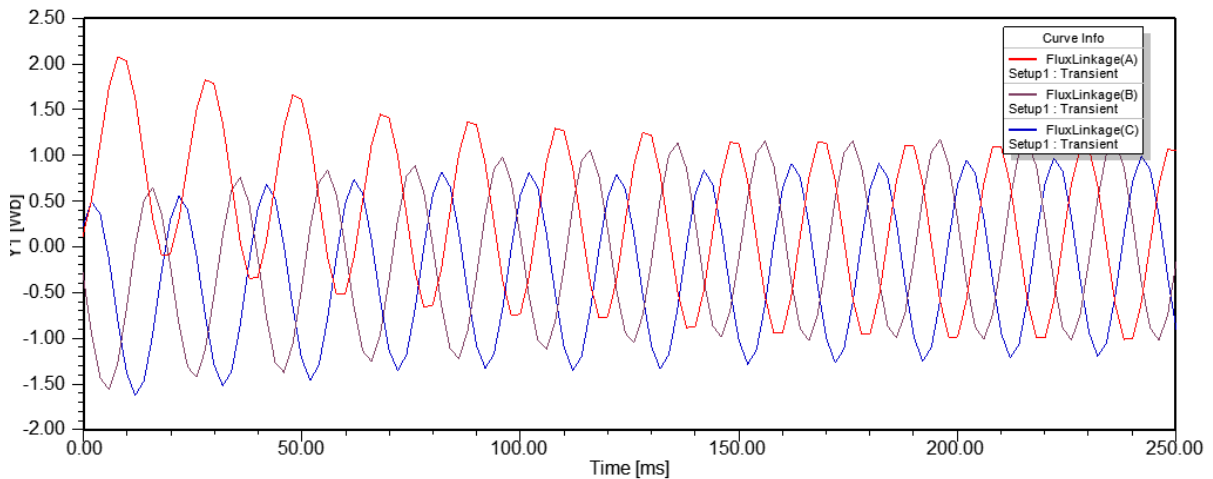
(c) LSAFPMSM type 1 copper inductor at no load



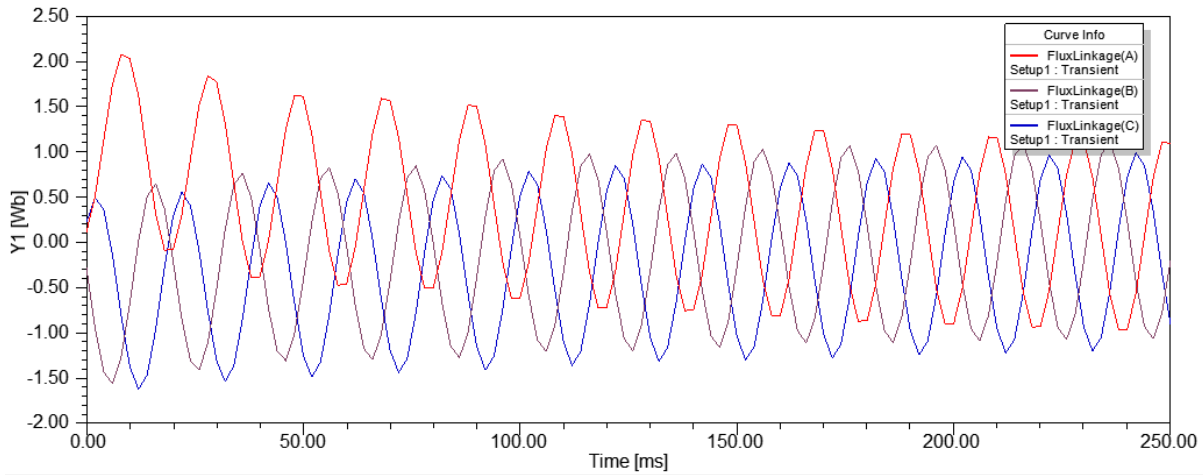
(d) LSAFPMSM type 2 aluminium inductor at 2Nm load



(e) LSAFPMSM type 2 copper inductor at 2Nm load



(f) LSAFPMSM type 3 aluminium inductor at 2Nm load



(g) LSAFPMSM type 3 copper inductor at 2Nm load

Fig.4.7: Magnetic flux linkage at 2Nm load

From the figure 4.7, it can be seen that the magnetic flux linkage at 2Nm load is identical to the no load flux linkage. But, there is small difference in the shape and amplitude of the waveform. During the starting performance of motor there is some fluctuation in the waveform but after that it should be sinusoidal waveform for all machine. One of the reason to increase in core loss is increasing the alternating flux frequency. The adjustment in magnetic flux linkage has directly affect the induced EMF. The expanded frequency and diminished magnitude of the flux linkage is directly relative to expansion in frequency and decrease in the magnitude of EMF.

4.4 Summary of Magnetostatic Analysis

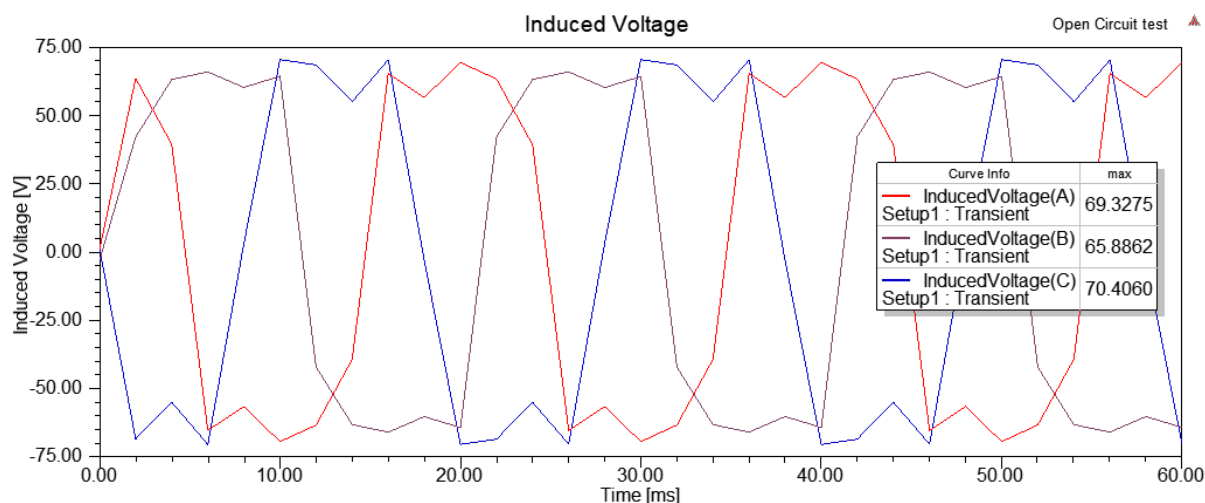
In this section, the magnetostatic analysis is implemented for the all designed machines. The magnetic flux density plot for all machine is achieved. From the flux density plot, the performance of magnetic circuit is carried out in this analysis. The flux density shows the magnetic behaviour of the different parts of machine. The magnetic vector shows the direction and filed of the flux in the machine. The magnetic flux linkage is carried out for all machine, which shows the relation to the EMF of the machines. The flux linkage of all machine has almost same but there is minor difference in the magnitude and shape of waveform. There is also some phase difference of waveform at no load and 2Nm load conditions. But, overall the flux linkage of all machine is sinusoidal. Finally, the magnetostatic analysis is performed for magnetic performance of machine using FEA.

4.5 No load test analysis

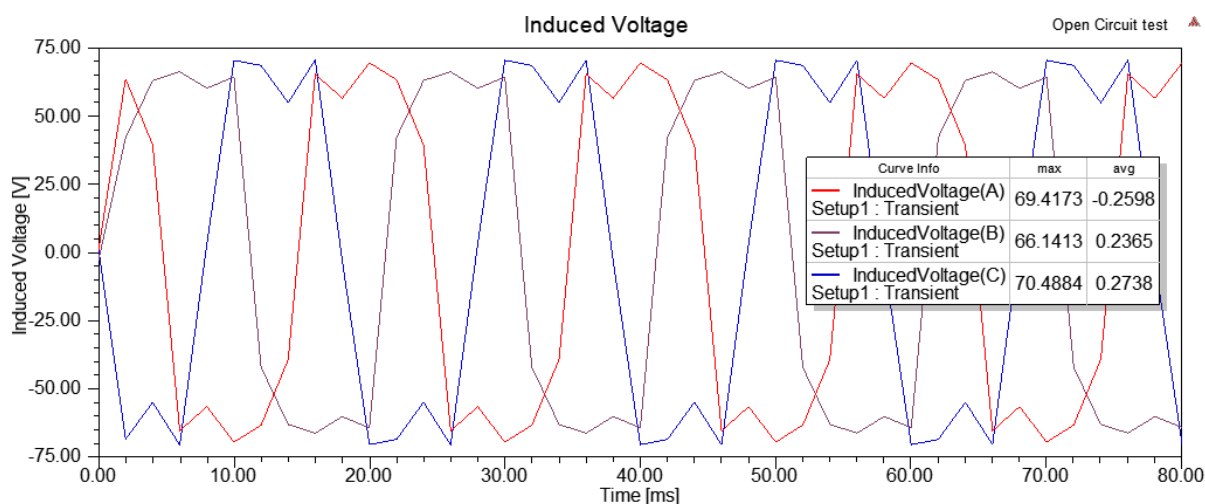
In the open circuit test, the machine is operated on no electrical load. Mostly, the open circuit test is used to measure induced voltage at rated speed.

4.5.1 Induced voltage measurement

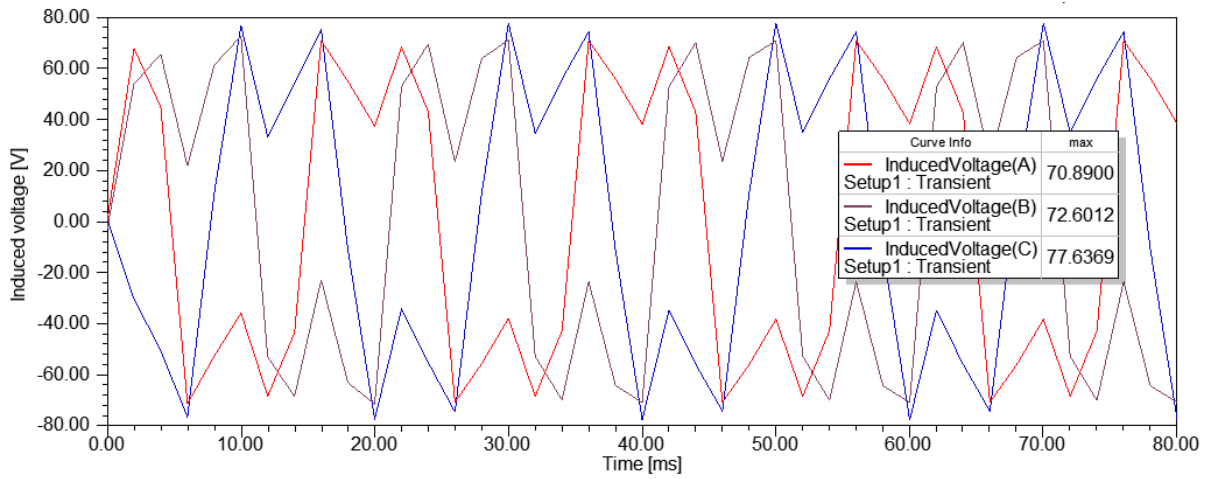
The induced voltage can be measured at rated speed under open circuit test of machine. The induced voltage is obtained by permanent magnets in LSAFPMSM which is measured at rated speed of 750 rpm. There is no excitation given to the stator winding. The induced voltage is measured for 1.25s with time step of 0.002s.



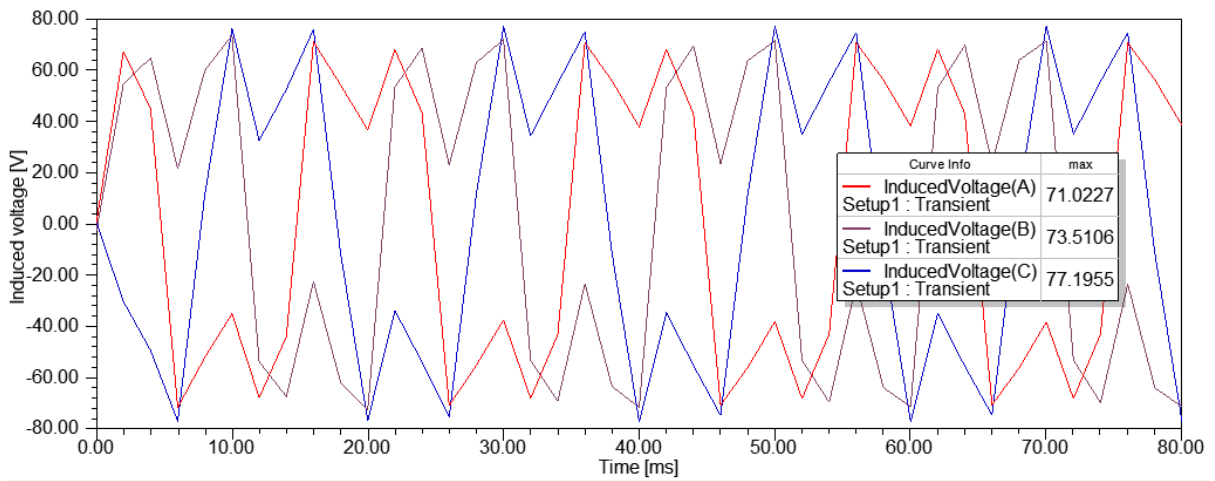
(a) LSAFPMSM type 1 aluminium inductor



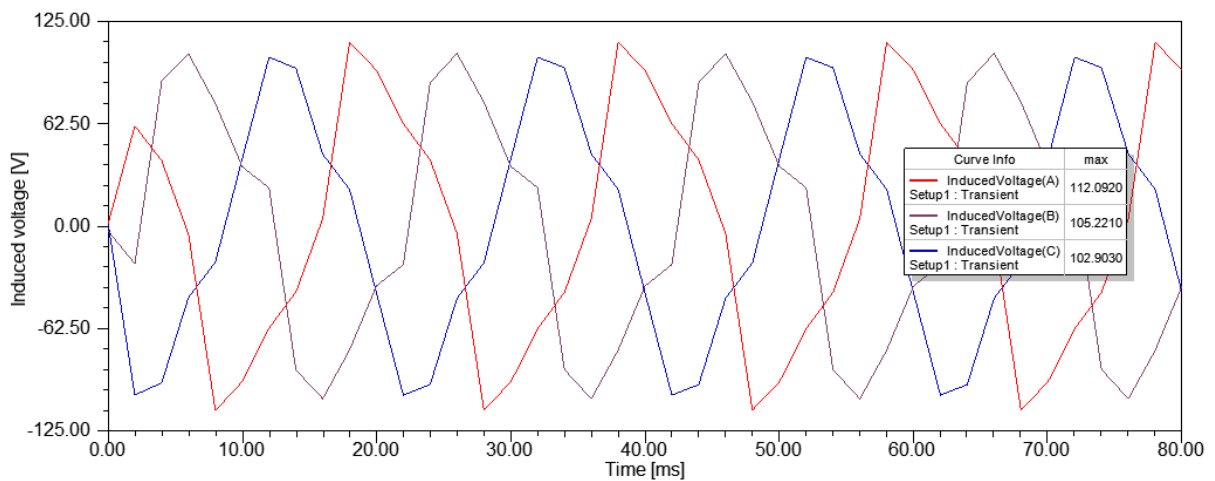
(b) LSAFPMSM type 1 copper inductor



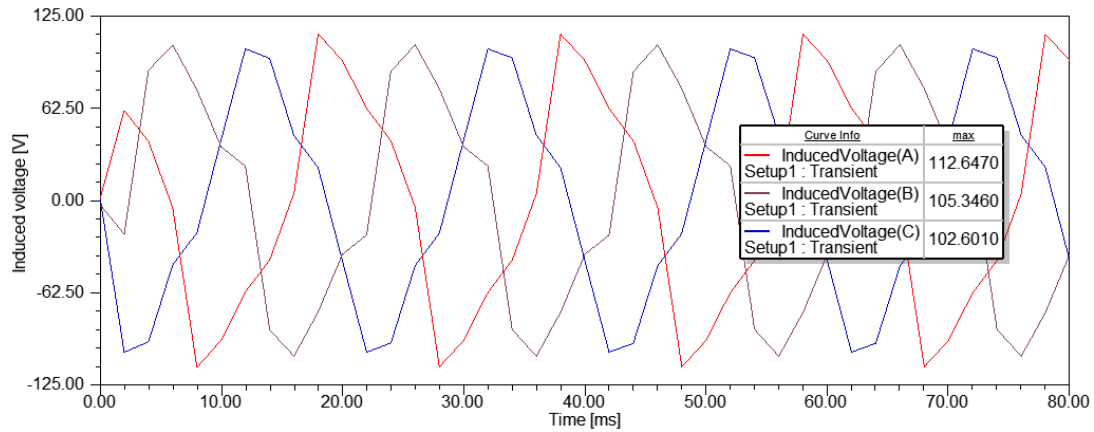
(c) LSAFPMSM type 2 aluminium inductor



(d) LSAFPMSM type 2 copper inductor



(e) LSAFPMSM type 3 aluminium inductor



(f) LSAFPMSM type 3 copper inductor

Fig.4.8: Induced voltage waveform of LSAFPMSM

Figure 4.8 shows the three-phase induced voltage waveform of different model of LSAFPMSM. For better represent the waveform are displayed for first 80ms of total run time with 50Hz frequency. The type 3 inductor model have maximum induced voltage for all three phases as compared to other two models. The table 4.1 shows the summary of peak induced voltage at open circuit test.

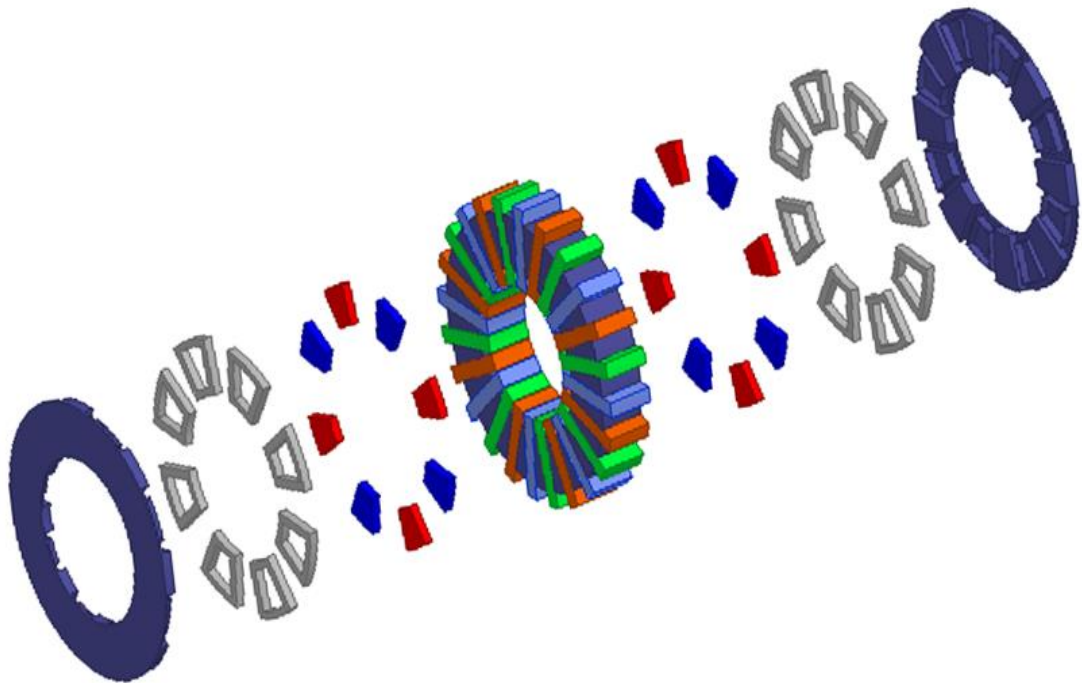
Table.4.1: Summary of peak Induced voltage of Open circuit test

LSAFPMSM Model	Induced voltage (V) Peak value of Phases		
	Phase A	Phase B	Phase C
Type 1 Aluminium inductor	69.32	65.88	70.40
Type 1 copper inductor	69.41	66.14	70.48
Type 2 aluminium inductor	70.8	72.8	77.6
Type 2 copper inductor	71.02	73.51	77.19
Type 3 aluminium inductor	112.09	106.22	102.90
Type 3 copper inductor	112.6	105.34	102.60

4.6 Transient analysis

In the transient analysis, the machine is tested under different loading condition. For this project, the all designed models are tested for no load condition and under load condition at 2Nm. In starting, mechanical load is not given to the machine which means it operate under no load condition. During the no load condition, the motor performance such as speed, current, losses, torque, power rating, efficiency and power factor of the machine is tested. But the efficiency at no load condition is always zero. The next step, 2Nm mechanical load is applied to machine and the same motor performance is tasted for given load condition. The results of no load and 2Nm load condition is obtained and represented in graph with respect to time. All the result of transient analysis is described in the next chapter.

Chapter 5: Results and Discussion



5.1 Start-up of the Motor

In this section, the speed of the different motor design is examined. It can be also observed the starting speed of motor in how much time motor reach to 750 rpm and stable average speed. The first analysis of different motor designs is starting with graph of speed vs time. The simulation was tested for 1.25 seconds with time step of 2ms. The starting performance of motor is tested for no load and under load conditions. The moment of inertia 0.01kg m^2 was used for all motor.

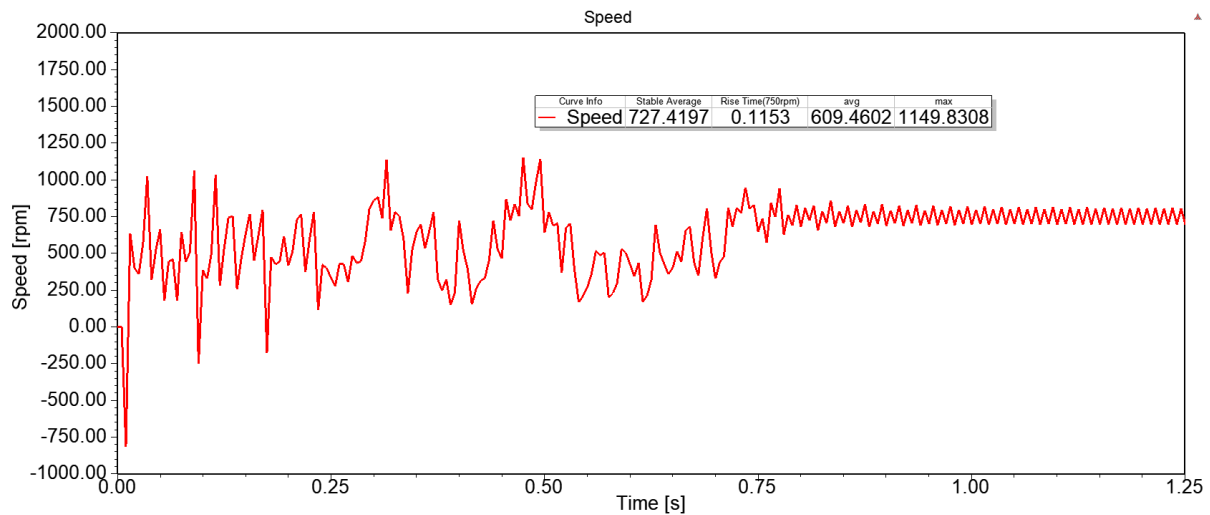


Fig.5.1: Speed of induction Motor at no load

The above figure 5.1 indicate the speed vs time graph of the induction motor. The stable average speed of this motor is 727.41 rpm. Here, stable average is calculated between 0.75s to 1.25s, during this period the speed of the motor is stable. The speed of induction motor is fluctuating around 750rpm.

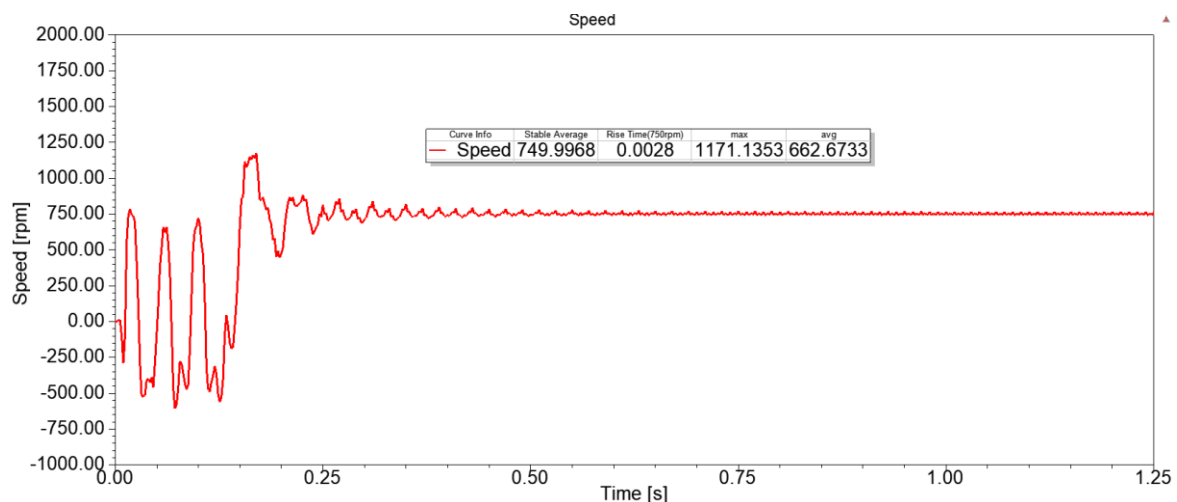


Fig.5.2: Speed of LSAFPMSM type 1 aluminium inductor at no load

The figure 5.2 shows the speed graph of line-start axial-flux permanent magnet synchronous motor (LSAFPMSM) with type 1 aluminium inductor at no load. The motor reach to synchronous speed in very short time 2.8ms. The stable average speed is 750 rpm. This motor takes less time for stable time as compare to induction motor.

The same model with copper inductor material, speed graph is shown in figure 5.3. Due to copper material, the speed is fluctuating in starting period, but it takes 4.9ms to rise at 750 rpm. The maximum speed of this model is 1407 rpm after that the speed is stable at 750 rpm.

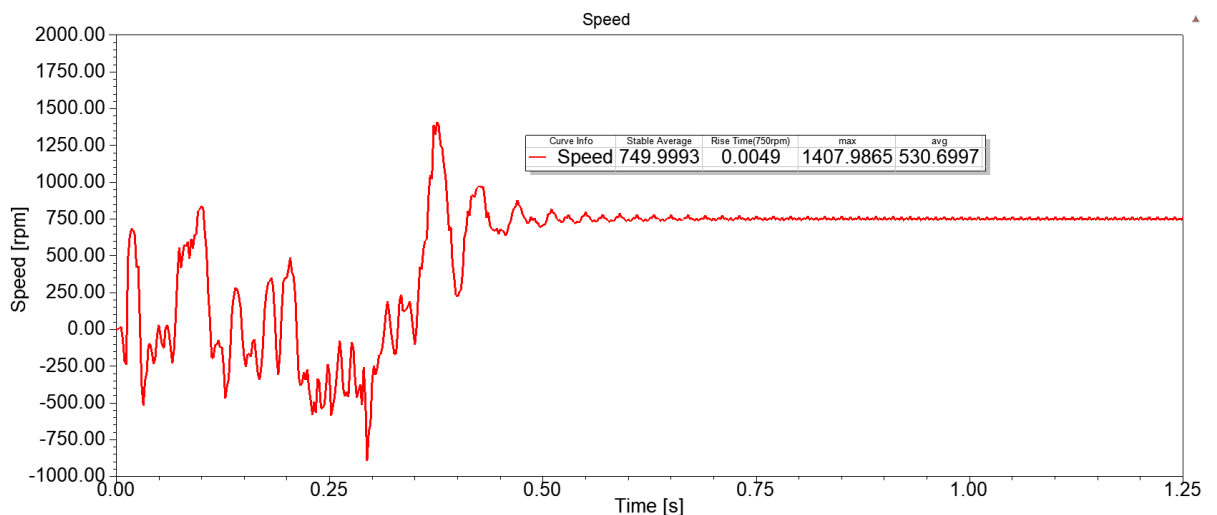


Fig.5.3: Speed of LSAFPMSM type 1 copper inductor at no load

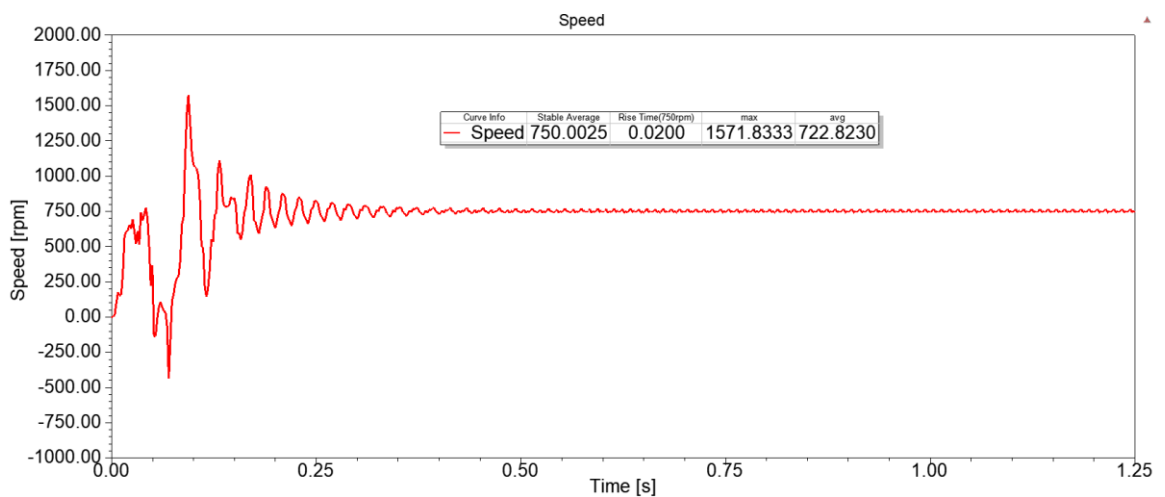


Fig.5.4: Speed of LSAFPMSM type 2 aluminium inductor at no load

Figure 5.4 and 5.5 indicate the speed vs time graph of LSAFPMSM type 2 inductor with aluminium and copper material respectively. Both the model have same synchronous speed 750 rpm. But the in terms of maximum value the copper inductor have maximum speed of 1711 rpm. Both the motor takes same time to stable around the synchronous speed which is 750 rpm. The rise time at 750 rpm of both model is 0.020s and 0.035s respectively.

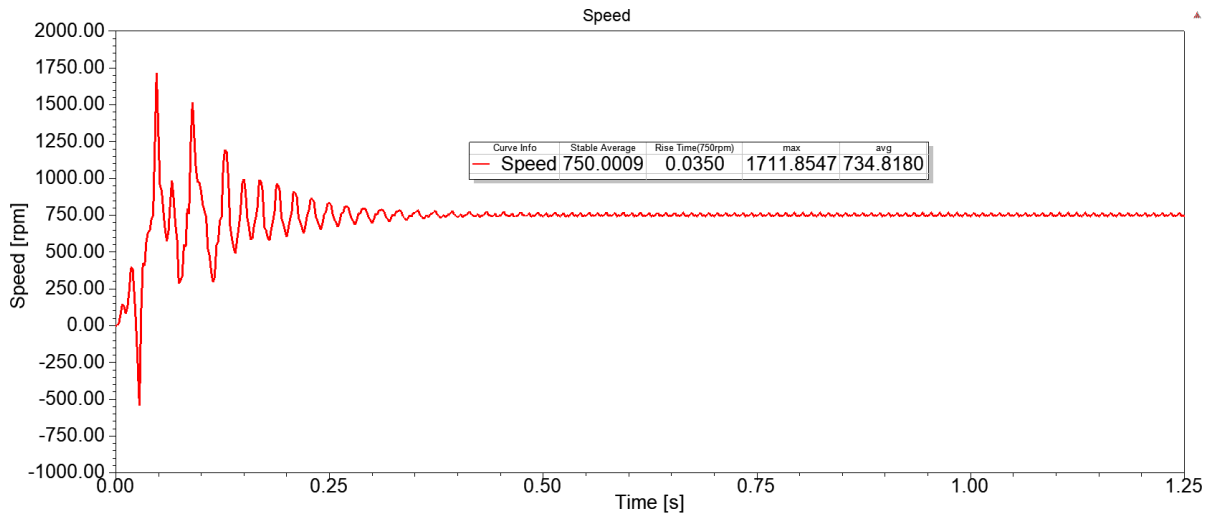


Fig.5.5: Speed of LSAFPMSM type 2 copper inductor at no load

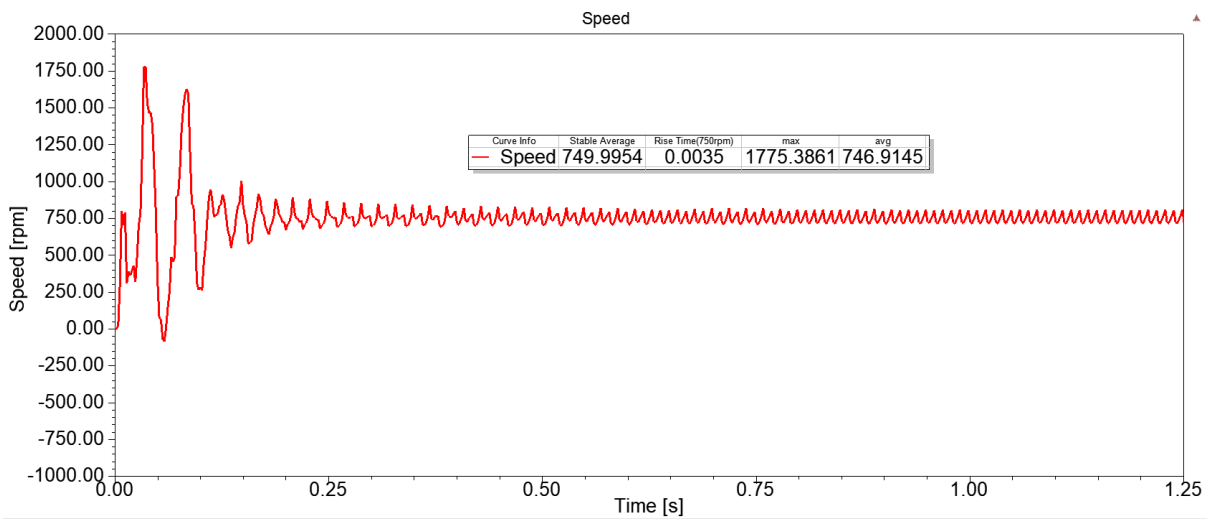


Fig.5.6: Speed of LSAFPMSM type 3 aluminium inductor at no load

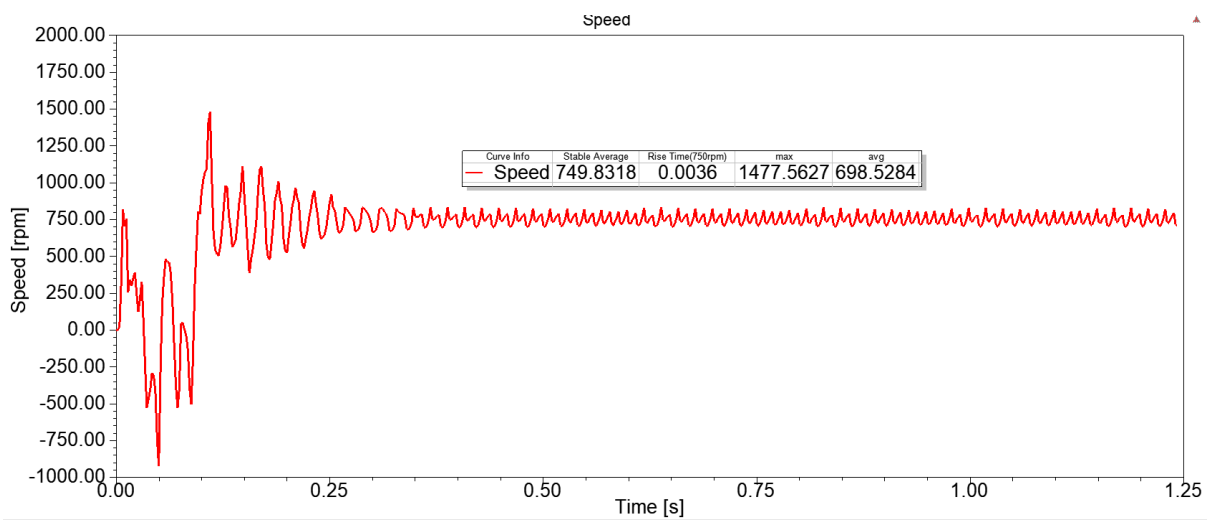


Fig.5.7: Speed of LSAFPMSM type 3 copper inductor at no load

The Speed plot of LSAFPMSM type 3 inductor with both aluminium and copper material is shown in figure 5.6 and 5.7. It can be seen that; the speed is more fluctuating than other two models at synchronous speed. But the stable speed is same 750 rpm as other two models.

From the above all speed graph of all model, the speed is 750 rpm for all model. But the speed of induction motor is fluctuating around 750 rpm. While the type 1 and type 2 model get almost flat synchronous speed 750 rpm. The induction motor takes more time to become stable speed while LSAFPMSM takes very less time. The rise time (750 rpm) is also less for LSAFPMSM as compared to induction motor.

Now, the speed graph is obtained for underload condition at 2Nm load. The results shown as below:

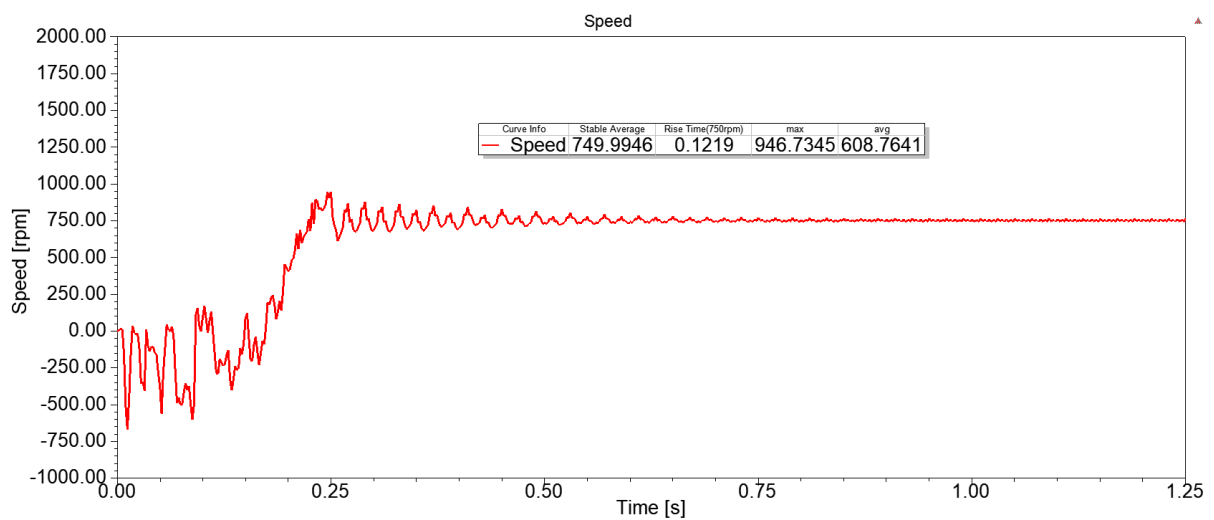


Fig.5.8: Speed of Induction motor at 2Nm load

The speed of induction motor under 2Nm load is shown in figure 5.8. Due to the load induction motor take much time to stable and to rise 750 rpm speed. The speed is fluctuating as shown in figure around 750 rpm.

Figure 5.9 and 5.10 indicates the speed graph of type 1 inductor with aluminium and copper material of LSAFPMSM. For both material, the speed is synchronising at 750 rpm. But there is difference in rise time. Copper is heavy material, so the rise time of this model is high as compare to aluminium inductor type. But both the model have same stable speed at 750 rpm.

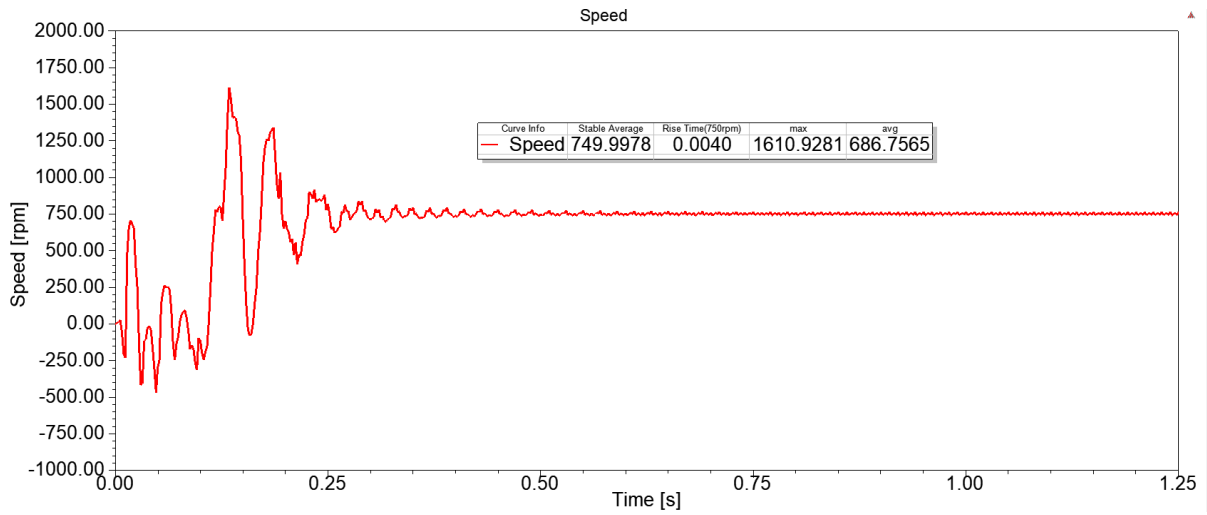


Fig.5.9: Speed of LSAFPMSM type 1 aluminium inductor at 2Nm load

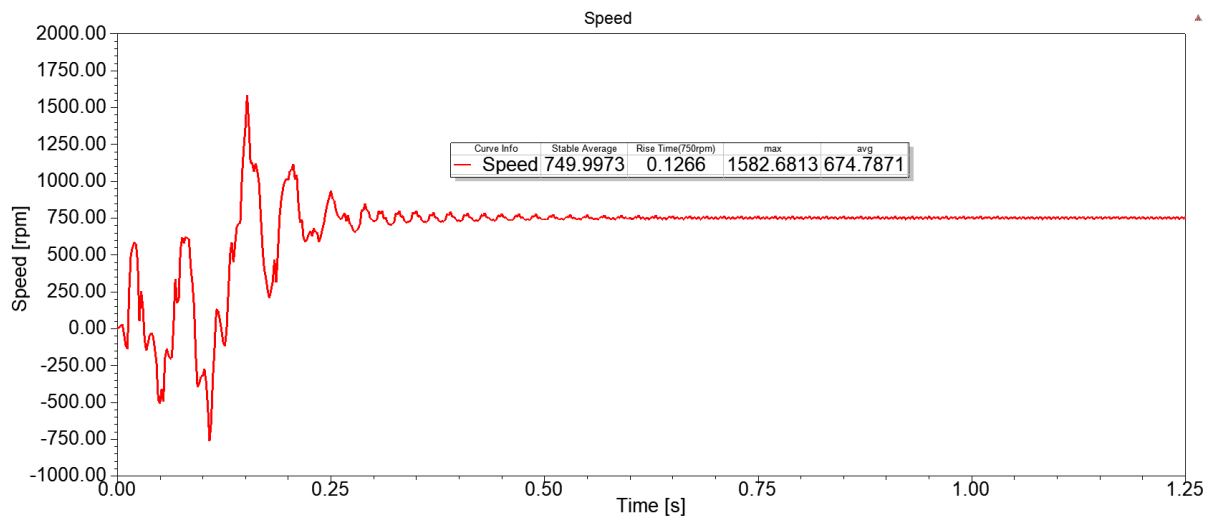


Fig.5.10: Speed of LSAFPMSM type 1 copper inductor at 2Nm load

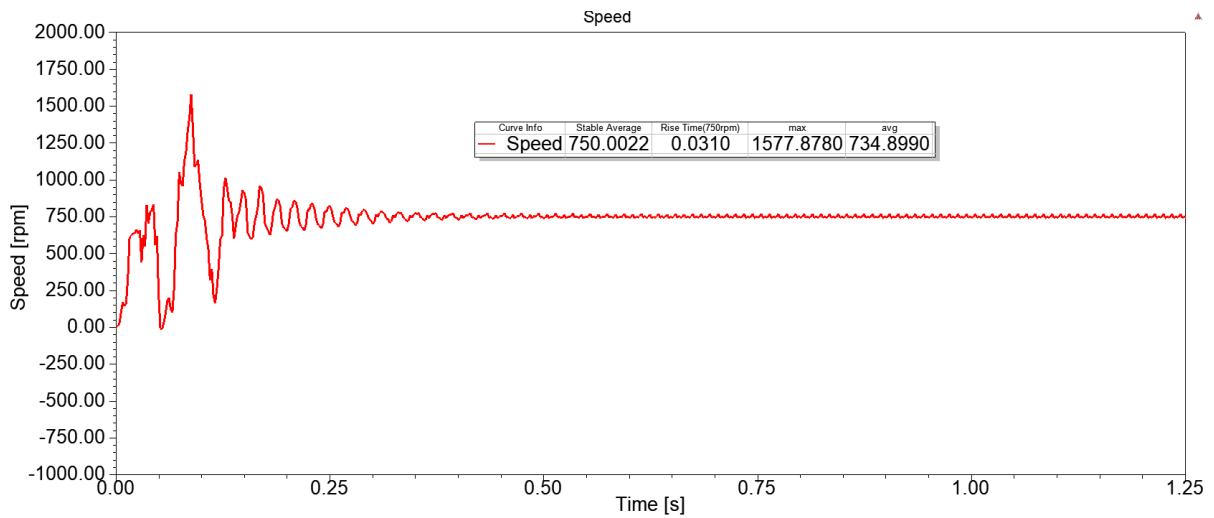


Fig.5.11: Speed of LSAFPMSM type 2 aluminium inductor at 2Nm load

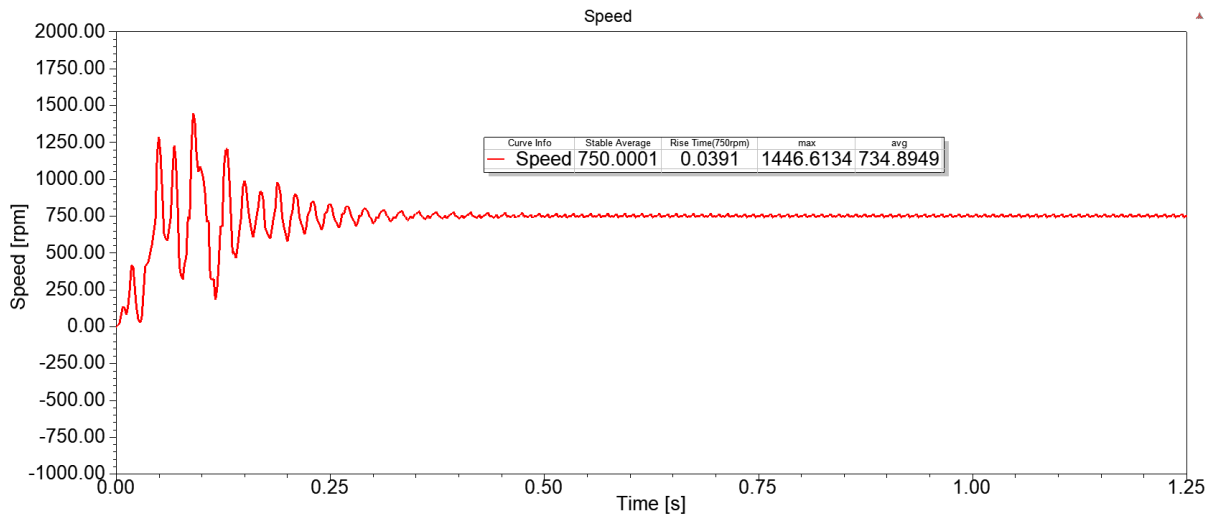


Fig.5.12: Speed of LSAFPMSM type 2 copper inductor at 2Nm load

Figure 5.11 and 5.12 illustrate the speed graph of type 2 inductor with both material. The speed performance of both model is same under 2Nm load condition. The rise time 0.03s is same for these two model and speed is synchronising.

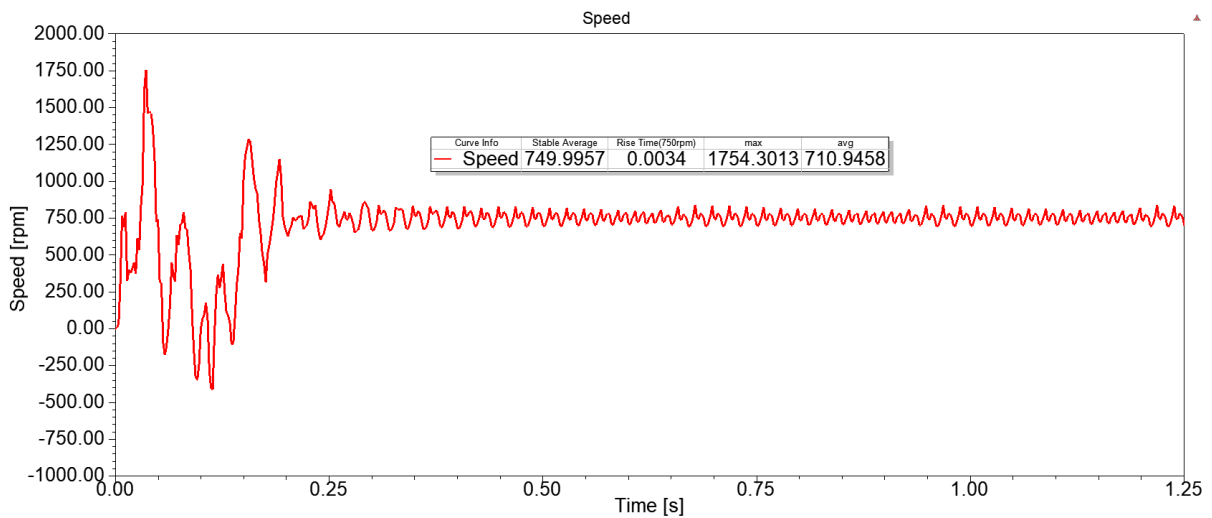


Fig.5.13: Speed of LSAFPMSM type 3 aluminium inductor at 2Nm load

The speed vs time graph of type 3 inductor of both material is shown in figure 5.13 and 5.14. The rise time to reach 750 rpm is almost same 0.0034s for both material at 2Nm load. But it can be seen that the speed is fluctuating around synchronous speed.

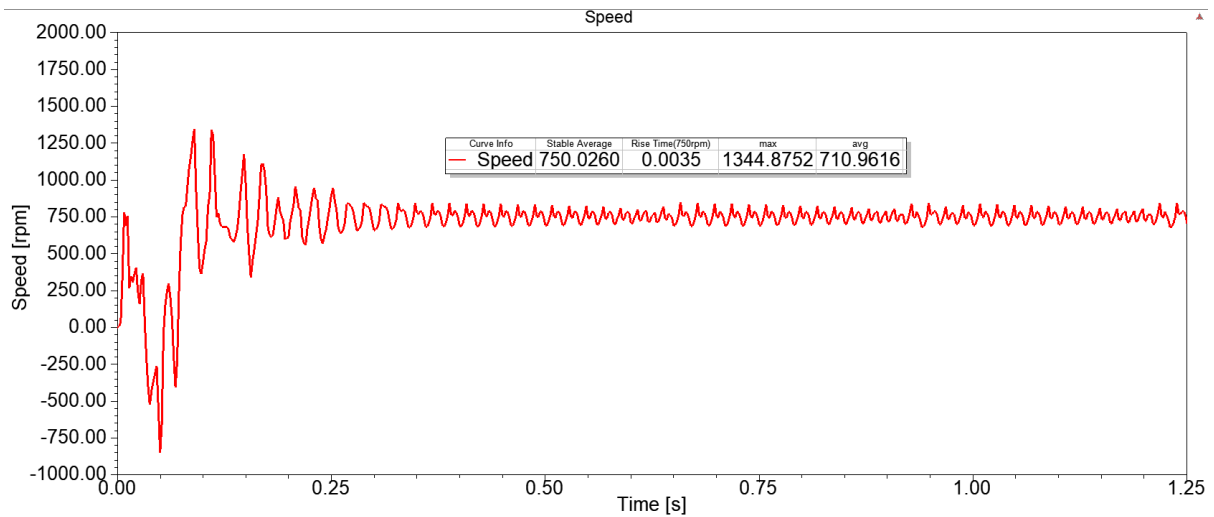


Fig.5.14: Speed of LSAFPMSM type 3 copper inductor at 2Nm load

From the above results of speed at no load and 2Nm load, the starting characteristics of LSAFPMSM models have same as induction motor.

Moreover, speed graph is obtained for full load condition at 14Nm load. The results shown as below:

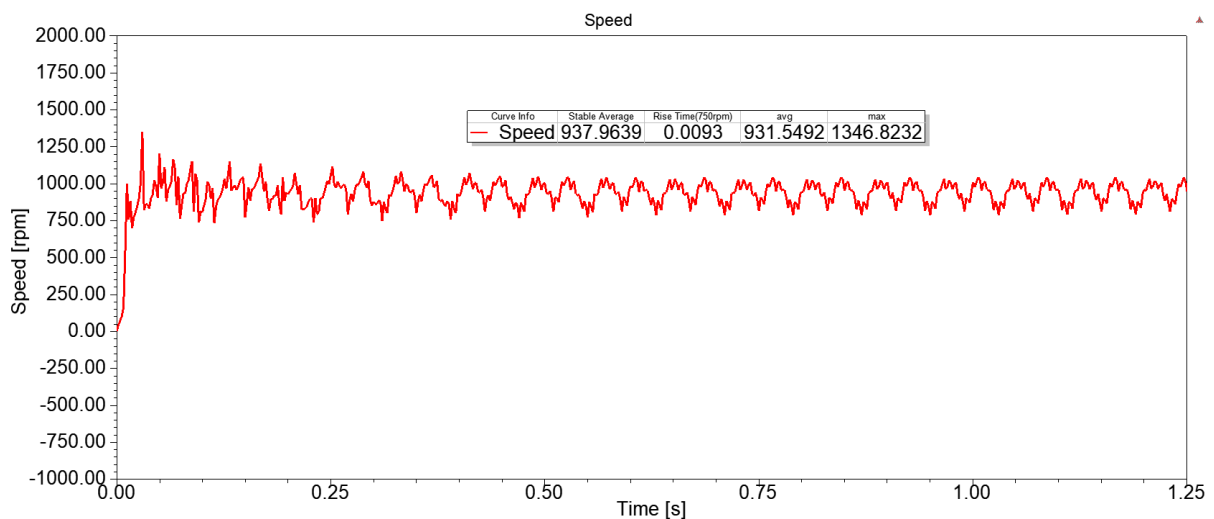


Fig.5.15: Speed of Induction motor at 14Nm load

The speed of induction motor at full load condition 14Nm load is shown in figure 5.15. Due to the full load induction motor take much time to stable and to rise 750 rpm speed. The speed is fluctuating as shown in figure around 930rpm due to full load 14Nm of motor.

Figure 5.16 and 5.17 indicates the speed graph of type 1 inductor with aluminium and copper material of LSAFPMSM. For both material, the speed is synchronising at 750 rpm under full load 14Nm condition.

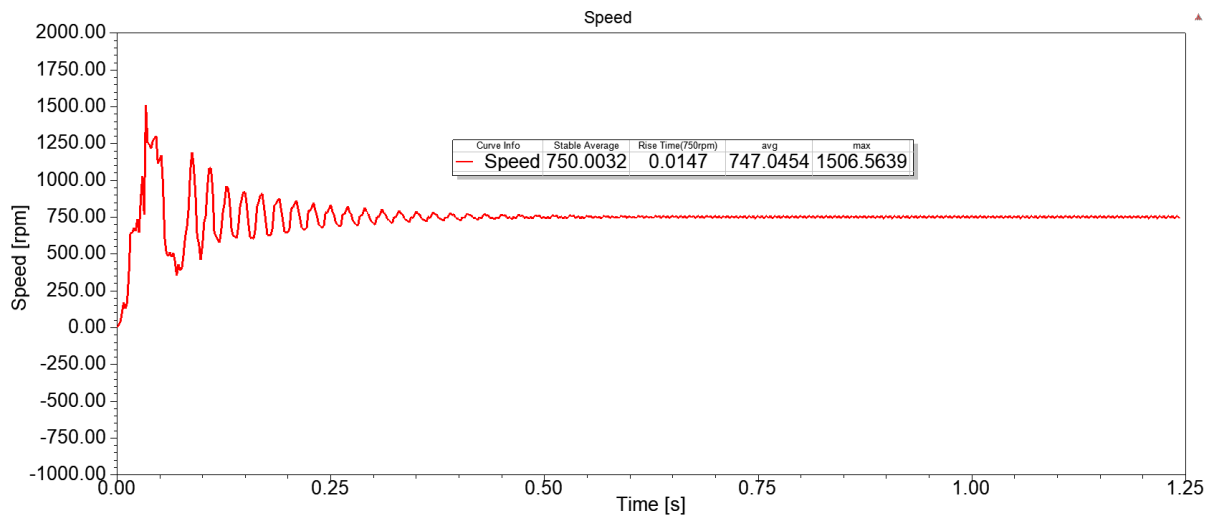


Fig.5.16: Speed of LSAFPMSM type 1 aluminium inductor at 14Nm load

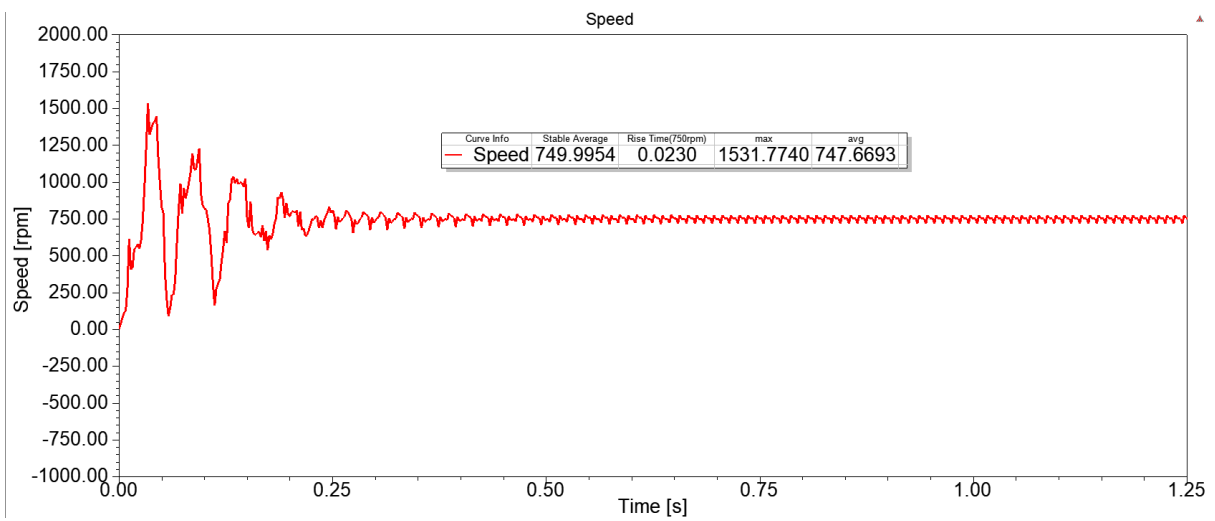


Fig.5.17: Speed of LSAFPMSM type 1 copper inductor at 14Nm load

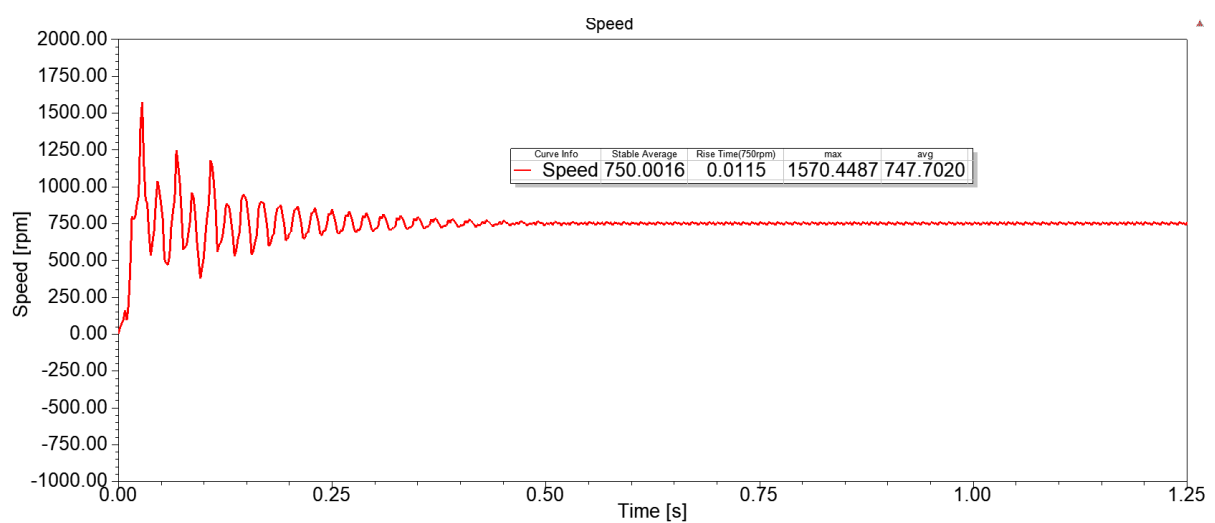


Fig.5.18: Speed of LSAFPMSM type 2 aluminium inductor at 14Nm load

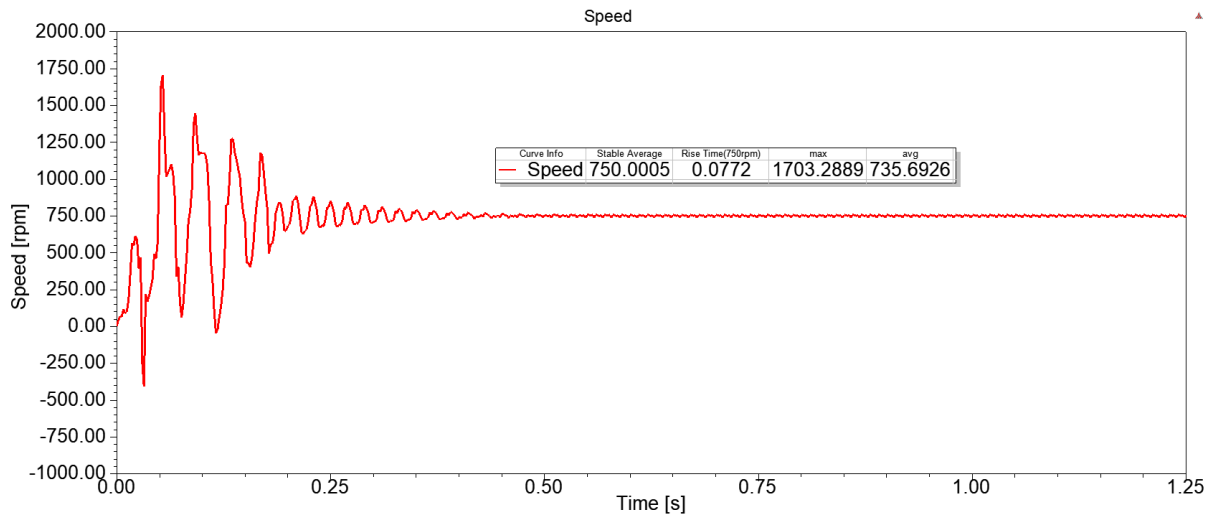


Fig.5.19: Speed of LSAFPMSM type 2 copper inductor at 14Nm load

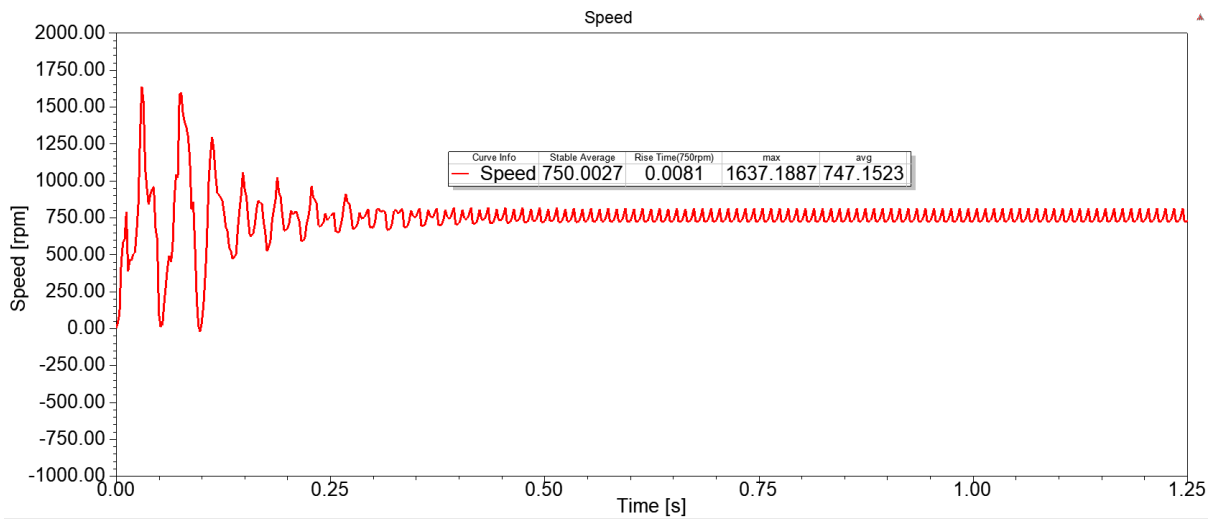


Fig.5.20: Speed of LSAFPMSM type 3 aluminium inductor at 14Nm load

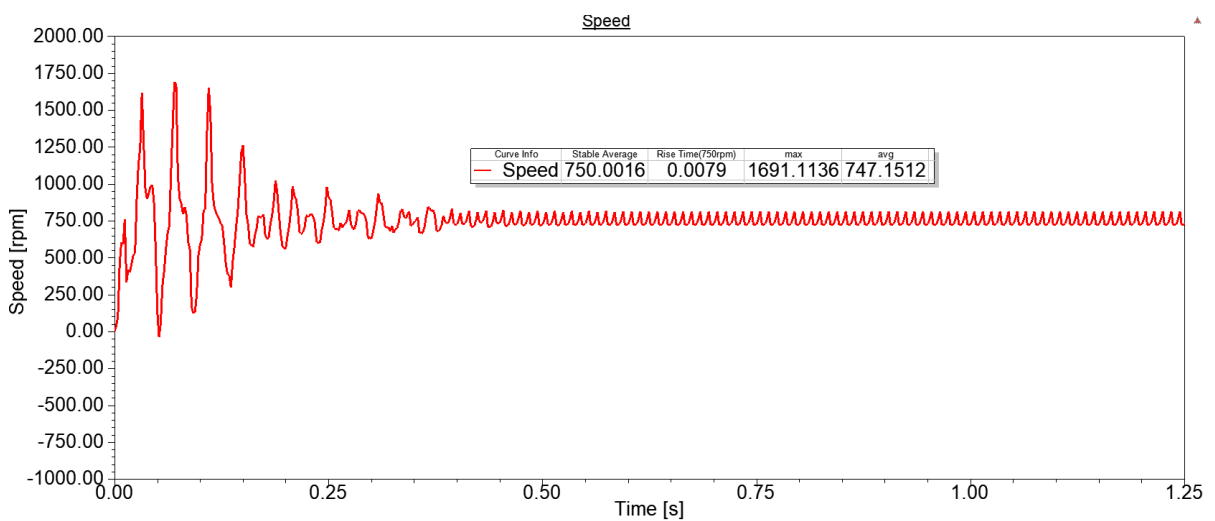


Fig.5.21: Speed of LSAFPMSM type 3 copper inductor at 14Nm load

The advantage of LSAFPMSM model is that it takes less time to reach 750 rpm and also stable time is very fast as compared to induction motor under loaded conditions. Moreover, under full load condition 14Nm, the induction motor runs over the synchronous speed while the LSAFPMSM are running at synchronous speed at 750rpm. Under the any load condition the LSAFPMSM are running at synchronous speed which is desired to take over induction motor. So, this kind of motor is run at constant speed which doesn't required any external circuit drive. Finally, the LSAFPMSM can be replace to the induction motor for constant speed application.

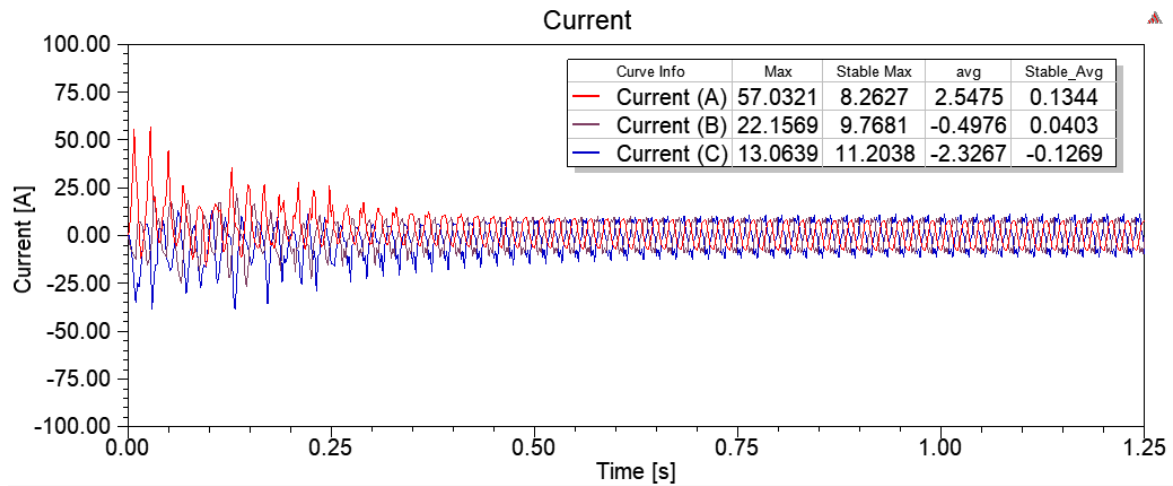
Table.5.1: Speed response of motor under different load condition

Speed response of motors under different load condition					
Load	Motor Type		Maximum Speed (rpm)	Steady state Average Speed (rpm)	Rise time (sec) at 750 rpm
No Load	Induction motor		1149.83	727.41	0.1153
	LSAFPMSM	Alu inductor type 1	1171.13	750	0.0028
		Copper inductor type 1	1407.98	750	0.0049
		Alu inductor type 2	1571.83	750	0.0200
		Copper inductor type 2	1711.85	750	0.0350
		Alu inductor type 3	1775.36	750	0.0035
		Copper inductor type 3	1477.56	750	0.0036
	2Nm load	Induction motor		946.75	749
LSAFPMSM		Alu inductor type 1	1610.92	750	0.0040
		Copper inductor type 1	1582.13	750	0.1266

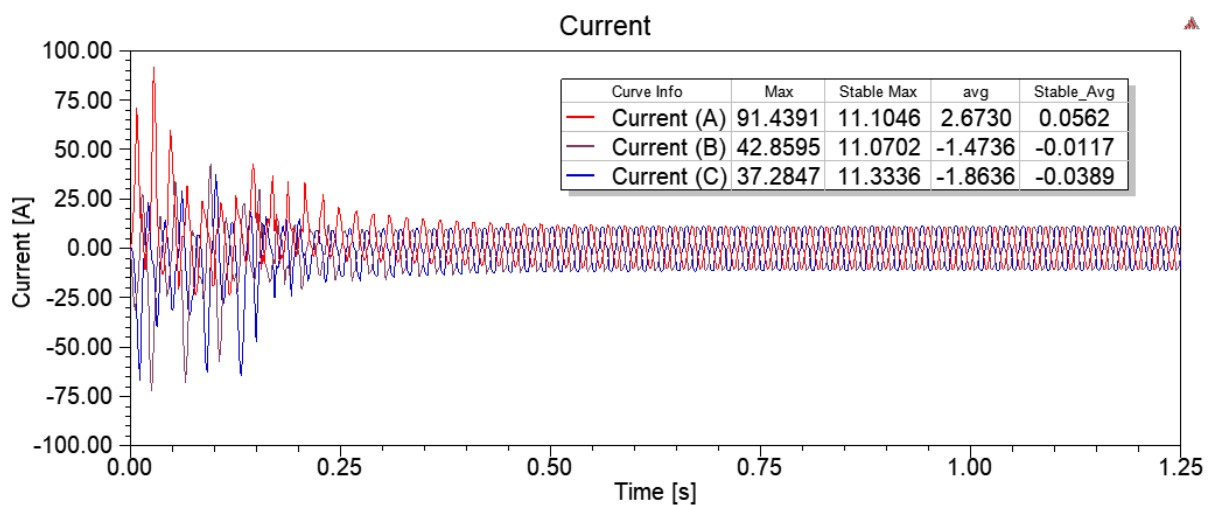
		Alu inductor type 2	1577.87	750	0.0310
		Copper inductor type 2	1446.61	750	0.0391
		Alu inductor type 3	1754.30	750	0.0034
		Copper inductor type 3	1344.87	750	0.0035
	Induction motor		1346.82	938	0.0093
Full load 14Nm	LSAFPMSM	Alu inductor type 1	1506.56	750	0.0147
		Copper inductor type 1	1531.77	750	0.0230
		Alu inductor type 2	1570.44	750	0.0115
		Copper inductor type 2	1703.28	750	0.0772
		Alu inductor type 3	1637.18	750	0.0018
		Copper inductor type 3	1691.11	750	0.0079

5.2 Winding current of Motors

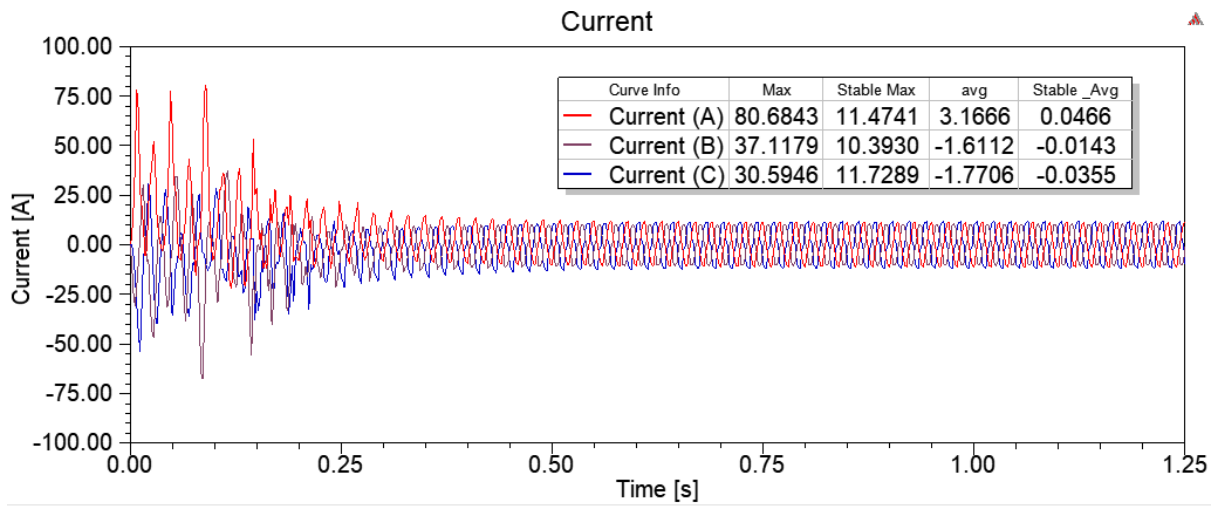
The current of winding is observed in this section. The simulation and test were conducted for all motor and the winding current of all the motor design was observed. For the better performance of the motor, winding current should be sinusoidal waveform. The graph of current vs time of all model under no load condition is illustrated in figure 5.22.



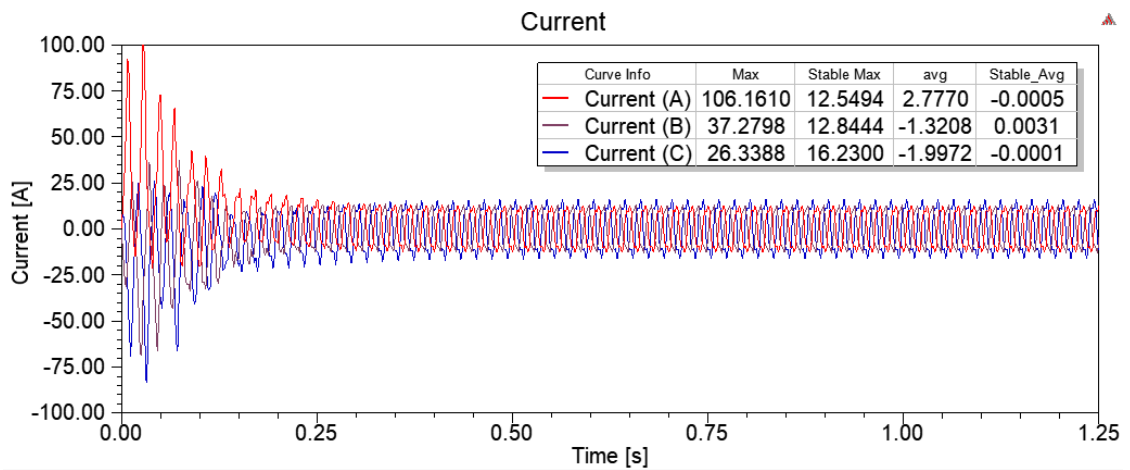
(a) Winding current for induction motor



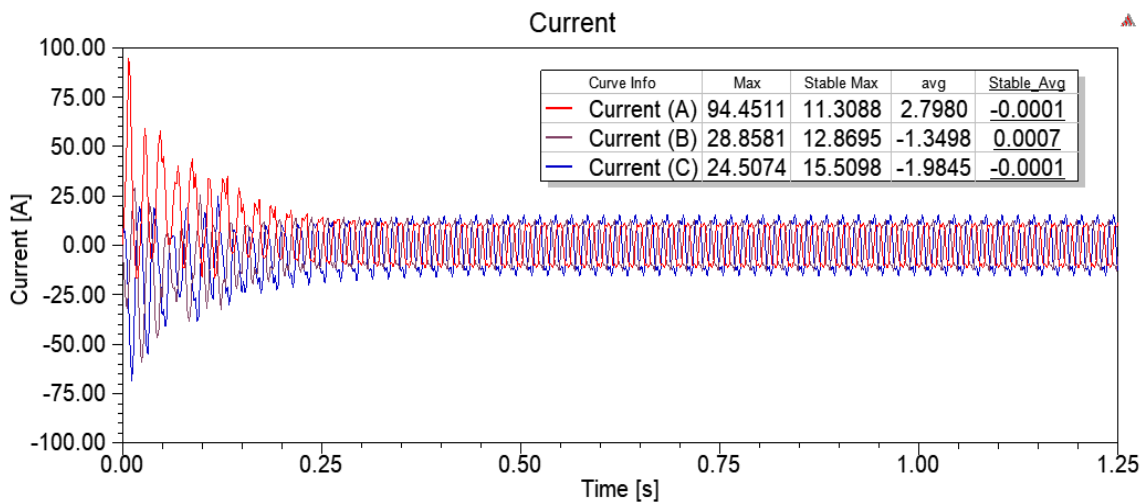
(b) Winding current of LSAFPMSM type 1 aluminium inductor



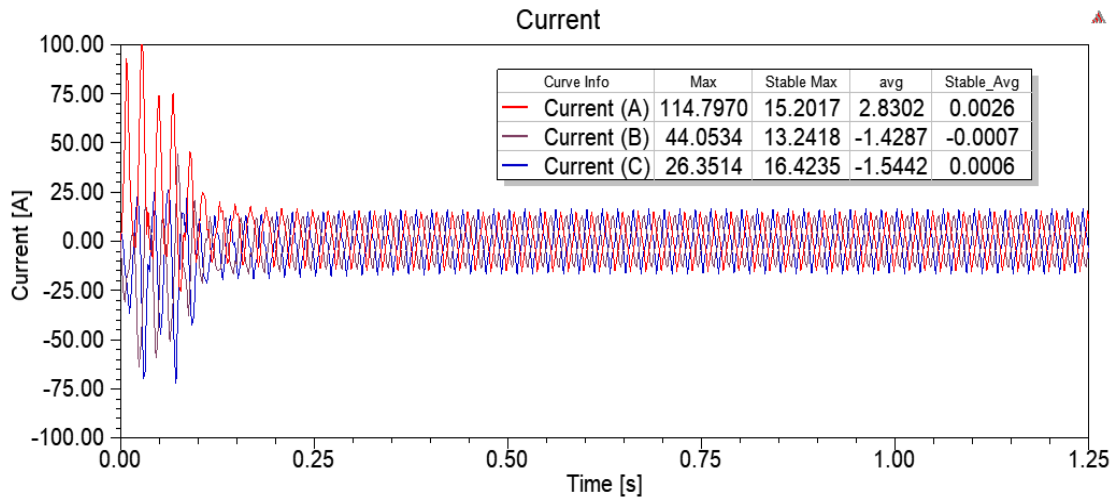
(c) Winding current of LSAFPMSM type 1 copper inductor



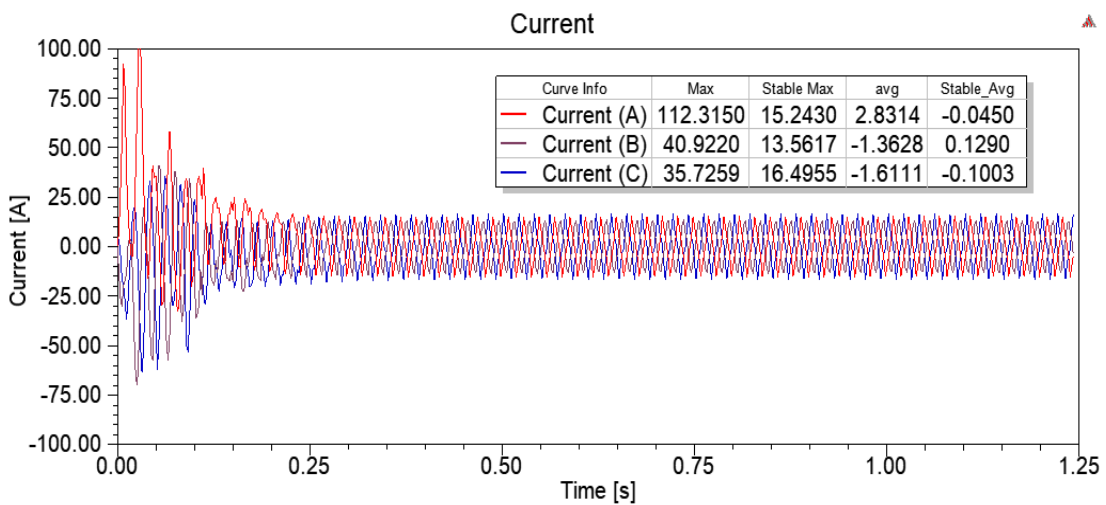
(d) Winding current of LSAFPMSM type 2 aluminium inductor



(e) Winding current of LSAFPMSM type 2 copper inductor



(f) Winding current of LSAFPMSM type 3 aluminium inductor



(g) Winding current of LSAFPMSM type 3 copper inductor

Fig.5.22: Winding current vs Time graph of all model at no load

From the figure 5.22, it can be seen that the winding current of all model is in the balanced condition. The magnitude and phase shift of all model are in balanced condition. Here, the stable max current is calculated between the interval of time 0.75s to 1.25s. The stable max value for all model is ranging between 10 to 15 A winding current for three-phases. The stable average is average current value between 0.75s to 1.25s. During this period, the winding current for three-phases almost stable. The stable average value for all model is zero.

If the winding current of motor is unbalanced the main reason is reactance of the three-phase motor. Due to unbalance winding current, may have adverse effect on efficiency and speed of motor. It has also bad effect on the torque of motor due to unbalancing of current. The main reason for motor vibration is unbalance torque which lead motor to damage from connected

system. There are also many bad effects on motor due to unbalanced current such as heating problem and losses of the motor is increase. So, motor cannot be run on the desired output.

But, in this case the winding current of all model are in balanced with magnitude and phase shift. The motor performance of all model is better which is shown in figure 5.22.

5.3 Losses of the machine

In this part, the different losses of all model are tested and analysed. Mostly, the three type of losses such as core loss, eddy current loss and hysteresis loss are tested. These losses are tested under no load and under load 2Nm. The core loss depends on the frequency of supply voltage. The core is made from iron which rotate in magnetic field and small current induced in the armature of core. The core loss is divided in to eddy current loss and hysteresis loss. The eddy current losses can be reason of due to small induced electromagnetic force (emf) a large current flow due to low resistance of core. Hysteresis loss is due to some magnetization effect of armature core. The losses of induction motor are high due to more iron armature. The losses vs time graph of all model is illustrated in below figures.

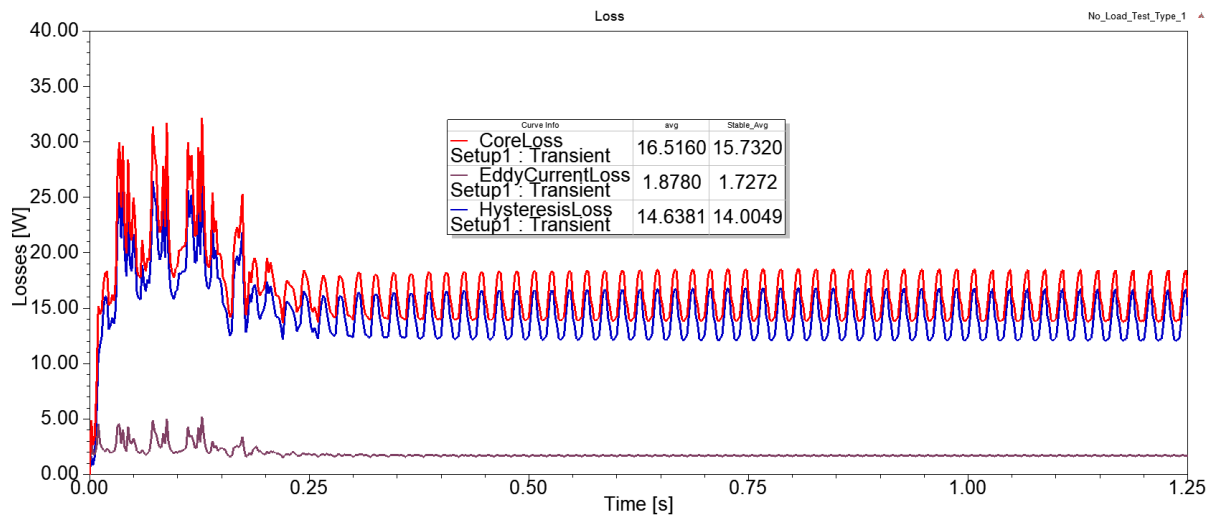


Fig.5.23: Losses of Induction motor at no load

Fig 5.23 shows the losses of induction motor. The core loss of induction motor is 15.7W. The eddy current and hysteresis loss of induction motor is 1.72W and 14W respectively. These three losses are very high among all the motor tested in this project.

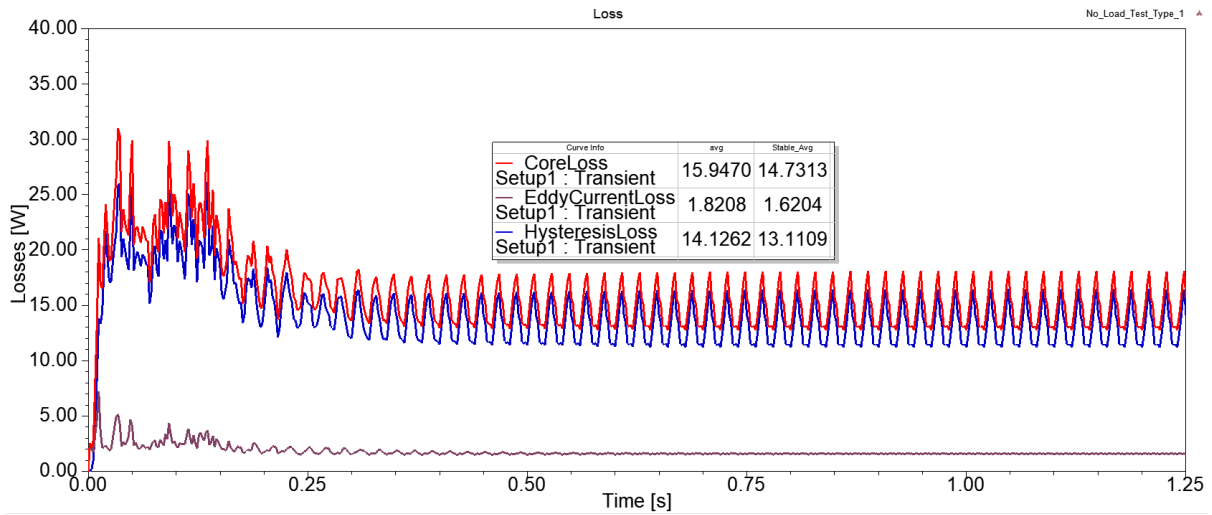


Fig.5.24: Losses of LSAFPMSM type 1 aluminium inductor at no load

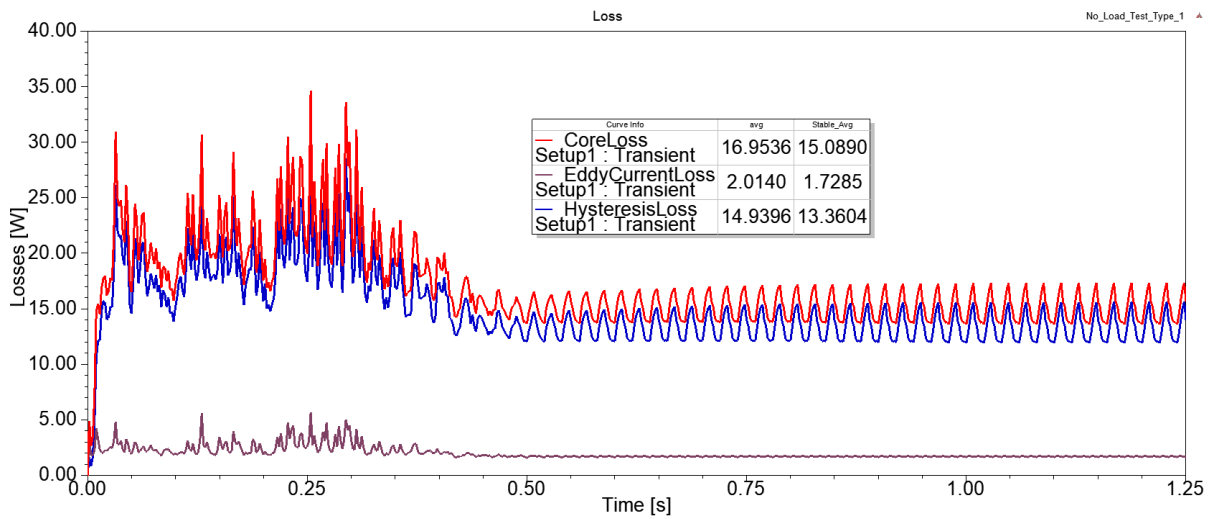


Fig.5.25: Losses of LSAFPMSM type 1 copper inductor at no load

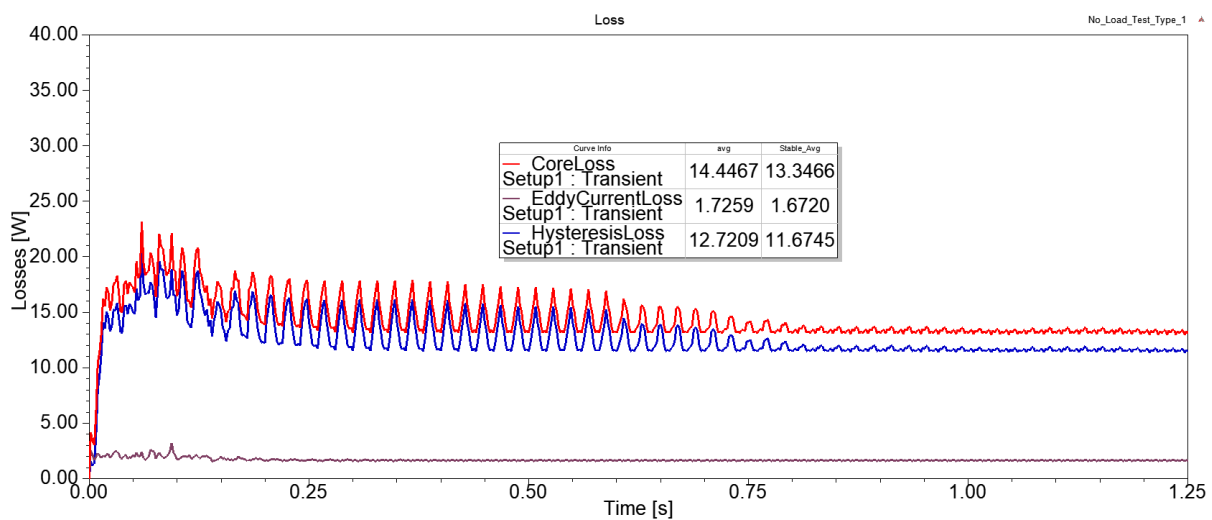


Fig.5.26: Losses of LSAFPMSM type 2 aluminium inductor at no load

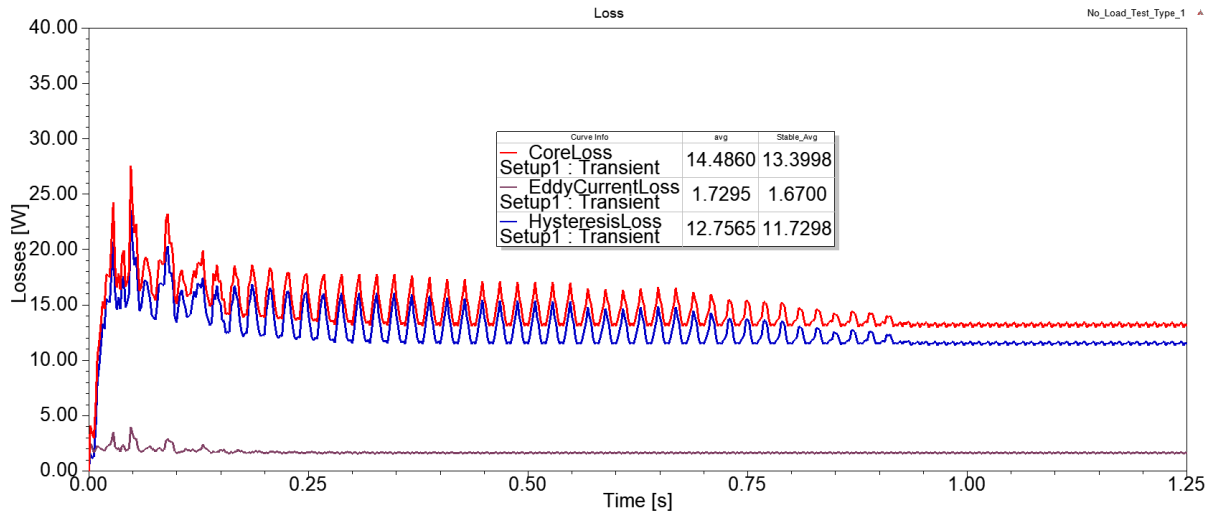


Fig.5.27: Losses of LSAFPMSM type 2 copper inductor at no load

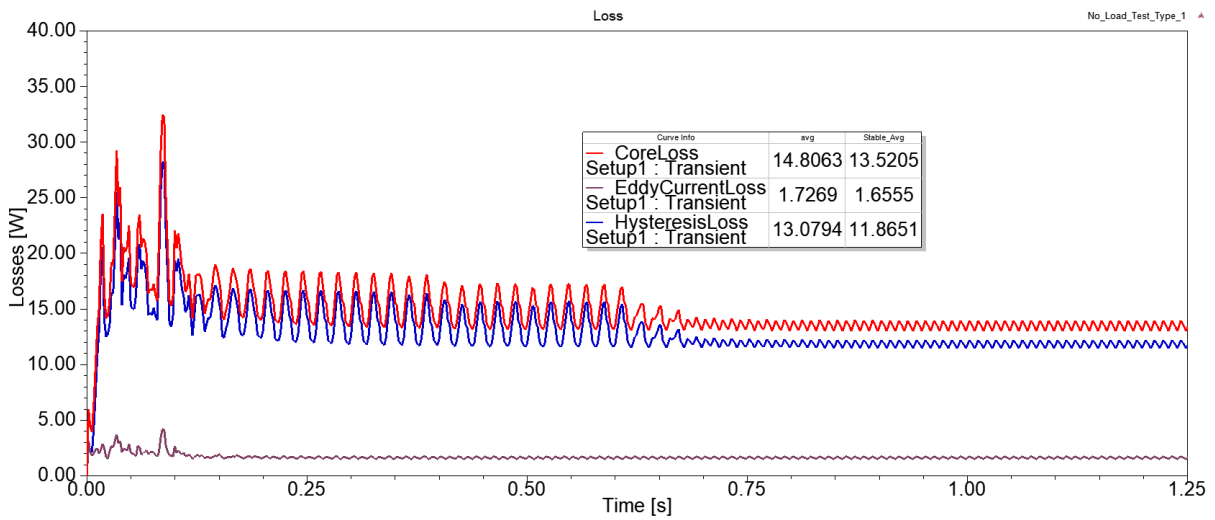


Fig.5.28: Losses of LSAFPMSM type 3 aluminium inductor at no load

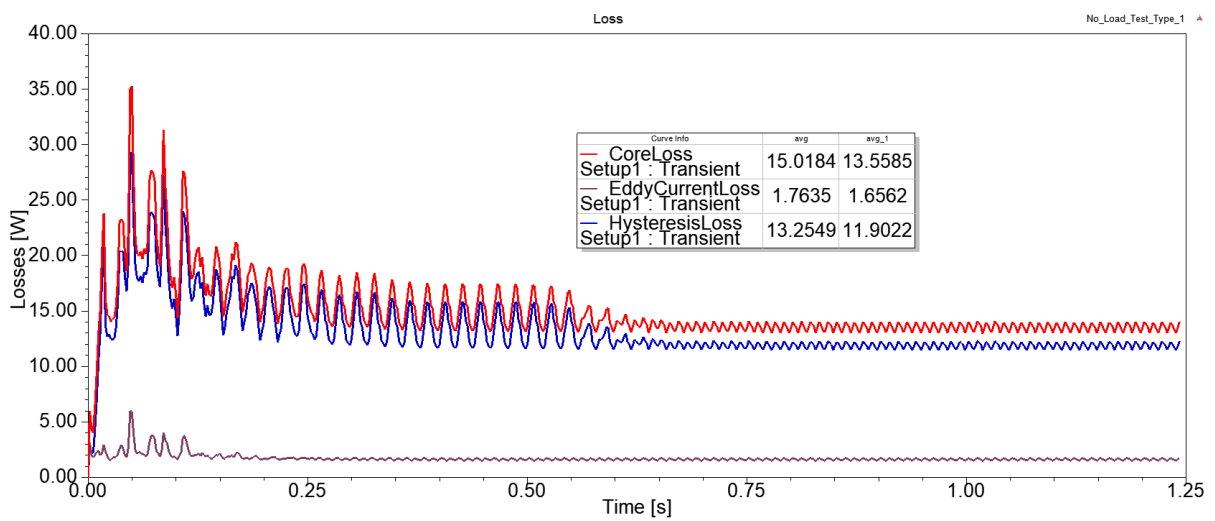


Fig.5.29: Losses of LSAFPMSM type 3 copper inductor at no load

Figure 5.24 to 5.29 shows the losses of LSAFPMSM for mentioned different design of motors. The core loss of all LSAFPMSM is around 13.5W except type 1 copper material model. Due to the copper material, the core loss is high because of mass of material is very high at inductor and rotor. These all losses are tested at no load condition of motor.

Now, the losses under 2Nm load is tested for all model and graph of losses vs time as flow,

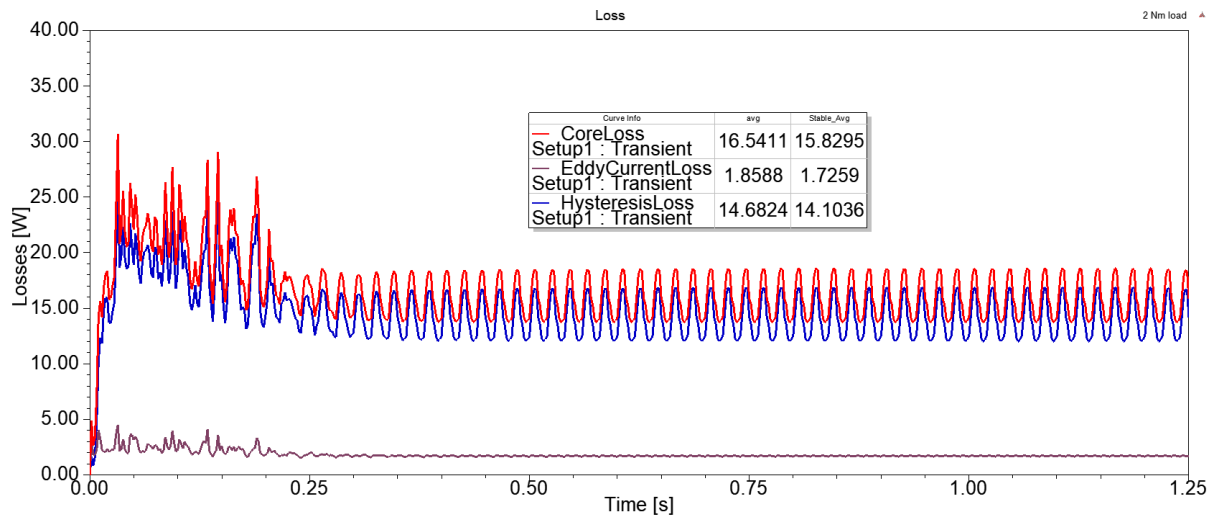


Fig.5.30: Losses of Induction motor at 2Nm load

The losses of induction motor at 2Nm load is shown in figure 5.30. The induction motor has high core loss of 15.8W as compare to other models. Due to the high losses, the efficiency of the motor is decrease and power factor is also reduced.

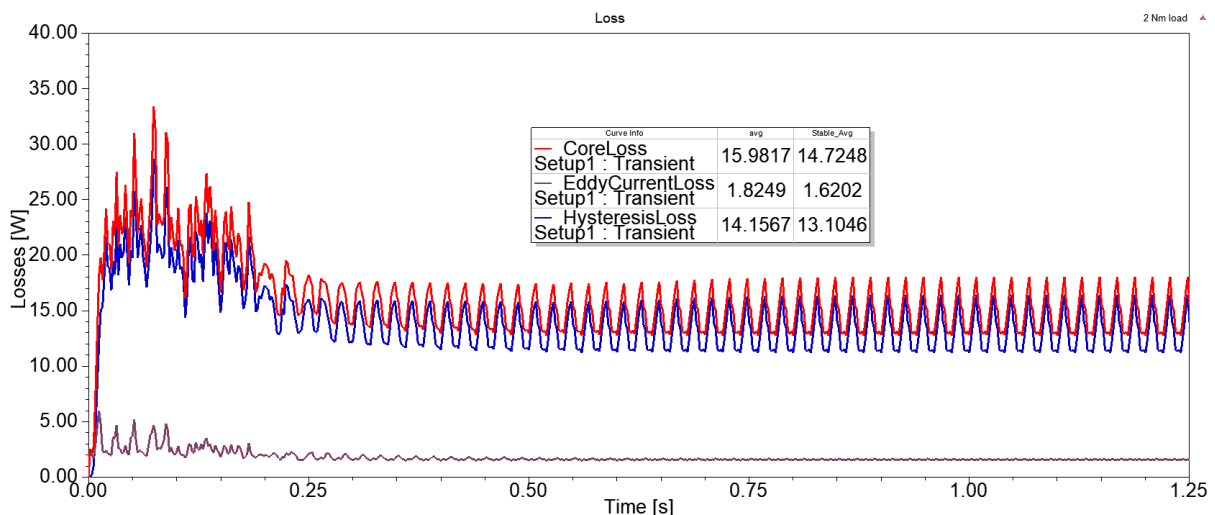


Fig.5.31: Losses of LSAFPMSM type 1 aluminium inductor at 2Nm load

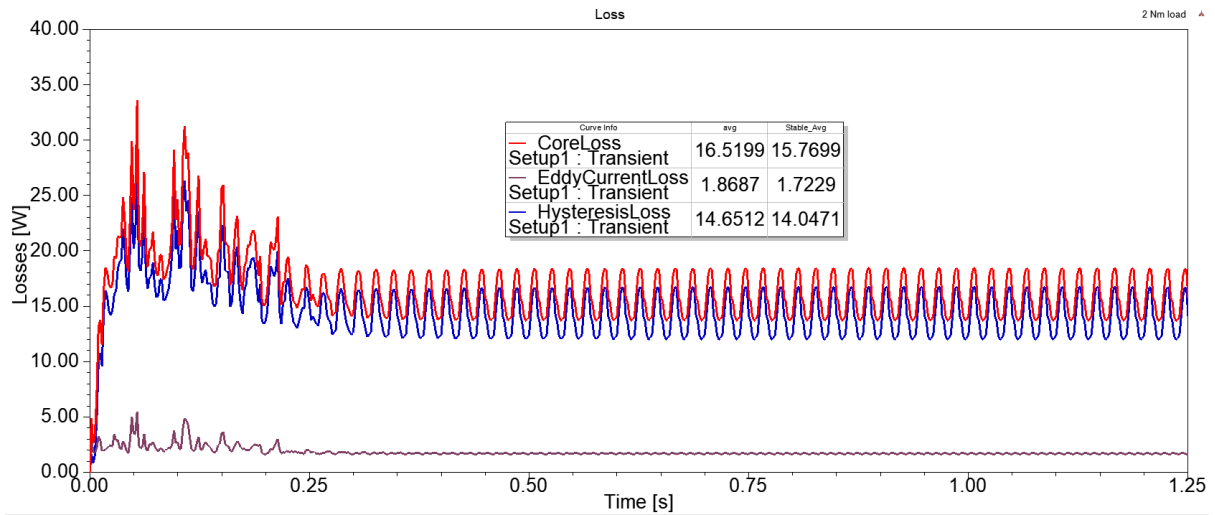


Fig.5.32: Losses of LSAFPMSM type 1 copper inductor at 2Nm load

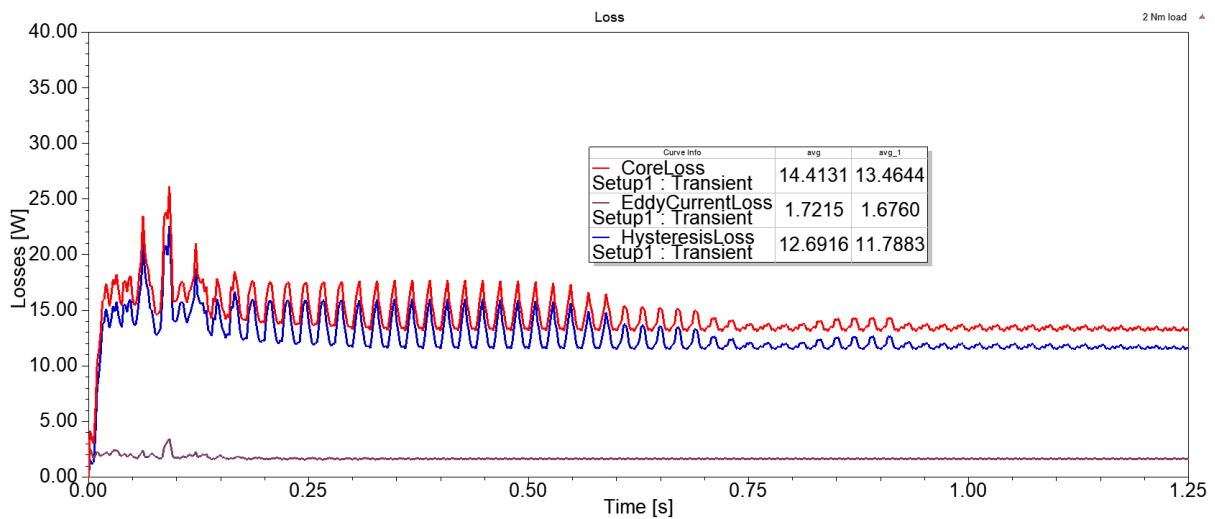


Fig.5.33: Losses of LSAFPMSM type 2 aluminium inductor at 2Nm load

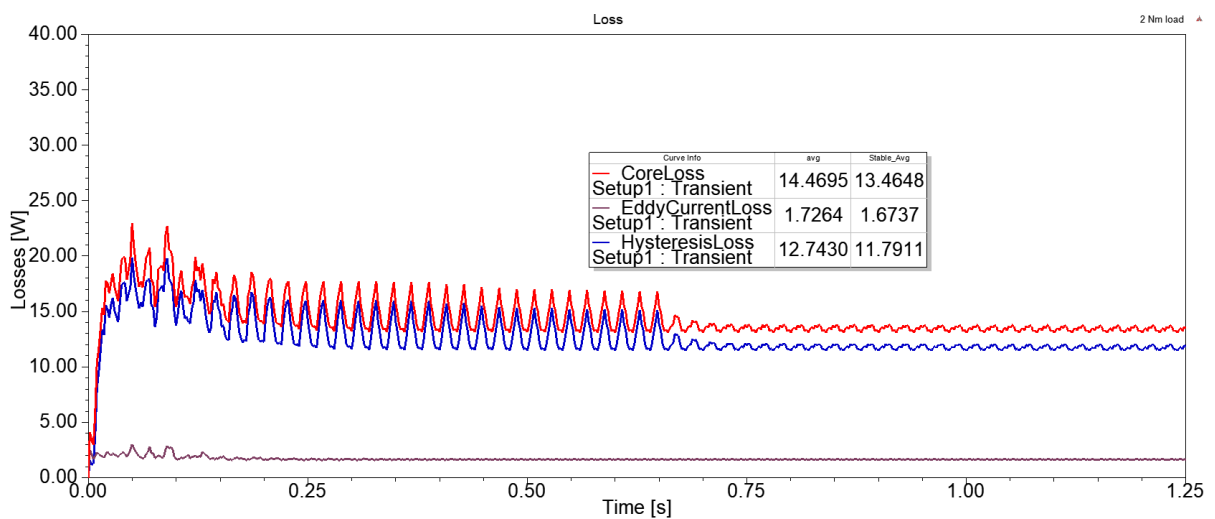


Fig.5.34: Losses of LSAFPMSM type 2 copper inductor at 2Nm load

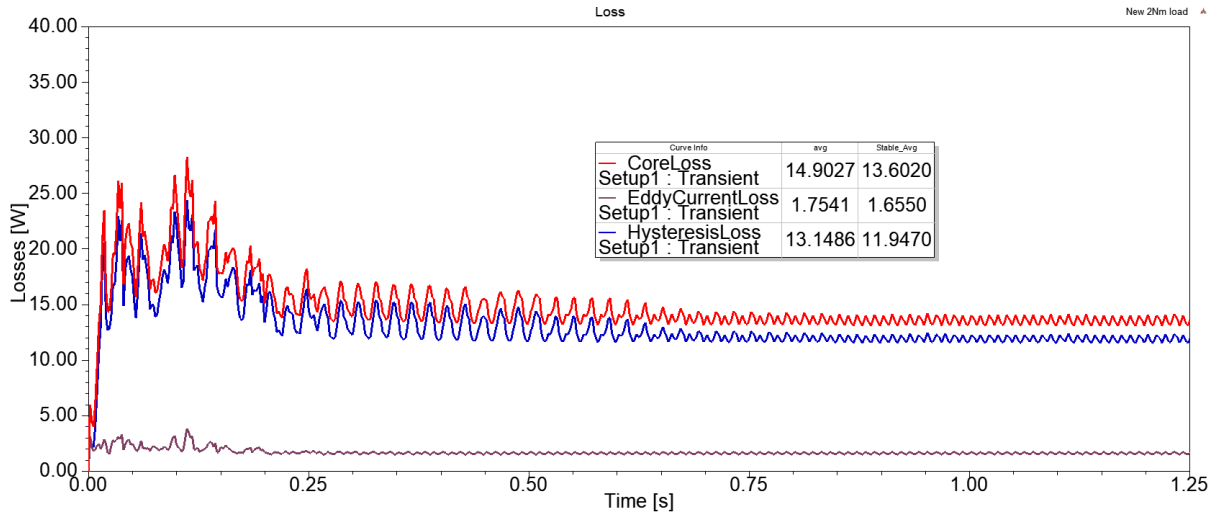


Fig.5.35: Losses of LSAFPMSM type 3 aluminium inductor at 2Nm load

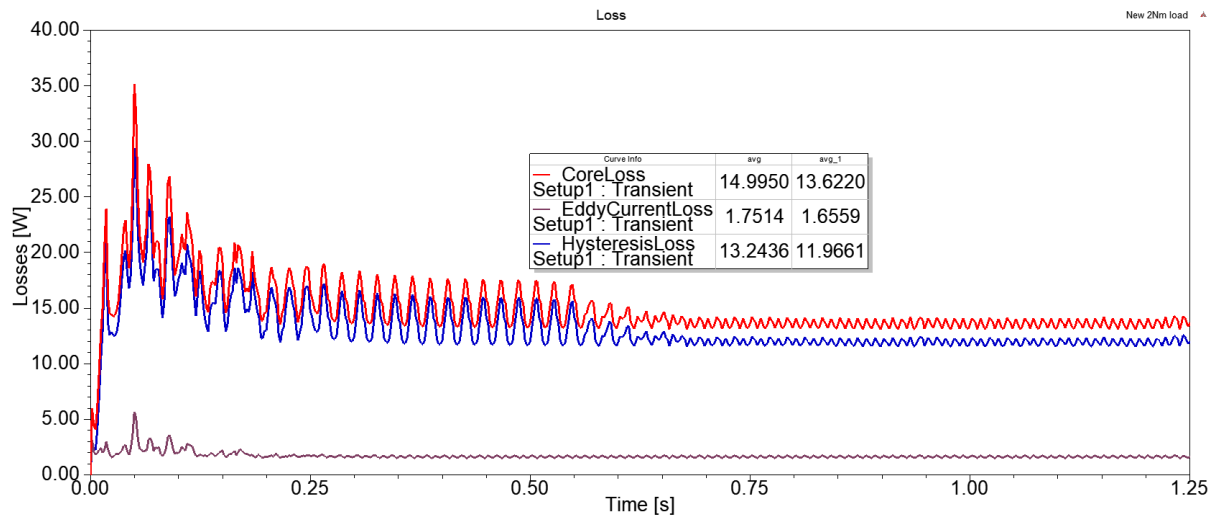


Fig.5.36: Losses of LSAFPMSM type 3 copper inductor at 2Nm load

From the above results of losses at no load and 2Nm load, it can be seen that the induction motor has very high losses as compared to LSAFPMSM. The average core losses of induction motor are 16.5W and the losses in other models are average of 13.5W. Due to the less losses the efficiency of LSAFPMSM becomes high as compared to induction motor.

5.4 Torque produced by Machine

In this section, the performance of torque is studied for all design motor. Torque is produced due to rotating force to radius of machine. The motor start from zero to maximum speed, during this period torque is developed. Here, the torque plot is obtained to check the starting torque performance of motor. The torque studied under no load condition and with 2Nm load. The graph of torque vs time is listed below.

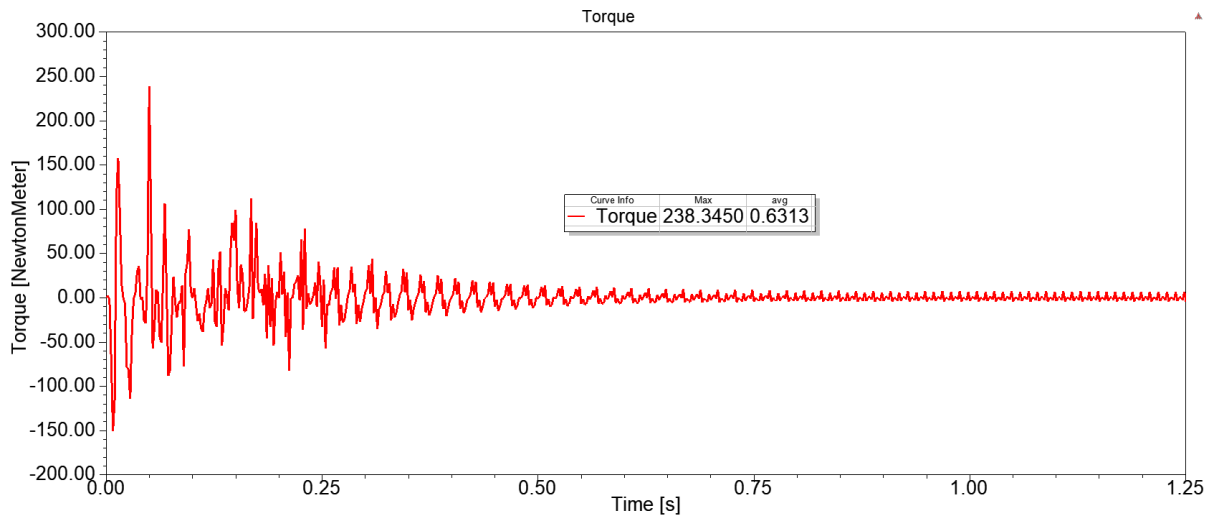


Fig.5.37: Torque of Induction motor at no load

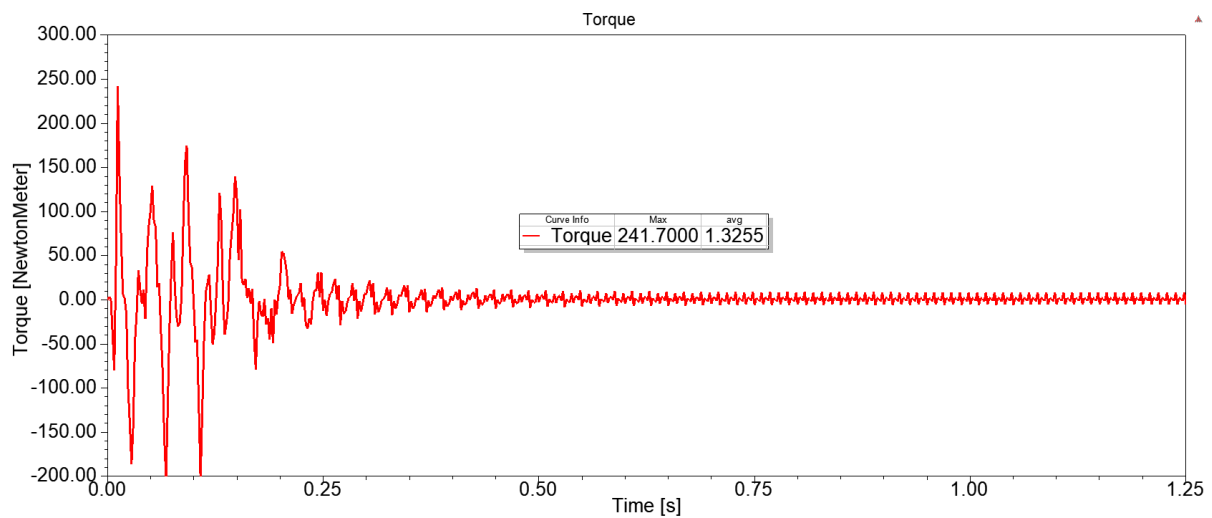


Fig.5.38: Torque of LSAFPMSM type 1 aluminium inductor at no load

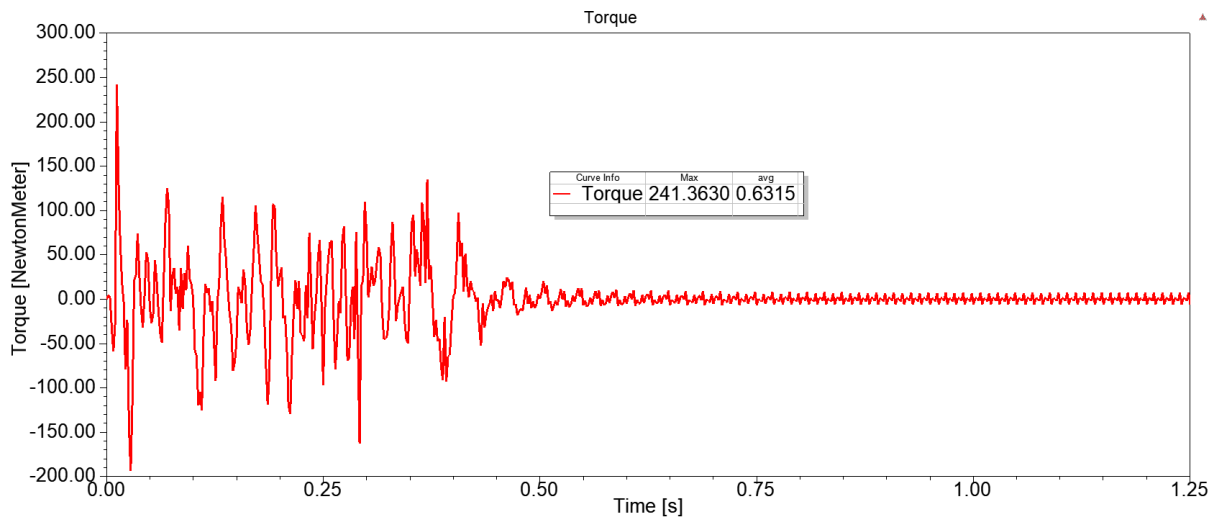


Fig.5.39: Torque of LSAFPMSM type 1 copper inductor at no load

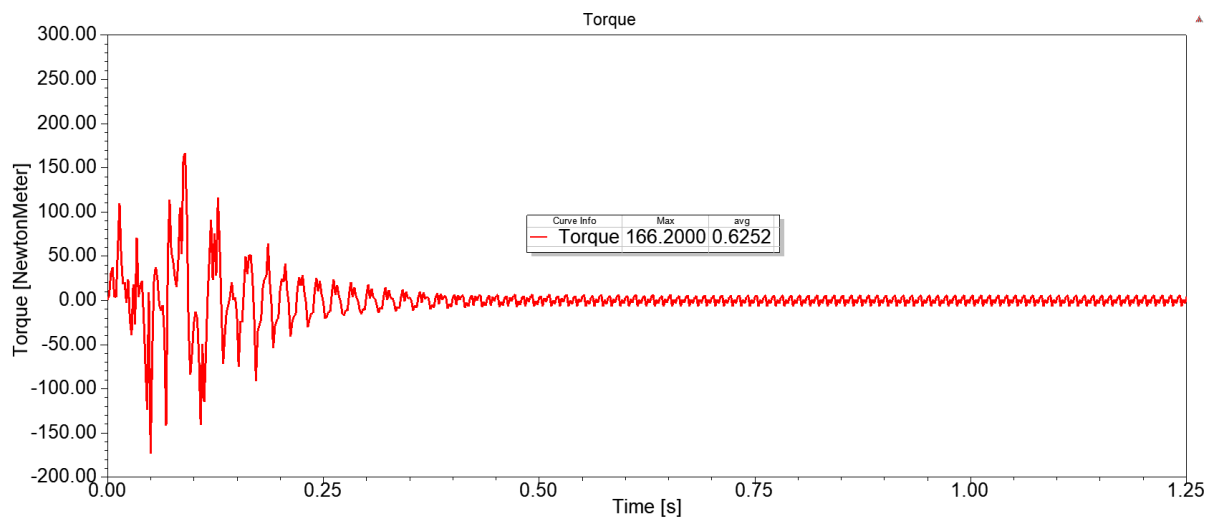


Fig.5.40: Torque of LSAFPMSM type 2 aluminium inductor at no load

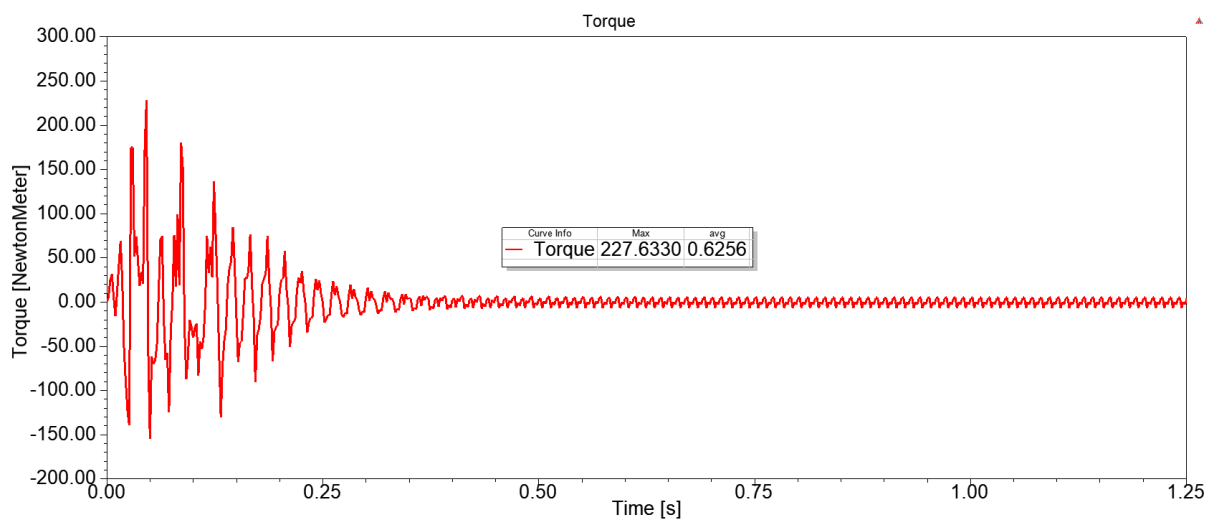


Fig.5.41: Torque of LSAFPMSM type 2 copper inductor at no load

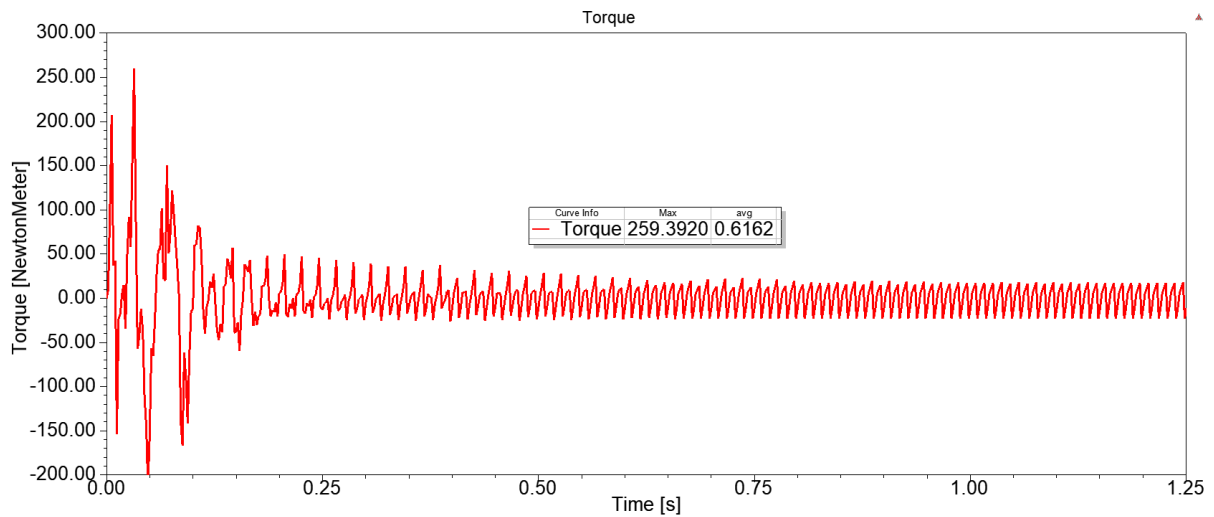


Fig.5.42: Torque of LSAFPMSM type 3 aluminium inductor at no load

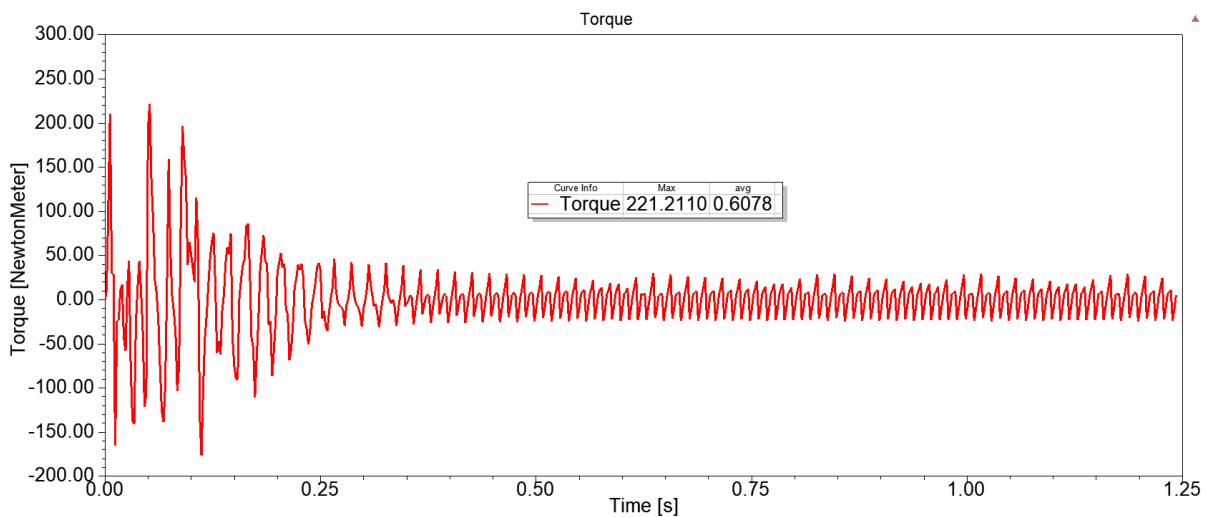


Fig.5.43: Torque of LSAFPMSM type 3 copper inductor at no load

From the figure 5.37 to 5.43, the starting torque of all motor at no load condition is high. The maximum torque of the motor is listed in the graphs. Motor produce high starting torque for the rotation from steady condition. The all motor is run to 1.25s with time step of 2ms. The stable average torque of all model is about 0.6Nm with high starting torque. Due to high starting torque, these types of motor is mostly used in industrial application.

The performance of torque is also tested under loading condition of 2Nm load. The mechanical load of 2Nm is applied for all model and tested.

The 2Nm load torque graph is obtained and illustrated in the following figures.

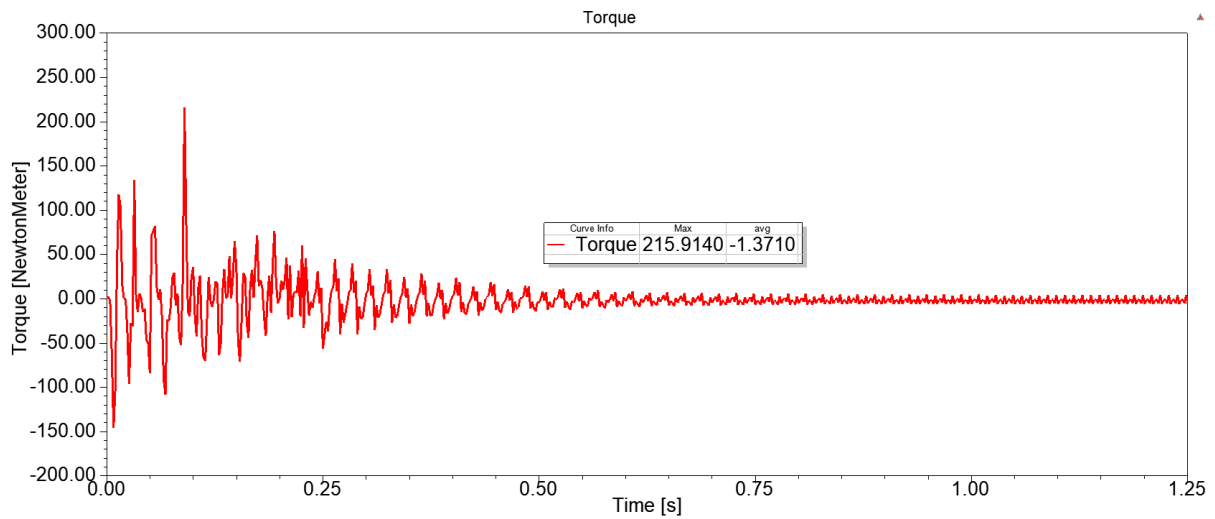


Fig.5.44: Torque of Induction motor at 2Nm

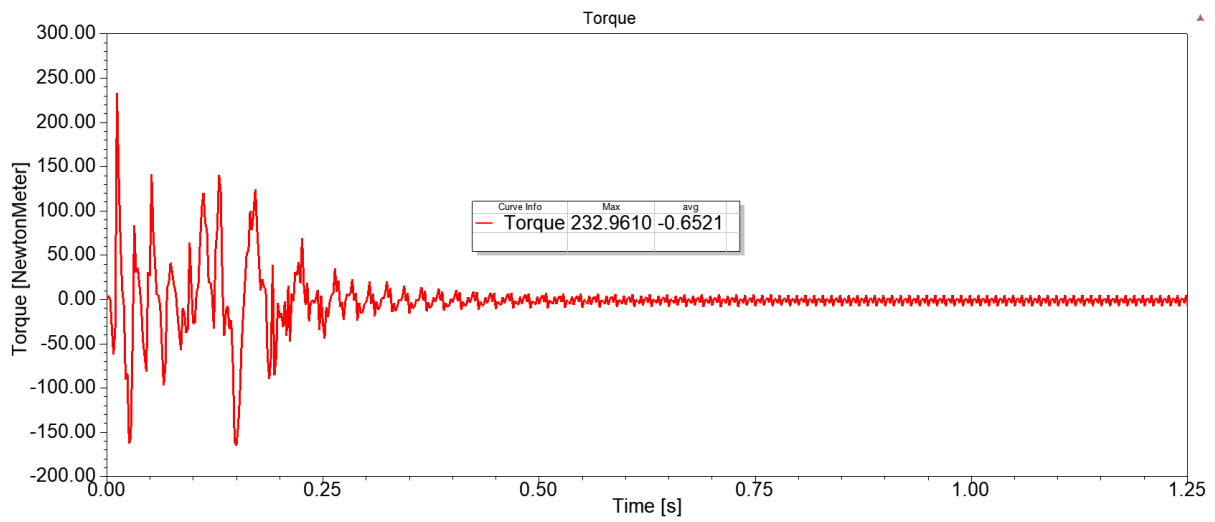


Fig.5.45: Torque of LSAFPMSM type 1 aluminium inductor at 2Nm

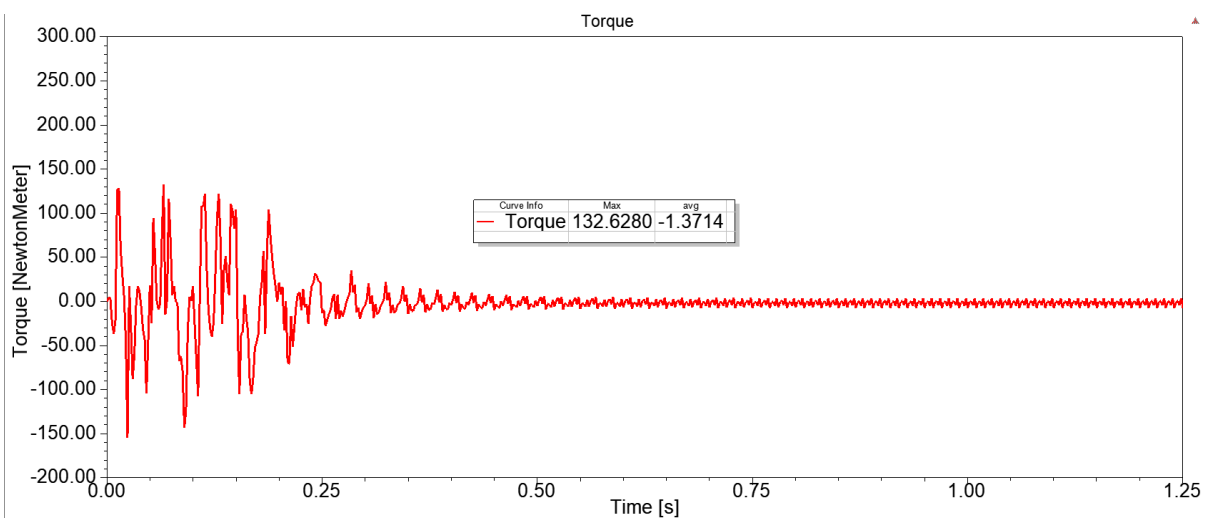


Fig.5.46: Torque of LSAFPMSM type 1 copper inductor at 2Nm

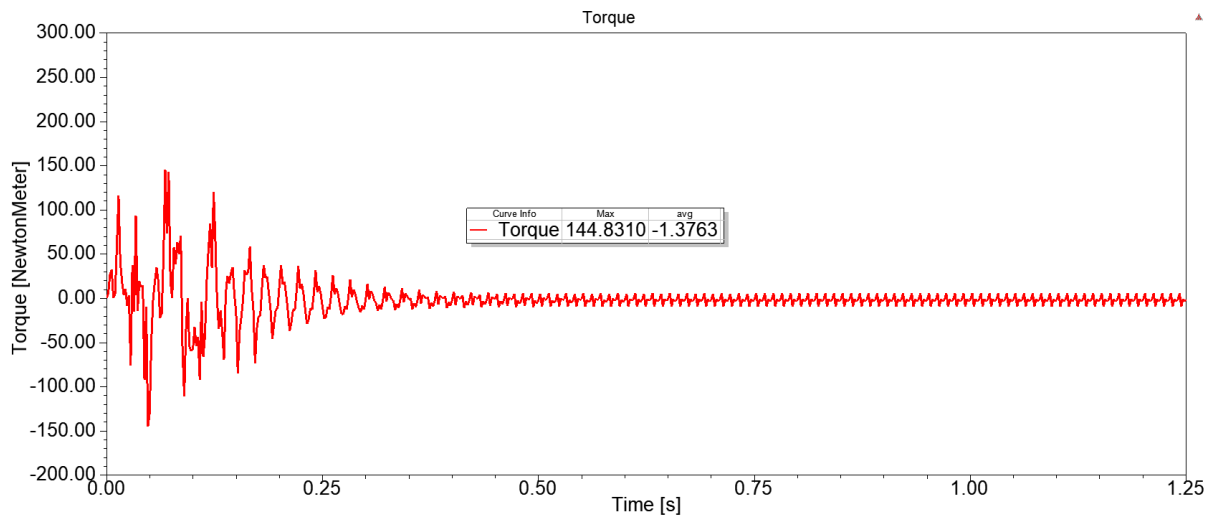


Fig.5.47: Torque of LSAFPMSM type 2 aluminium inductor at 2Nm

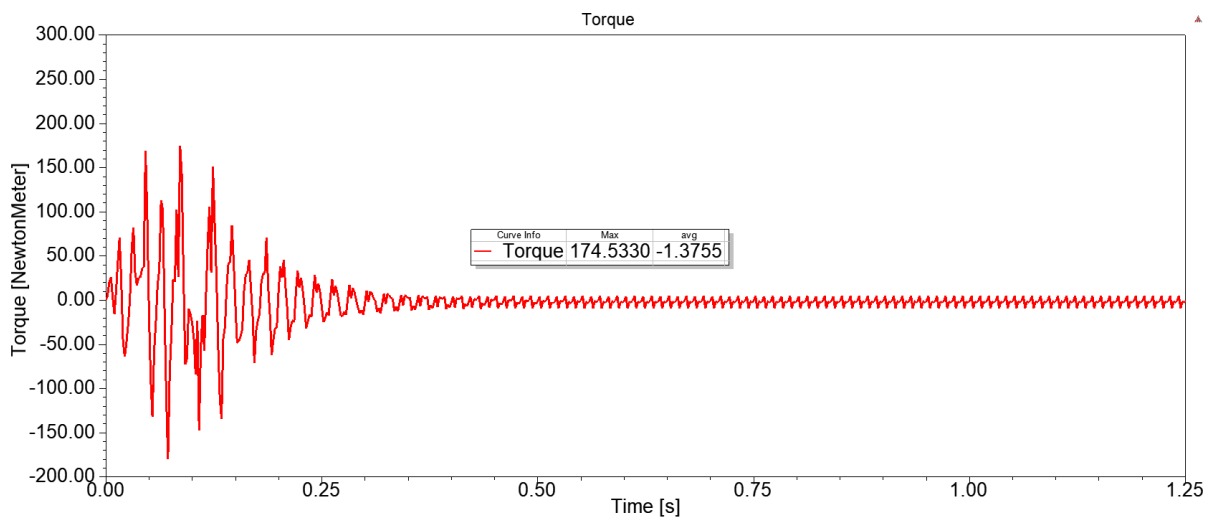


Fig.5.48: Torque of LSAFPMSM type 2 copper inductor at 2Nm

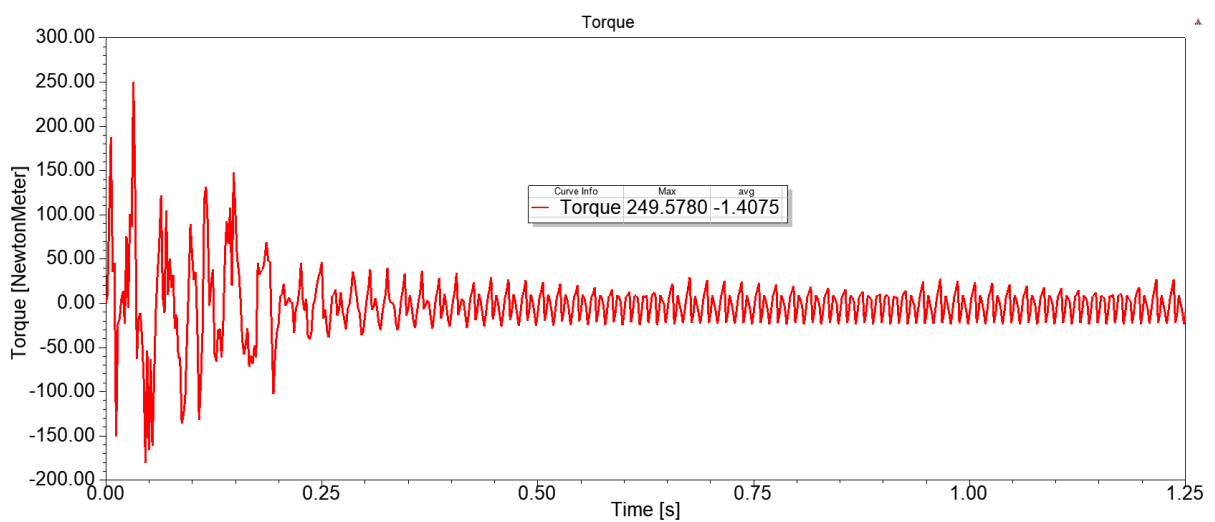


Fig.5.49: Torque of LSAFPMSM type 3 aluminium inductor at 2Nm

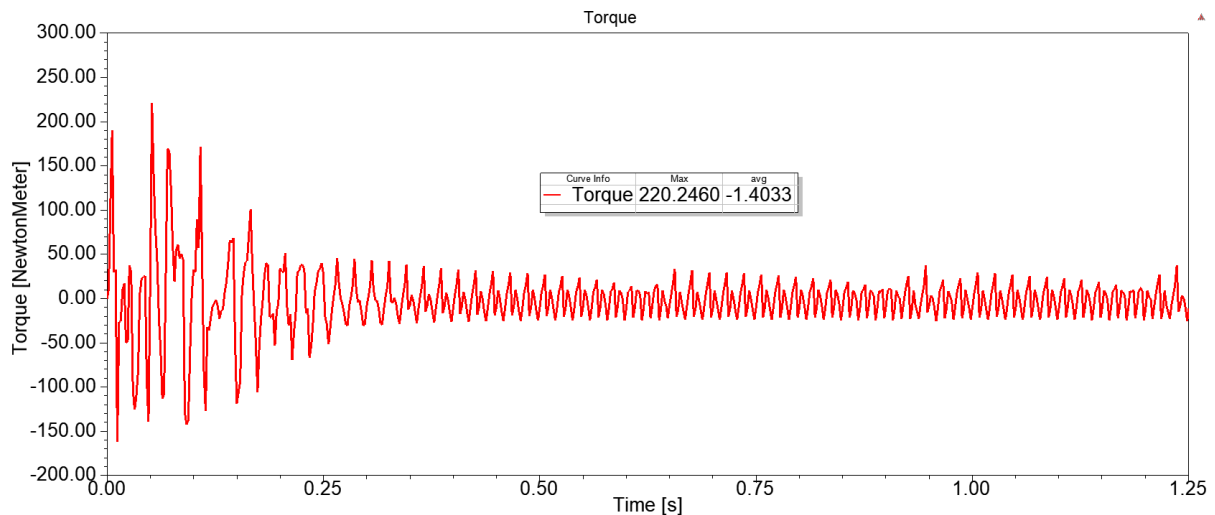


Fig.5.50: Torque of LSAFPMSM type 3 copper inductor at 2Nm

The torque at 2Nm load for all model is shown in figure 5.44 to 5.50. The induction motor has 215Nm maximum torque. The designed all models of LSAFPMSM have high starting torque and the maximum torque is depended on the design construction of all models. The type 2 model of has relatively low maximum torque because of double inductor bar design. Overall, the LSAFPMSM have high maximum torque to rotate the machine. This is the reason that, LSAFPMSM takes less time to reach synchronous speed. So, this kind of motor is replaced to induction motor for industrial application.

5.5 Power Rating of machine

In this part, the input power and output power of all design is carried out. The input power and output power are measured at no load and 2Nm under load condition.

Here, the formula directly used in software for input power and output power is:

$$\text{Power_In} = \text{abs}(\text{Current}(\text{A}) * \text{InputVoltage}(\text{A}) + \text{Current}(\text{B}) * \text{InputVoltage}(\text{B}) + \text{Current}(\text{C}) * \text{InputVoltage}(\text{C}))$$

$$\text{Power_Out} = \text{Power_In} - \text{Total_Losses}$$

$$\text{where, Total_Losses} = \text{CoreLoss} + \text{SolidLoss} + \text{StrandedLoss} + \text{StrandedLossR}$$

The power rating at no load condition is shown in the following figures.

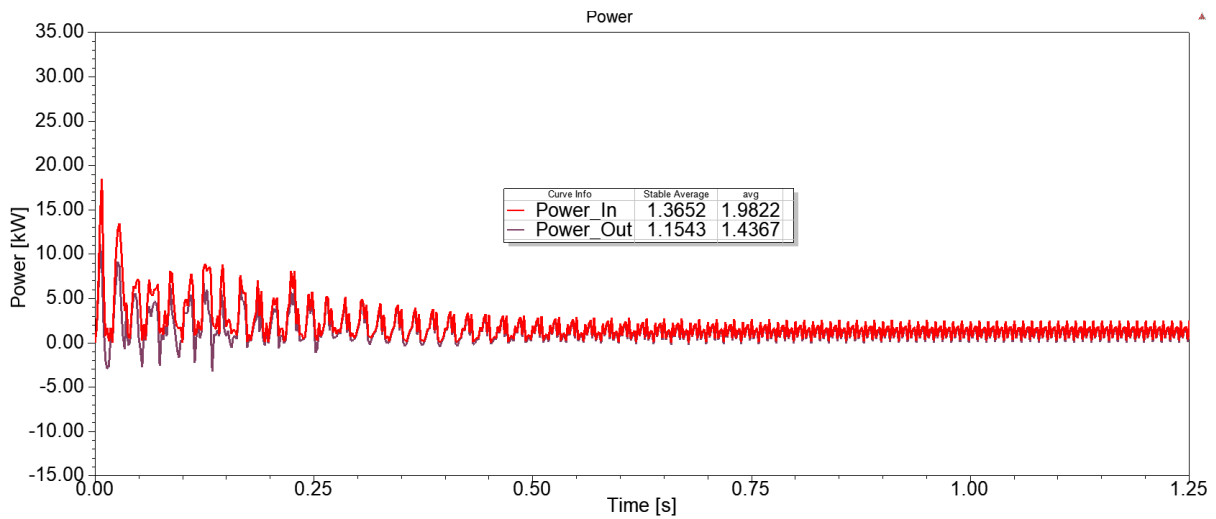


Fig.5.51: Input and output power of Induction motor at no load

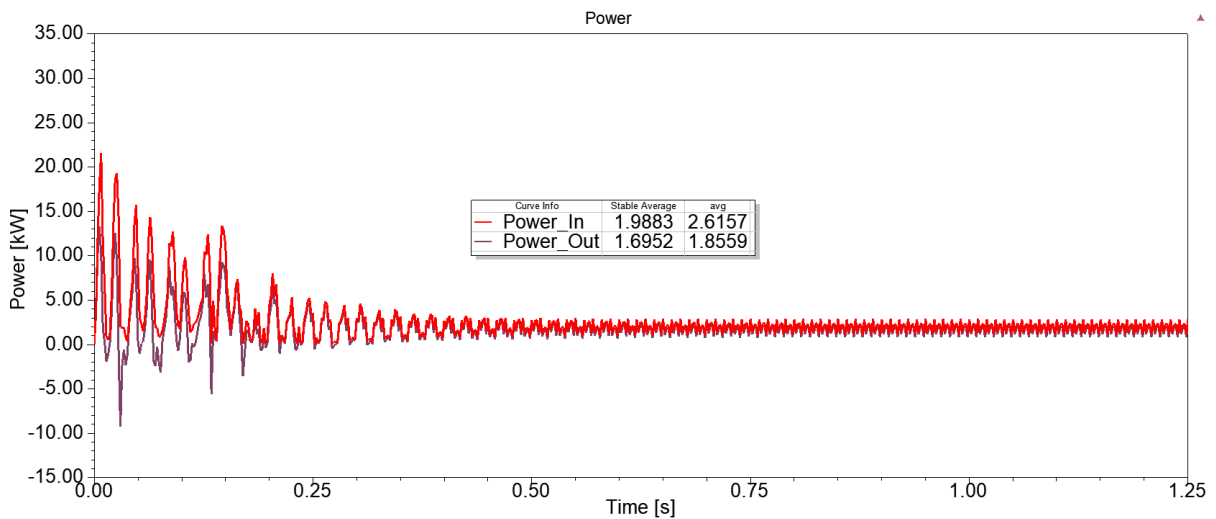


Fig.5.52: Input and output power of LSAFPMSM type 1 aluminium inductor at no load

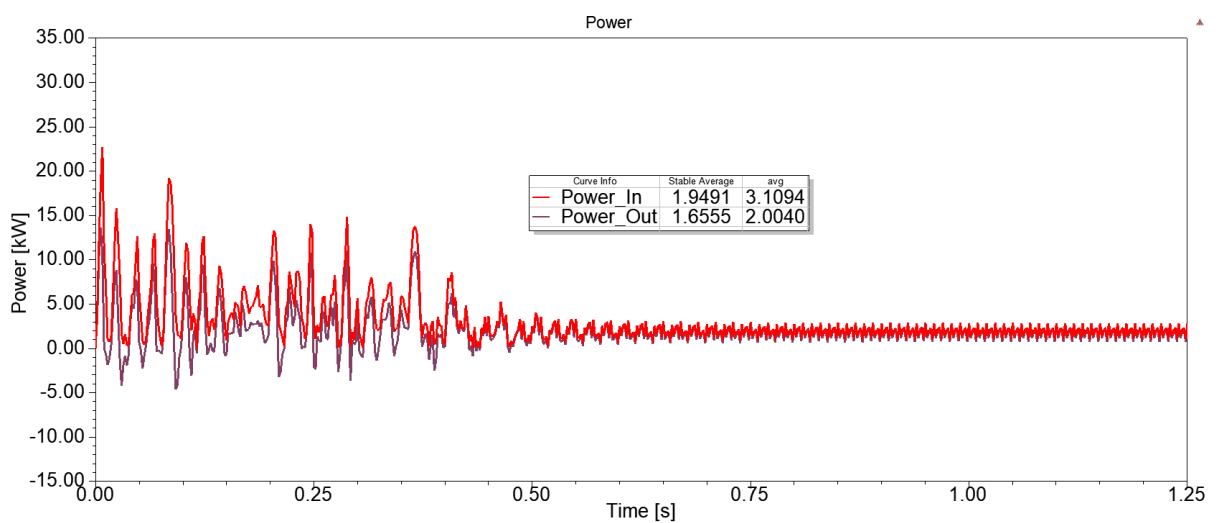


Fig.5.53: Input and output power of LSAFPMSM type 1 copper inductor at no load

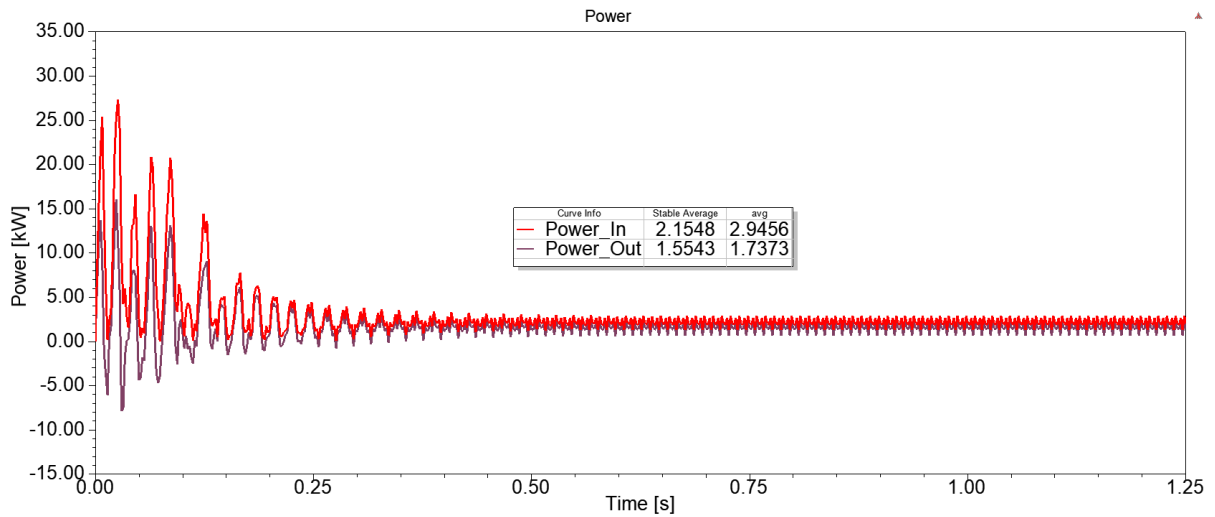


Fig.5.54: Input and output power of LSAFPMSM type 2 aluminium inductor at no load

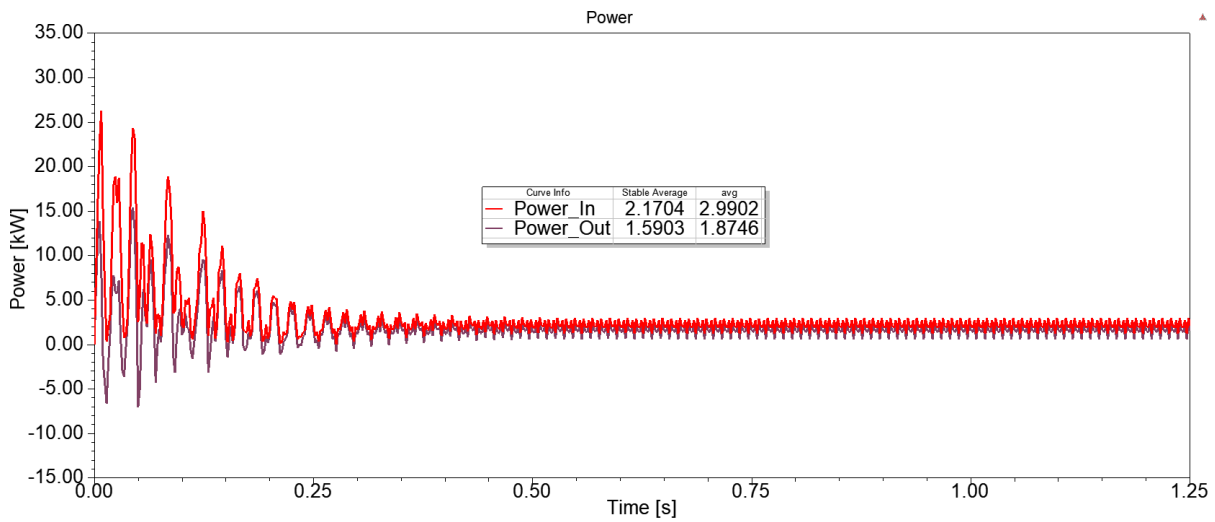


Fig.5.55: Input and output power of LSAFPMSM type 2 copper inductor at no load

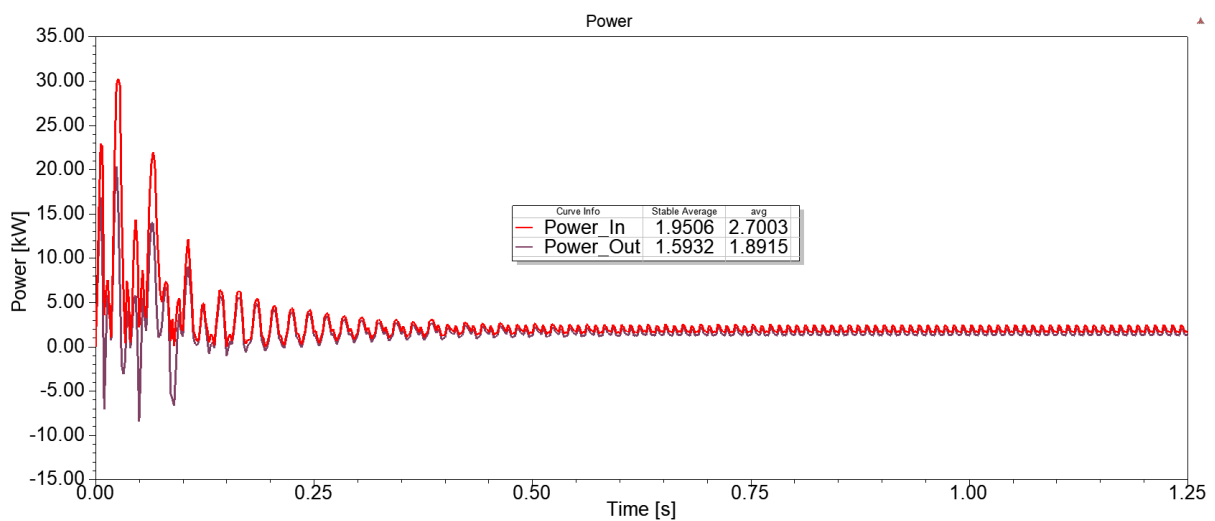


Fig.5.56: Input and output power of LSAFPMSM type 3 aluminium inductor at no load

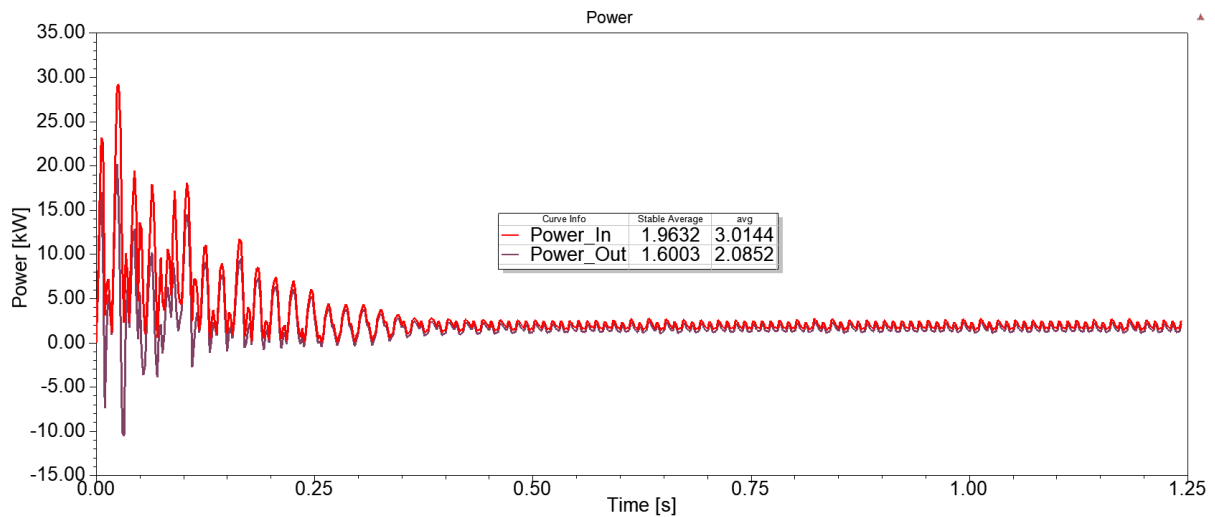


Fig.5.57: Input and output power of LSAFPMSM type 3 copper inductor at no load

The input and output power of induction motor is low as compared to LSAFPMSM in figure 5.51. The input and output power of LSAFPMSM type 1 and type 3 has almost same value as input power of 1.9kW and output power is 1.6kW. This is because the same design of inductor with different position on the rotor. While, the type 2 motor has input power 2.1kW and output power is 1.5kW because of double inductor design as discussed in design chapter. So, at no load LSAFPMSM have high power rating as compared to induction motor.

In the second part, the input power and output power are tested for 2Nm under load condition and the graph for given load is as following.

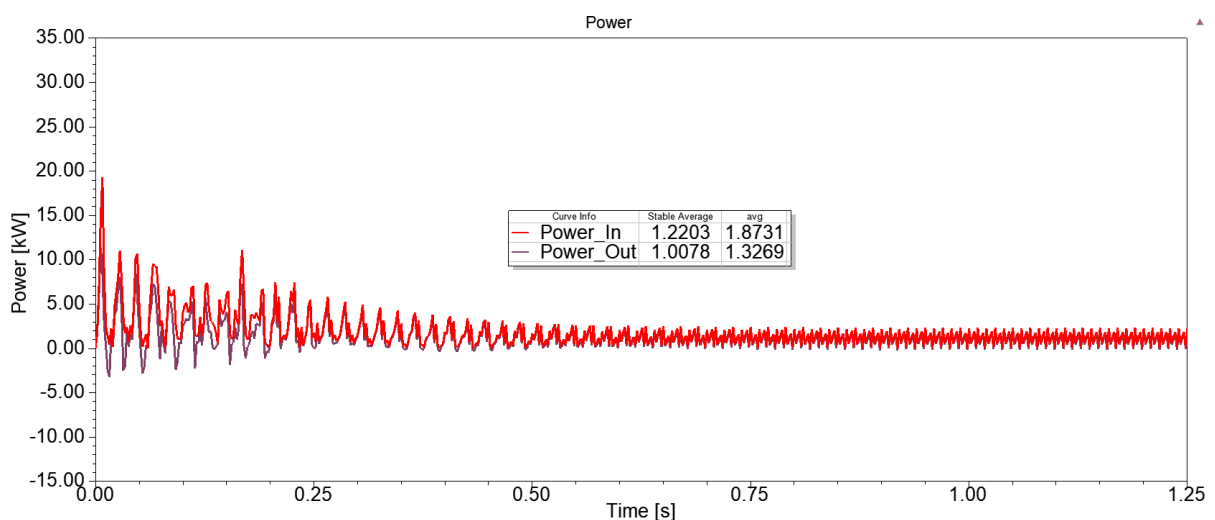


Fig.5.58: Input and output power of Induction motor at 2Nm load

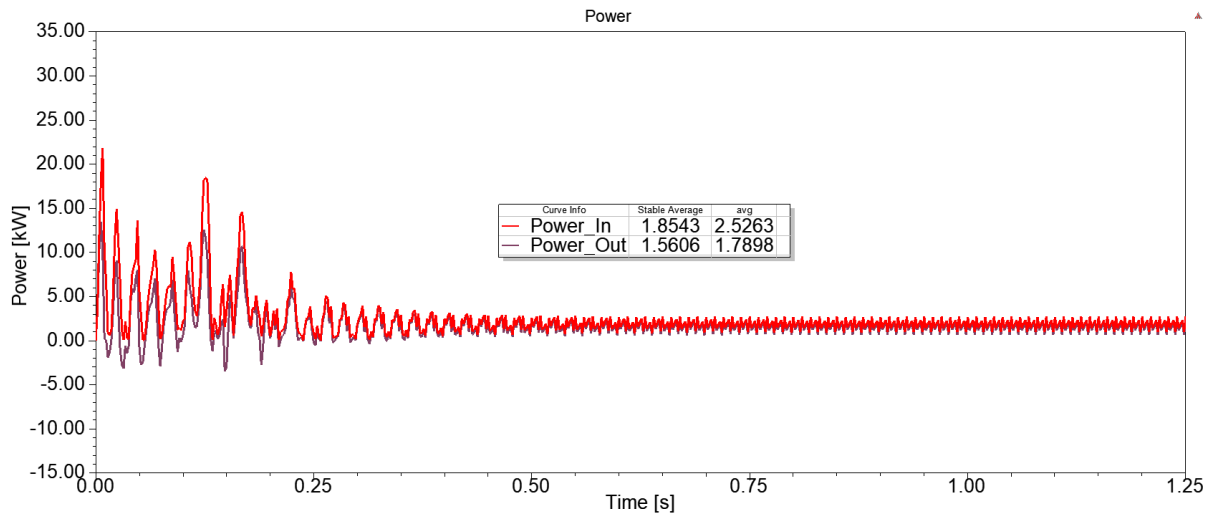


Fig.5.59: Input and output power of LSAFPMSM type 1 aluminium inductor at 2Nm load

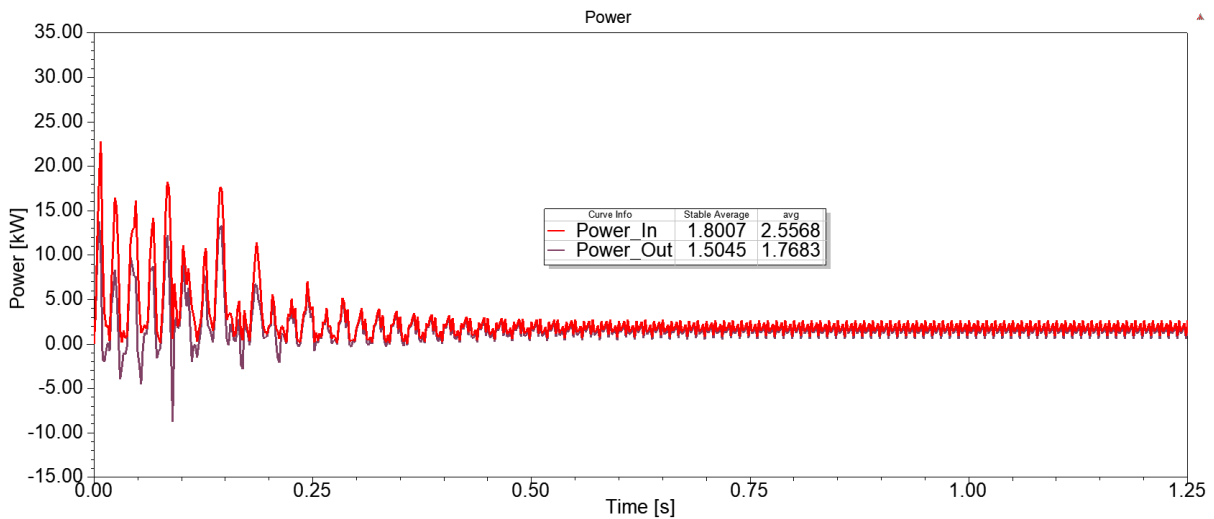


Fig.5.60: Input and output power of LSAFPMSM type 1 copper inductor at 2Nm load

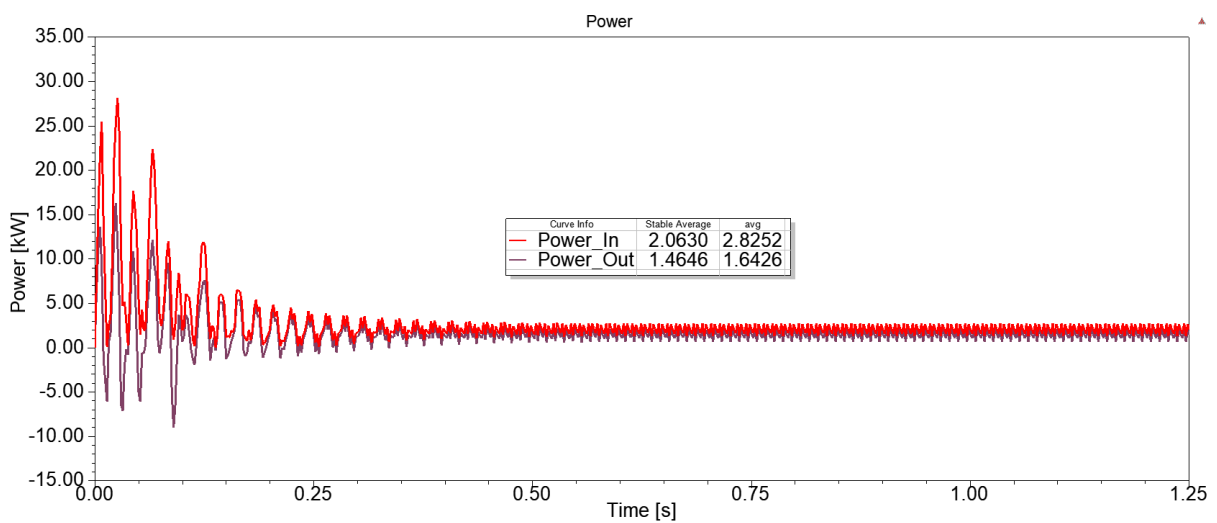


Fig.5.61: Input and output power of LSAFPMSM type 2 aluminium inductor at 2Nm load

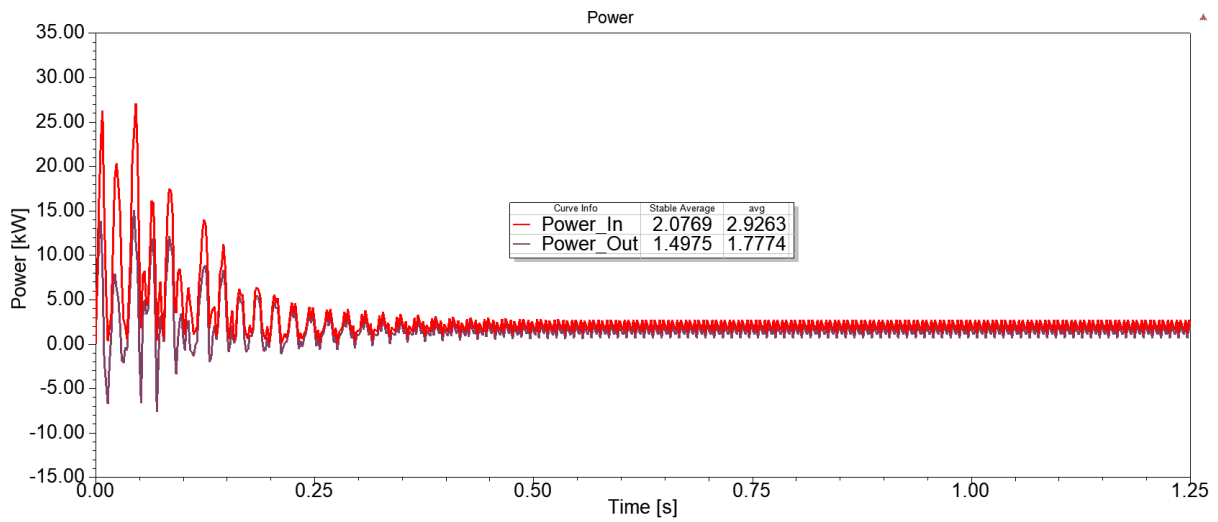


Fig.5.62: Input and output power of LSAFPMSM type 2 copper inductor at 2Nm load

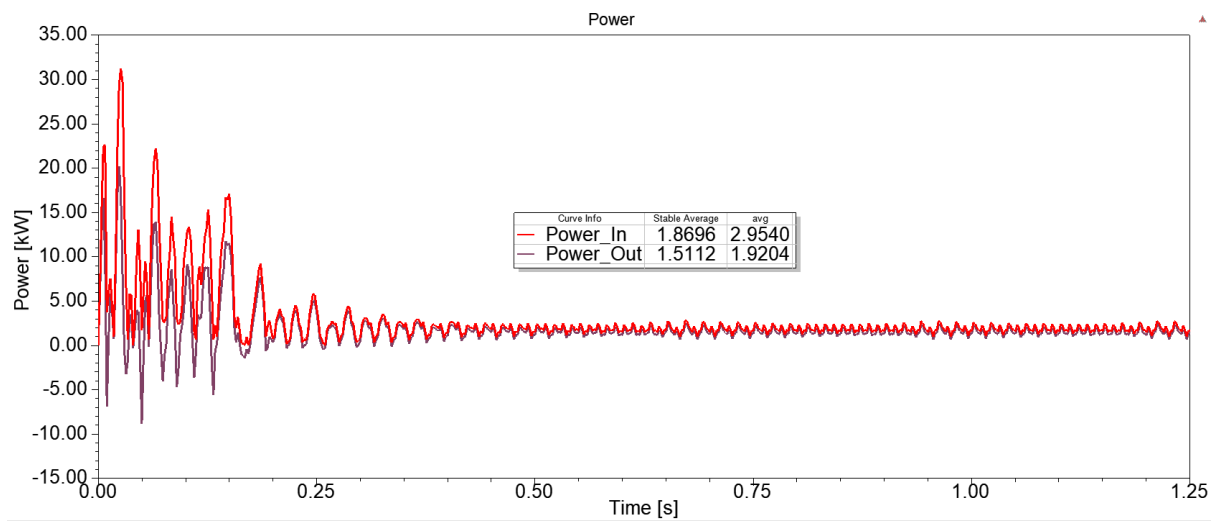


Fig.5.63: Input and output power of LSAFPMSM type 3 aluminium inductor at 2Nm load

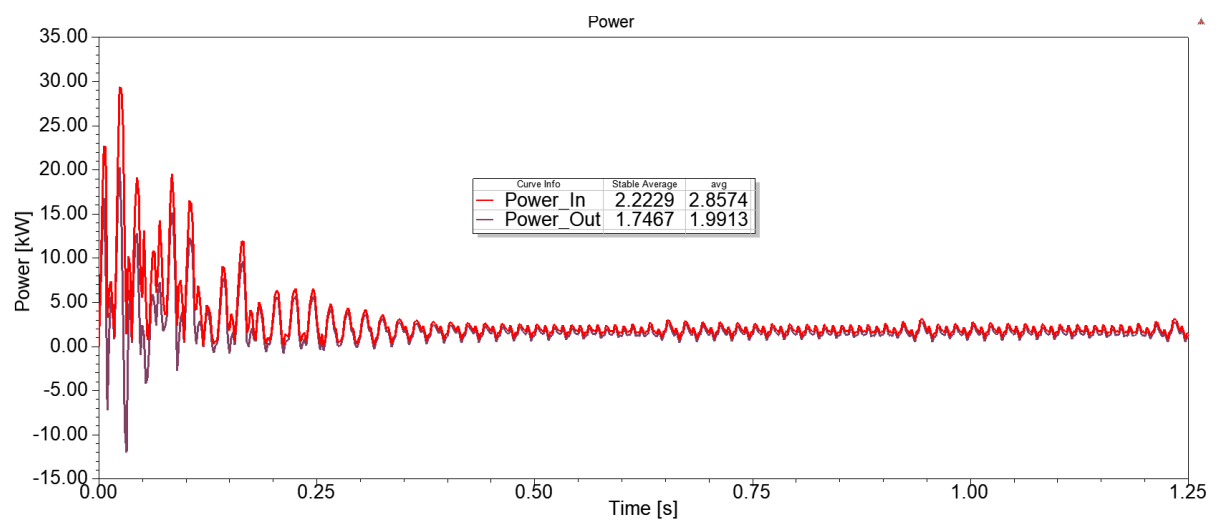


Fig.5.64: Input and output power of LSAFPMSM type 3 copper inductor at 2Nm load

At 2Nm load, the output power of induction motor 1.3kW. The LSAFPMSM have relatively high output power as compared to induction motor. The all models of LSAFPMSM have almost same 1.5kW output power as indicated in the above graphs. This value of input power and output power are used to calculate the efficiency of motors.

5.6 Efficiency of motor

The ratio between output power to input power is called efficiency. In this section, the efficiency of all model motor is obtained. The efficiency of motor is depended on the design, construction, power rating, load and construction of motor. For this project, the efficiency of all model is calculated manually.

The efficiency of the motor at no load is zero. The under 2Nm load condition the efficiency of all models are shown in figure 5.65.

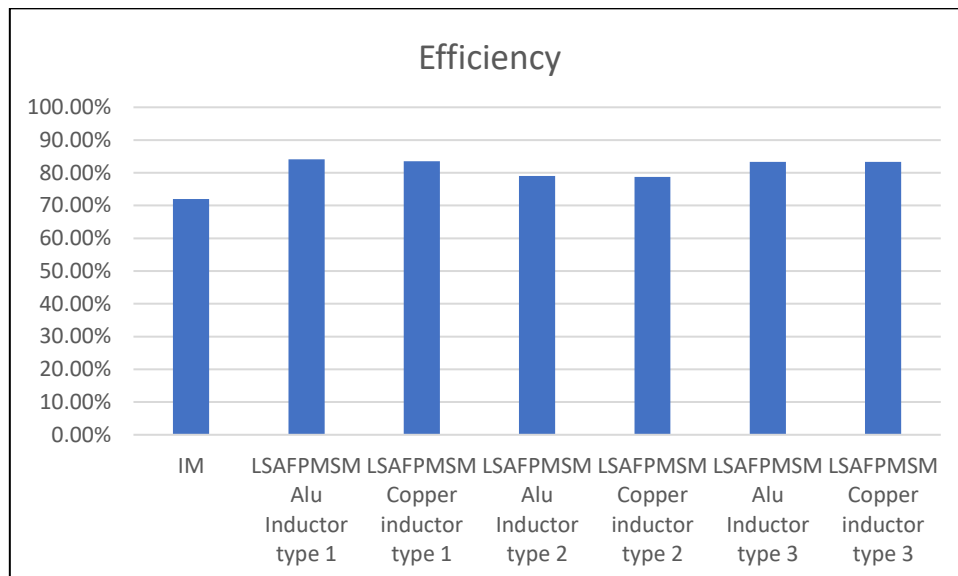


Fig.5.65: Efficiency of all motors at 2Nm load

Form the results, it can be seen that the all new design models of line-start axial-flux permanent magnet synchronous motor has higher efficiency. The new LSAFPMSM has around 83% efficiency of all models at 2Nm load. While, the efficiency of the induction motor is 72% at 2Nm load. Due to higher efficiency, this kind of motor is used for industrial purpose to overcome the disadvantages of the induction motor.

5.7 Power Factor

Power factor is one of the important factor of the motor. The energy cost of motor can be reduced by improving the power factor. Sometimes, power factor is overlook while designing of the motor which causes higher cost of motor. Normally, the power factor is defined as ration of kilowatts (kW) and kilovolt-amp (KVA). It is also defined as phase angle between voltage and current.

The formula which is used to calculate power factor in software is given below.

$$\text{Power_Factor} = (\text{Mechanical_Power})/\text{Power_In}$$

Where, $\text{Mechanical_Power} = \text{Power_In} - \text{Electrical_Loss}$

The Power factor of all motor is illustrated in the following figure 5.66.

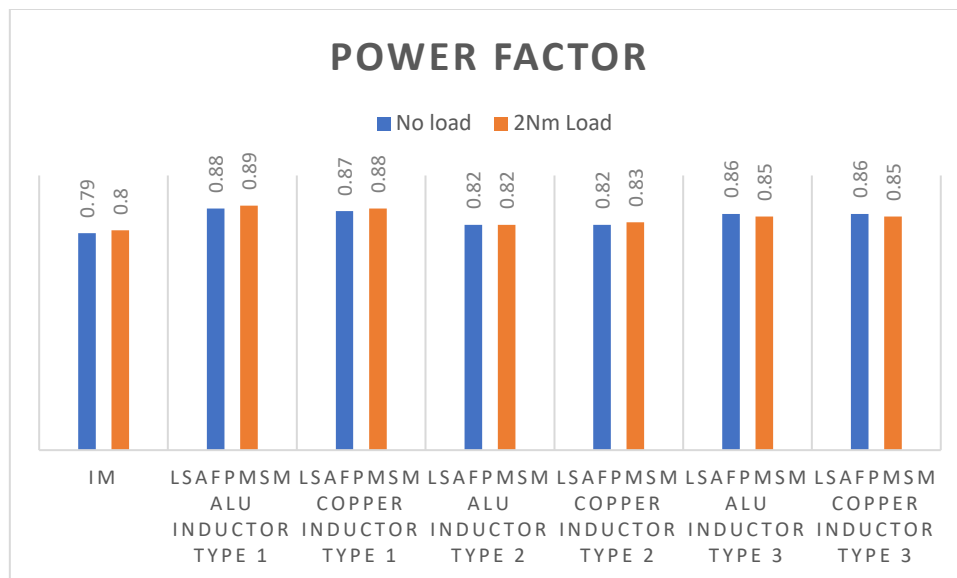


Fig.5.66: Power factor of motor at no load and 2Nm load

The power factor of induction motor at no load is 0.79 and 0.8 at 2Nm load. On the other side, the new developed models of LSAFPMSM have higher power factor at no load and at 2Nm load as compared to induction motor. The type 1 model has 0.88 and 0.89 power factor at no load and 2 Nm load. Type 2 model has low power factor among the three models of LSAFPMSM but higher power factor than induction motor.

Table.5.2: Overall performance of all motors

		Line-start Axial flux permanent magnet synchronous motor					
	Induction motor	Alu type 1 inductor	Copper type 1 inductor	Alu type 2 inductor	Copper type 2 inductor	Alu type 3 inductor	Copper type 3 inductor
Speed (rpm)	727	750	750	750	750	750	750
Rated Output power (kW)	1.1	1.5	1.5	1.49	1.49	1.5	1.5
Number of pole	8	8	8	8	8	8	8
Frequency (Hz)	50	50	50	50	50	50	50
Airgap (mm)	1	1	1	1	1	1	1
Losses (W)	16.5	15.9	16.5	14.4	14.4	13.6	13.6
Efficiency (%)	72	84.16	83.55	79.05	78.7	83.33	83.33

Table 5.2 shows the overall performance of the all motors. The line-start axial flux permanent magnet synchronous motor (LSAFPMSM) has better performance as compared to induction motor. The constant synchronous speed is achieved in all models of LSAFPMSM. This motor has less losses as compared to induction motor which leads to better efficiency of the motor. The 1mm air gap is selected for all motors and supply frequency 50Hz. LSAFPMSM models have higher output power at no load and at 2Nm load. At last, the LSAFPMSM have higher efficiency than induction motor at 2Nm load. So, this kind of motor replace induction motor for industrial application. The LSAFPMSM does not require any external circuit to start the motor. It is directly work on three-phase supply voltage.

The main advantage of LSAFPMSM is higher efficiency. The rotor cage loss is very low in the LSAFPMSM except the harmonic of motor so due to less losses the efficiency is high. While, the induction motor has high rotor cage loss which results increase in the total number of losses which leads to the lower efficiency of motor.

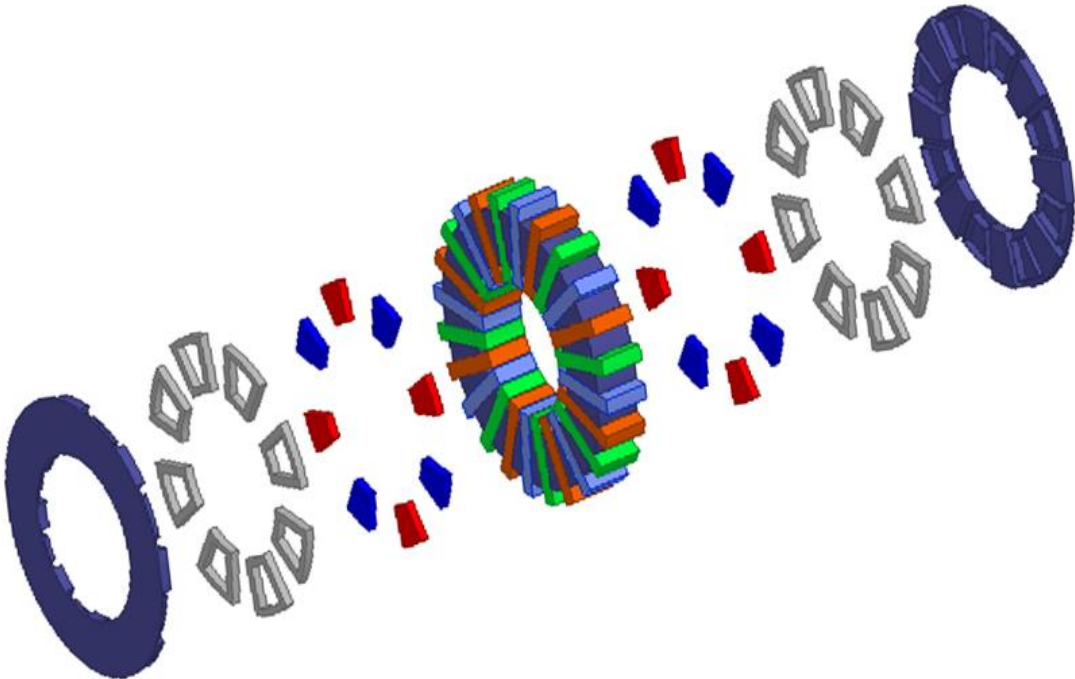
Because of inductive behaviour of induction motor has low power factor. Due to low power factor, the heating problem is occurred. But, the LSAFPMSM have higher power factor than induction motor. LSAFPMSM almost work near to unity power factor with same power rating.

The torque and rated output power of LSAFPMSM is high as compared to induction motor as from the results performance of both motor.

From the above all results of LSAFPMSM and Induction motor, it can be noticed that the LSAFPMSM is superior in performance than induction motor.

In terms of Cost, the LSAFPMSM has higher price as compared to induction motor. The permanent magnet is reason of high cost of LSAFPMSM. So, the material cost and manufacturing cost of the motor is high. This is the main disadvantage of line start axial flux permanent magnet synchronous motor.

Chapter 6: Conclusion and Future work



6.1 Conclusion

The objective of this thesis was to design double sided rotor line start axial flux permanent magnet synchronous motor with different design of inductor bars. The performance of double sided rotor line-start axial flux permanent magnet synchronous motor (LSAFPMSM) is compared with the Induction motor. The three phase 8-pole, 50Hz, 750 rpm speed axial flux motor were designed with same stator design but there was different in rotor design. The LSAFPMSM has permanent magnet on rotor which is absent in induction motor. The three types of inductor bar were designed for LSAFPMSM and performance of this model was carried out with aluminium and copper material of inductor bar. The finite element analysis is used with ANSYS Maxwell 3D software for better accurate results. The magnetostatic analysis, open circuit test and transient analysis was performed in this thesis.

6.2 Key Findings

The results of different analysis of the motors shows that Double sided rotor line-start axial flux permanent magnet synchronous motor (LSAFPMSM) have better performance than Induction motor (IM). The LSAFPMSM has high rated output power as compared to Induction motor. In terms of efficiency, the LSAFPMSM have higher efficiency than induction motor under given load condition. The all model of LSAFPMSM have efficiency around 83% except type 2 model. While, the efficiency of induction motor is low 72%.

The flux density of the all designed models is obtained in magnetostatic analysis. The magnetic flux density of LSAFPMSM shows better density at different parts of motor under no load and under load condition. The flux vector shows the direction of flux. The magnetic flux linkage is carried out for all motor. The all motor has almost same flux linkage with minor difference in shape and magnitude.

The open circuit test is carried out on all models of LSAFPMSM with no mechanical load at rated speed. The no load induced voltage is obtained for all models. Type 3 model has high peak induced voltage as compared to other two types.

The all model of LSAFPMSM have achieved constant speed during the no load condition and at 2Nm load condition but the induction motor has fluctuating speed at both load condition. The speed of LSAFPMSM takes very less time to reach synchronous speed than induction motor. So, the LSAFPMSM is used for constant speed application under different loading conditions.

Starting torque of the LSAFPMSM is high as compared to Induction motor. Due to high starting torque response, the rotation of motor start very fast. After that, torque is stable at around 0Nm for all model. The core loss of the induction motor is high as compared to LSAFPMSM at no load and at 2Nm load.

The rated output power of all models of LSAFPMSM is high as compared to Induction motor. The LSAFPMSM models have 1.5kW rated output power. The induction motor obtained 1.1kW output power.

As mentioned before, the LSAFPMSM has better efficiency than induction motor. The power factor is also improved for LSAFPMSM models as compared to Induction motor. Due to high efficiency and constant speed, LSAFPMSM is suitable to replace induction motor for industrial application. The drawback of LSAFPMSM is the cost. The cost of LSAFPMSM is high because of permanent magnet used in rotor.

6.3 Future work

Optimisation of design

This thesis discussed the design and performance of double sided rotor line start axial flux permanent magnet synchronous motor with three type of inductor bar design. In the future, the performance of motor can be optimized by changing the shape and size of magnets, different arrangement of inductor bar and by changing the winding properties.

Prototyping

The working models of LSAFPMSM can be optimised in future for better accurate and actual experimental results.

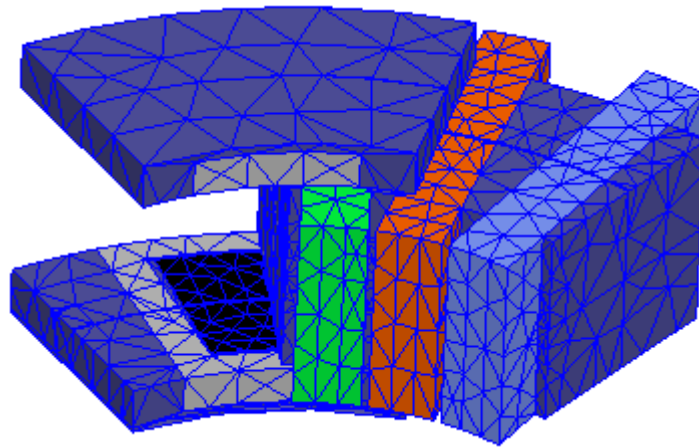
References

- [1] Energy Efficiency Series, “Energy-Efficiency policy opportunity for electric Motor-Driven System”. Accessed on: 08 October 2017, Online available at: <http://citeseerx.ist.psu.edu/viewdoc/download?doi=10.1.1.378.4854&rep=rep1&type=pdf>
- [2] Electric Motors, “Energy Rating, Accessed: 08 October 2017,
< <http://www.energyrating.gov.au/products/electric-motors#toc2> >
- [3] L. Livadaru, A. Simion, A. Munteanu and O. Dabija, “Design and FEM based Simulation of High Power Induction Motor with severe Start-up Constraints”, AGIR, Romania, Tech. Rep. 101-106, 2012. [Online]. Available: <http://www.agir.ro/buletine/1521.pdf>.
- [4] S. Contreras, C. Cortes, M. Guzman, “Modelling of squirrel cage induction motors for a bio-inspired multi-objective optimal design”, IET Electr. Power appl. 2017. Iss 4, pp. 512-523.
- [5] Ruthes, J.R., Nau, S.L. and Nied, A., 2016, November. “Performance analysis of induction motor under non-sinusoidal supply voltages”. In *Industry Applications (INDUSCON), 2016 12th IEEE International Conference on* (pp. 1-6). IEEE.
- [6] Srinivasan, J., Selvaraj, K., Chitrrasu, J. and Resmi, R., 2016, October. Design and analysis of squirrel cage induction motor in short pitch and full pitch winding configurations using FEA. In *Emerging Technological Trends (ICETT), International Conference on* (pp. 1-10). IEEE.
- [7] Pyrhonen J, Jokinen T and Hrabovcova V, “Design of Rotating Electrical Machines”, 2nd ed. Chichester, United Kingdom: Wiley, 2014, pp. 293-456
- [8] Cavagnino, A., Lazzari, M., Profumo, F. and Tenconi, A., 2002. A comparison between the axial flux and the radial flux structures for PM synchronous motors. *IEEE Transactions on Industry Applications*, 38(6), pp.1517-1524.
- [9] Patterson, D.J., Colton, J.L., Mularcik, B., Kennedy, B.J., Camilleri, S. and Rohoza, R., 2009, May. A comparison of radial and axial flux structures in electrical machines. In *Electric Machines and Drives Conference, 2009. IEMDC'09. IEEE International* (pp. 1029-1035). IEEE.
- [10] Upadhyay, P.R. and Rajagopal, K.R., 2005. Comparison of performance of the axial-field and radial-field permanent magnet brushless direct current motors using computer aided design and finite element methods. *Journal of applied physics*, 97(10), p.10Q506.

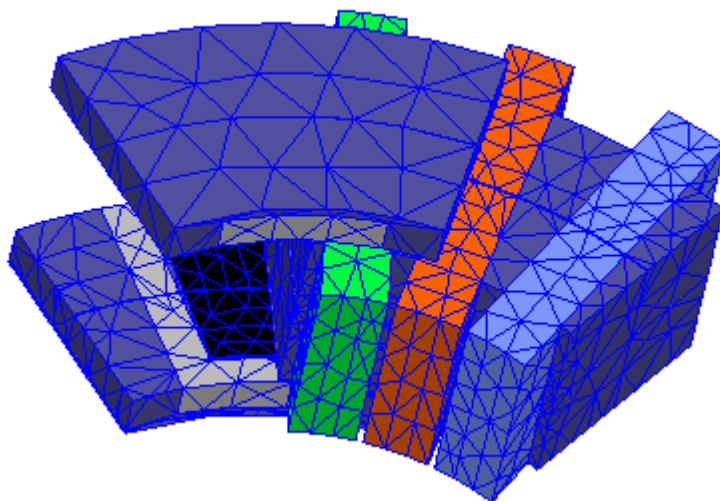
- [11] Sitapati, K. and Krishnan, R., 2001. Performance comparisons of radial and axial field, permanent-magnet, brushless machines. *IEEE Transactions on industry applications*, 37(5), pp.1219-1226.
- [12] Parviainen, A., Niemela, M., Pyrhonen, J. and Mantere, J., 2005, May. Performance comparison between low-speed axial-flux and radial-flux permanent-magnet machines including mechanical constraints. In *Electric Machines and Drives, 2005 IEEE International Conference on* (pp. 1695-1702). IEEE.
- [13] Mahmoudi, A., Kahourzade, S., Uddin, M.N., Rahim, N.A. and Hew, W.P., 2013, September. Line-start axial-flux permanent-magnet synchronous motor. In *Energy Conversion Congress and Exposition (ECCE), 2013 IEEE* (pp. 3210-3216). IEEE.
- [14] Ugale, R.T., Bhanuji, A. and Chaudhari, B.N., 2009, January. A novel line start permanent magnet synchronous motor using two-part rotor. In *TENCON 2009-2009 IEEE Region 10 Conference* (pp. 1-5). IEEE.
- [15] Tsuboi, K., Takegami, T., Hirotsuka, I. and Nakamura, M., 2011. A general analytical method for a three-phase line-start permanent-magnet synchronous motor. *IEEJ Transactions on Industry Applications*, 131, pp.692-699.
- [16] Feng, X., Bao, Y., Liu, L., Huang, L. and Zhang, Y., 2012, September. Performance investigation and comparison of line start-up permanent magnet synchronous motor with super premium efficiency. In *Electrical Machines (ICEM), 2012 XXth International Conference on* (pp. 424-429). IEEE.
- [17] Fei, W., Luk, P.C.K., Ma, J., Shen, J.X. and Yang, G., 2009. A high-performance line-start permanent magnet synchronous motor amended from a small industrial three-phase induction motor. *IEEE Transactions on Magnetics*, 45(10), pp.4724-4727.
- [18] Kül, S., Bilgin, O. and Mutluer, M., 2015. Application of finite element method to determine the performances of the line start permanent magnet synchronous motor. *Procedia-Social and Behavioral Sciences*, 195, pp.2586-2591.

Appendices

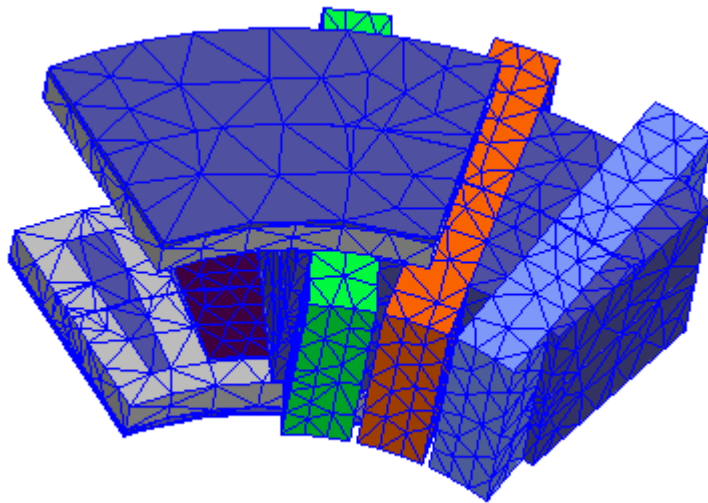
Appendix A: Mesh plots



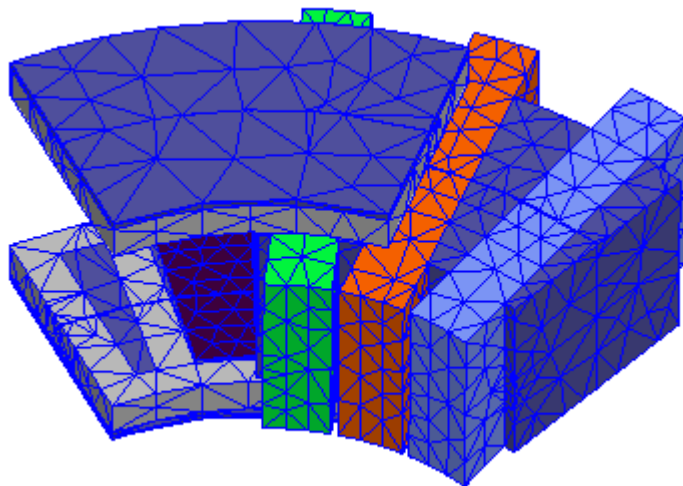
Mesh plot of LSAFPMSM type 1 Alu inductor



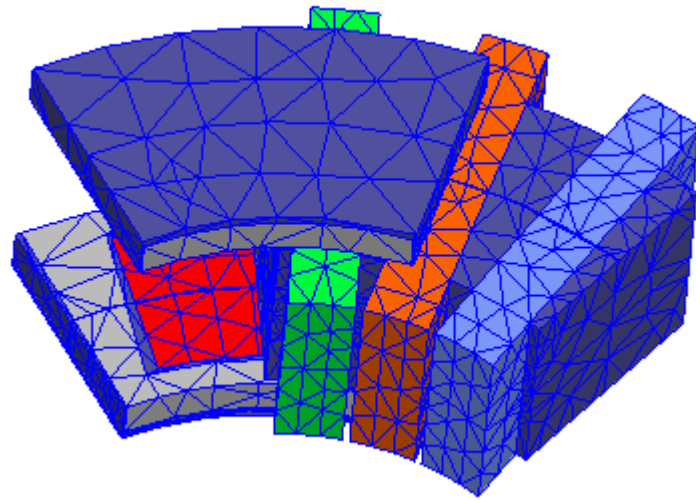
Mesh plot of LSAFPMSM type 1 copper inductor



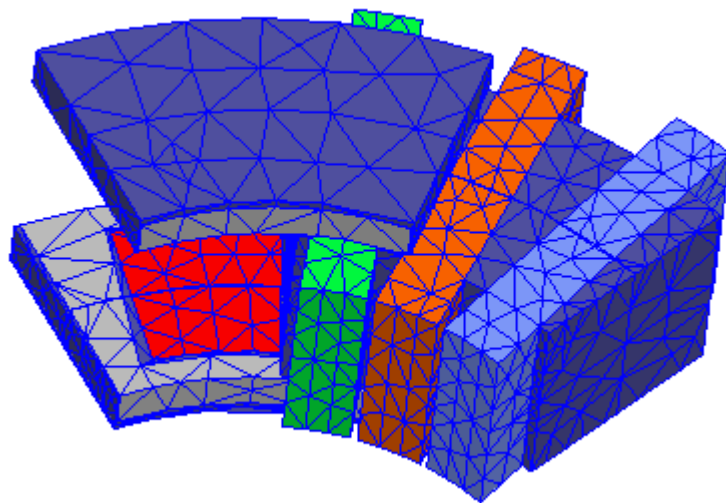
Mesh plot of LSAFPMSM type 2 Alu inductor



Mesh plot of LSAFPMSM type 2 copper inductor



Mesh plot of LSAFPMSM type 3 Alu inductor



Mesh plot of LSAFPMSM type 3 copper inductor